

Techniques from the neonatal brain

*Use of advanced
cranial ultrasound
to study the
neonatal brain*

Edited by **Dr. David A. Hirsch**

Ginette Ecury-Goossen

Echoes from the neonatal brain

*Use of advanced cranial ultrasound
to study the neonatal brain*

Printing of this thesis was kindly supported by Esaote Benelux B.V.

Layout and Printing: Optima Grafische Communicatie (www.ogc.nl)

ISBN: 978-94-6169-968-8

Copyright ©

All rights reserved. No part of this thesis may be reproduced, stored in a retrieval system, or transmitted in any form or by any means, electronically, mechanically, by photocopying, recording, or otherwise, without prior permission of the author.

Echoes From The Neonatal Brain
Use of advanced cranial ultrasound
to study the neonatal brain

Echo's uit het neonatale brein
Gebruik van geavanceerde schedelechografie
voor onderzoek van het neonatale brein

Proefschrift

ter verkrijging van de graad van doctor aan de
Erasmus Universiteit Rotterdam
op gezag van de
rector magnificus

Prof.dr. H.A.P. Pols

en volgens besluit van het College voor Promoties.
De openbare verdediging zal plaatsvinden op

dinsdag 6 december 2016 om 13.30 uur

Ginette Marguerita Ecury-Goossen
geboren te Delft

Promotiecommissie

Promotor: Prof.Dr. I.K.M. Reiss

Overige leden: Prof.Dr. L.S. de Vries
Prof.Dr. A. van der Lugt
Prof.Dr. E.A.P. Steegers

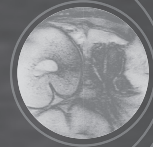
Copromotor: Dr. J. Dudink

Table of contents

Part I	Neonatal cerebral blood flow – use of advanced Doppler cranial ultrasound	7
Chapter 1	General introduction	9
Chapter 2	State of the art cranial ultrasound imaging in neonates	25
Chapter 3	Resistive index of cerebral arteries in very preterm infants: values throughout stay in the Neonatal Intensive Care Unit and impact of patent ductus arteriosus	43
Chapter 4	Calibrating Doppler imaging of preterm intracerebral circulation using a microvessel flow phantom	63
Part II	Neonatal focal brain lesions	79
Chapter 5	Risk factors, clinical presentation and neuroimaging findings of neonatal perforator stroke	81
Chapter 6	The clinical presentation of preterm cerebellar hemorrhage	97
Chapter 7	Serial cranial ultrasonography or early MRI for detecting preterm brain injury?	109
Chapter 8	Neurodevelopmental outcome following neonatal perforator stroke	127
Chapter 9	General discussion	145
Chapter 10	Summary	159
Part III	Appendices	171
	About the author	173
	List of publications	175
	PhD portfolio	177
	Dankwoord	179

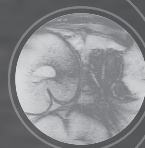
PART I

Neonatal cerebral blood flow – use of advanced Doppler cranial ultrasound



CHAPTER 1

General introduction



Introduction

Preterm birth is defined by the World Health Organization as birth before 37 completed weeks of gestation and is subdivided into extreme preterm (< 28 weeks of gestation), very preterm (28 to < 32 weeks of gestation) and late preterm birth (32 to < 37 weeks of gestation).¹ Worldwide, an estimated 14.9 million neonates were born preterm in 2010, 11.1% of all live births.² Preterm birth rates are increasing in most countries with reliable trend data.^{2,3} In the Netherlands the reported incidence of preterm birth is 7.4%, the incidence of very preterm birth is 1.4%.⁴ The associated morbidity of preterm birth may continue throughout life, with long term cognitive, motoric, and behavioral problems resulting in major socio-economic burdens.

Preterm infants are born in a critical period of brain development and maturation, in which the brain is extremely vulnerable. Cerebral vascular anatomy and physiology during preterm brain development are key factors in the sensitivity of the preterm brain to extra-uterine life.⁵ Ischemia and inflammation are main initiating factors in cerebral white matter injury. Ischemia and inflammation often co-exist and potentiate each other, leading to increased excitotoxicity and free radical attack.^{6,7} In the end, preterm brain injury seems to be an intricate combination of primary destructive disease and secondary trophic and maturational disturbances.⁸ Injury to the preterm brain may result in long term cognitive, motoric, and behavioral problems.

The brain of critically ill term born infants is also at risk for damage. However, brain injury in these term infants differs from that in preterm infants. Important developmental changes in the last trimester of pregnancy are: involution of the germinal matrix, maturation of a pressure-passive brain perfusion, and sensitivity of axons and oligodendrocytes to hypoxic injury.⁹ Perinatal brain injury in the term infant affects approximately 1 in 1000 live born neonates, and is most often a consequence of intracranial hemorrhage, cerebral infarction and hypoxic-ischemic injury.¹⁰

Neuroimaging of the neonatal brain

In order to detect acquired brain injury and congenital anomalies during the neonatal period, neuroimaging of infants admitted to the neonatal intensive care unit (NICU) has become part of routine clinical care. Neonatal neuroimaging has seen some major advances over the past decades. Since the early 1970's computed tomography (CT) was used for visualization of neonatal brain injury.¹¹⁻¹⁴ This provided insight into the correlation of brain lesions and outcome. Nowadays CT is hardly used anymore for neonatal brain injury because of exposure to a substantial radiation dosage and the availability of safer alternatives. For most indications for neonatal brain imaging, CT does not have

additional added value over current alternative neuroimaging modalities. Currently, cranial ultrasound (CUS) and magnetic resonance imaging (MRI) are used for imaging of the brain in critically ill neonates.

Cranial ultrasound (CUS)

Since its introduction in the late 1970's^{15, 16} CUS is widely used for neuroimaging in the neonatal period. In many NICU's CUS is currently used for routine brain imaging and has become indispensable in the care for critically ill neonates. This technique is relatively inexpensive, does not require sedation, is radiation-free, safe, can be performed at bedside –even when a patient is clinically unstable– and can be repeated as often as possible.¹⁷ In the neonate, the fontanels are still open and can be used as an acoustic window to visualize the brain. High frequency sound waves are sent from a transducer, propagate through the brain, and are reflected at surfaces between tissues of different density. The reflected echoes return to the transducer and are processed, leading to an image of the brain presented on a screen. Anatomical structures and lesions can be distinguished by differences in echogenicity. Typically, CUS is performed through the anterior fontanel and images are acquired in coronal and sagittal planes, which allows good visualization of most supratentorial structures.

Over time, imaging quality of CUS has improved considerably, with advancing techniques leading amongst others to better resolution, transducers, image processing and – display. Settings of the ultrasound machine can be optimized for neonatal brain imaging in order to provide the best possible visualization of important brain structures. However, evaluation of infratentorial structures through the anterior fontanel remains challenging, because these are located far away from the transducer and the highly echogenic tentorium impedes their assessment. Alternative acoustic windows, such as the mastoid, lateral and posterior fontanel, can be used to enable more detailed visualization of the posterior fossa, brain stem and occipital region, and thus detection of brain lesions in these regions. Unfortunately, only in few NICUs these supplemental acoustic windows are routinely used.^{18–21}

CUS also provides the possibility to use Doppler techniques to screen intracranial arteries and veins for patency. Flow velocities in cerebral vessels can also be obtained. Some manufacturers now provide hardware which enables visualization of vessels with flow around 2 cm/sec.²² This allows visualization of smaller cerebral arteries and veins, such as perforating arteries and subependymal veins tributary to the thalamostriate veins.

With the use of color Doppler techniques, different pathologies can be detected, such as vascular anomalies and sinovenous thrombosis. However, sometimes abnormalities in flow can be noted which are not directly related to pathology. Therefore, knowledge

of normal flow and principles of color Doppler techniques are required. These aspects are illustrated in the following clinical case.

Case

In a preterm neonate, born at 30 weeks of gestation, routine CUS was performed on the third day of life. While scanning through the anterior fontanel with a 8.5 MHz convex probe, obvious left dominance of the left transverse sinus was noted (see Figure 1A). Previous work showed that the right transverse sinus is dominant in the majority of neonates.²³ Thus, we evaluated flow in the right transverse and sigmoid sinus through the right mastoid fontanel with a high frequency linear probe (13 MHz). Initially, we visualized low flow through these sinuses, with reversed flow in the sigmoid sinus (see Figure 1B). Because the patient was in a prone position with extreme rotation of the neck to the right, we decided to change his position to lying on his left side with the neck in a more neutral position. Immediately repeating the imaging in this position, normal flow through the transverse and sigmoid sinus was visualized (Figure 1C).

We hypothesize that the reversed flow initially observed in the sigmoid sinus (figure 1B) was a result of obstructed venous outflow because of relative jugular venous occlusion due to extreme rotation of the neck. An increase in venous pressure as a result of jugular venous occlusion has been described before.²⁴

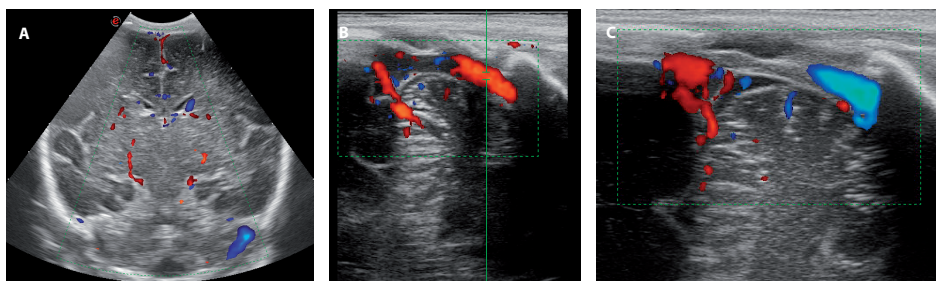


Figure 1. Doppler CUS imaging of transverse and sigmoid sinuses

MRI

MRI involves nonionizing radiation inside a strong magnetic field, using the properties of protons in their local chemical environment and their behavior to this magnetic field to obtain images. This neuroimaging technique is increasingly used for brain imaging of critically ill neonates and provides unique anatomical detail of neonatal brain tissue.²⁵ However, MRI is expensive and in most hospitals availability is limited. Also, sedation may be needed for adequate imaging, it requires transportation, and critically ill neonates may not be clinically stable enough to undergo MRI.

Conventional structural MRI imaging, such as T1- and T2-weighted imaging, is well suited to assess brain development and presence of brain lesions and relate these to neurodevelopmental deficits.^{26–28}

In recent years, quantitative MRI techniques have evolved, providing objective and reproducible measurements, which have improved understanding of brain development and cerebral pathology.²⁹ Examples of advanced MRI techniques are diffusion weighted imaging, diffusion tensor imaging, MR spectroscopy, susceptibility weighted imaging and functional MRI.

A selection of practical, logistical and technique-associated differences between CUS and MRI for neuroimaging in the NICU are presented in Table 1.

Table 1. Practical, logistical and technique-associated differences between CUS and MRI in the NICU

	CUS	MRI
Duration	Maximum 15 minutes for extensive (Doppler) CUS	45 minutes plus time necessary for transport of patient to MRI
Cost*	€ 96	€ 229
Resolution	± 100 microns (15 Hz Probe)	Voxel size commonly 1 to 4 mm3
Noise disturbance	Possibly some when scanning through mastoid fontanel, due to the mechanism of auditory response to pulses of radiofrequency energy. ³⁰	Sound pressure level for 1.5 T MRI exam is usually 81–117 dB. ^{31–33} Prevention: use of hearing protection (e.g. ear muffs, acoustic hood noise dampener ³¹) to reduce patient exposure to acoustic noise, 1.5 T NICU MRI scanner is quieter than conventional 1.5 T MRI scanners for identical imaging sequences and acquisition parameters. ³³
Imaging-associated safety	<ul style="list-style-type: none"> - Can be stopped immediately in case of cardiorespiratory instability. - Thermal and mechanical indices < 1 are generally accepted as safe.³⁴ 	<ul style="list-style-type: none"> - Minor adverse events during or after MRI scan are common (50% of preterm infants scanned at 30 weeks postmenstrual age)³⁵ - “Non-significant risk” in neonates at static magnetic field strengths below 4 T. Specific absorption rate limits that are considered safe: < 4 W/kg averaged over 15 minutes in the whole body and < 3.2 W/kg averaged over 10 minutes in the head.^{36, 37}
Detection of brain injury in preterm infants	More sensitive for detection of perforator stroke and cerebral sinovenous thrombosis ³⁸ and can be repeated as often as possible to evaluate evolution of brain injury.	More sensitive for detection of diffuse non-cystic white matter injury, small posterior fossa abnormalities. ³⁸

*According to price rates of the local Radiology Department in April 2015. Prices differ amongst hospitals.

Focal brain injury in neonates

In general, the two most commonly recognized types of brain injury in preterm born infants are (1) germinal matrix and intraventricular hemorrhage and (2) periventricular

white matter injury. Traditionally use of CUS in NICU's was mainly focused on detection of these types of brain injury. With improved techniques – leading amongst others to high resolution –, use of additional acoustic windows, and use of Doppler techniques other lesion patterns are recognized; e.g. cerebellar lesions, perforator strokes, and sinovenous thrombosis. In the following section these three types of brain injuries will be briefly discussed and examples of these lesions diagnosed with CUS imaging will be provided.

Cerebellar lesions

Cerebellar growth is extraordinarily rapid from 24 to 40 weeks of gestation, exceeding growth elsewhere in the brain. In vivo assessment by 3-dimensional volumetric ultrasound shows a 5-fold increase in cerebellar volume during this period.³⁹ Postmortem studies show exponential growth in foliation in this period, and as a consequence the cerebellar cortex surface area increases more than 30-fold between 24 and 40 weeks of gestation.^{40, 41} Because of its rapid growth and development in this period, the cerebellum is vulnerable to the multiple insults to which the preterm infant is exposed.⁴¹

Cerebellar hemorrhage in preterm infants was first described as a postmortem finding in case reports and in autopsy studies.^{42, 43} Because of increased use of CUS imaging through the mastoid fontanel and more widespread use of MRI, cerebellar injury is now considered an important complication of preterm birth and is also increasingly diagnosed in critically ill full-term infants.^{41, 44–48} Reported incidence of cerebellar hemorrhage in preterm infants ranges from 2.3% to 19%.^{45, 46, 48, 49} Incidence seems to depend on the degree of prematurity; in the largest reported study, the incidence was as high as 19.4% in infants with a birth weight < 750 grams, and 2% in those of 751 to 1499 grams at birth.⁴⁶

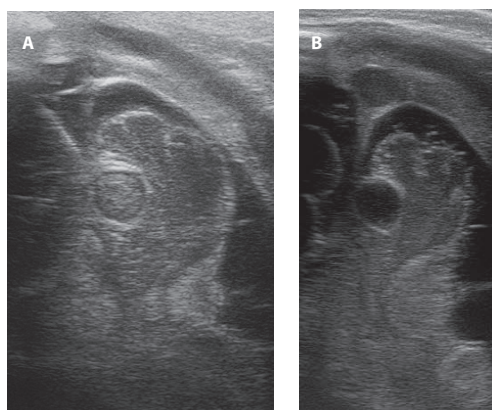


Figure 2. Imaging through the left mastoid fontanel

Images of a cerebellar abscess in an infant born at 25 weeks of gestation. A) At two weeks of age she developed ongoing *S. Aureus* sepsis and CUS 5 days later revealed a round lesion in the left cerebellar hemisphere, compatible with abscess formation. B) After prolonged high dose intravenous flucloxacillin without surgical intervention, a residual cavity was seen.

Cerebellar injury in preterm infants is associated with neurodevelopmental sequelae.^{50–52} Cerebellar hemorrhage may play a role in cognitive, learning and behavioral disorders known to affect survivors of preterm birth.⁵⁰

Figure 2 provides an example of a cerebellar lesion first diagnosed with CUS.

Perforator strokes

Improved neuroimaging techniques have greatly improved understanding and detection of neonatal stroke.⁵³ The incidence of neonatal stroke is thought to be as high as the annual incidence of stroke in adults.⁵⁴ In term newborns reported incidence of stroke ranges from 1 in 2300 to 1 in 5900.^{53–56} An even higher incidence of 7 in 1000 admissions was reported in a cohort of preterm infants, but this might also be a reflection of routine use of CUS in preterm newborns.⁵⁷ In the classification of perinatal stroke, venous and arterial mechanisms of occlusion can be distinguished.^{58–60} In case of arterial stroke, one or more of the main cerebral arteries and/or its perforator branches can be involved.⁶¹ Main branch involvement leads to cortical or pial stroke, while involvement of perforator branches leads to so-called perforator stroke.⁶¹ Neonatal perforator strokes are probably still under-recognized and little is known about incidence, clinical presentation, risk factors and implications for neurodevelopmental outcome.

In figure 3 CUS imaging of a term infant with a perforator stroke is presented.

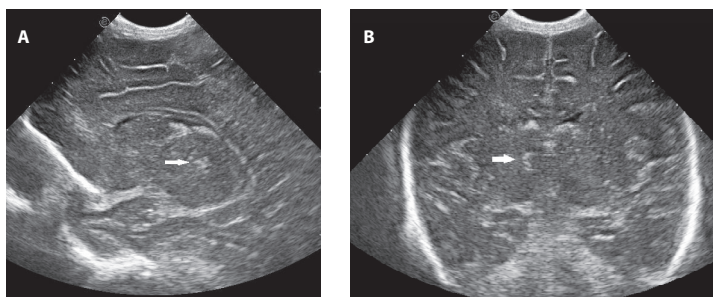


Figure 3. Perforator stroke

Term born infant with perinatal asphyxia due to hemorrhagic shock. CUS revealed a small perforator stroke in the right thalamus (indicated by arrow), as seen on the parasagittal (A) and coronal (B) images.

Sinovenous thrombosis

Neonatal cerebral sinovenous thrombosis (CSVT) has a lower reported incidence than that of perinatal arterial ischemic stroke. In a retrospective Dutch cohort study, an incidence of 1–12 per 100000 neonates was suggested.⁶² In a study by the Canadian Pediatric Ischemic Stroke Study Group an incidence of 0.67 per 100000 children per year was found and 43% of the included children were neonates.⁶³ These numbers are probably an underestimation, as only neonates with clinical symptoms suggestive of CSVT

are screened. Furthermore, clinical symptoms are thought to be non-specific or lacking and radiological diagnosis may be challenging, depending on the imaging modality and radiological expertise. In a recent prospective study in our NICU, an incidence of 4.4% was found with the use of systematic dedicated serial Doppler CUS in a cohort of 249 preterm infants with a gestational age of < 29 weeks.²¹

In preterm neonates, CSVT is associated with extensive white matter damage.⁶⁴ CSVT may lead to venous outflow obstruction, which may result in increased venous pressure, leading to hemorrhagic infarction and thus to parenchymal damage.⁶⁵ In figure 4 we present CUS imaging of a preterm infant with extensive sinovenous thrombosis and widespread white matter injury.

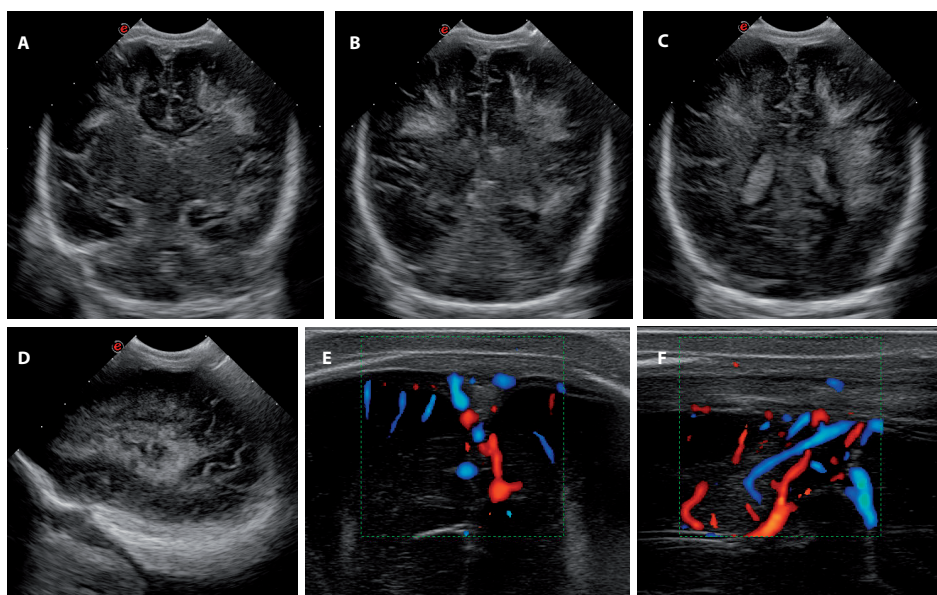


Figure 4. Sinovenous thrombosis

Infant born at 32 weeks of gestation, who presented with convulsions at the age of 1 week. CUS showed extensive bilateral white matter injury (A-D). Doppler CUS showed sinovenous thrombosis. Coronal (E) and midsagittal images (F) with a high frequency linear probe through the anterior fontanel show near-total occlusion of the superior sagittal sinus. The findings were confirmed with MRI.

Follow-up studies report neurodevelopmental sequelae in 48 to 79% of survivors with neonatal sinovenous thrombosis. These deficits include motor impairment, cognitive and behavioral concerns, visual defects, and epilepsy.^{62, 66, 67} Infants with associated thalamic injury have an increased risk of developing postneonatal epilepsy and electrical status epilepticus in slow wave sleep⁶⁸, possibly as a result of alterations in thalamocortical networks.⁶⁹

Aims and outline of this thesis

The general aim of this thesis was to provide more insight into neonatal cerebellar hemorrhage, perforator stroke and cerebral blood flow, with dedicated use of Doppler CUS in the NICU. In the first part of the thesis we focus on cerebral blood flow and use of advanced Doppler CUS.

In **chapter 2** we describe our approach of CUS imaging in the neonate, using additional acoustic windows and Doppler techniques. Using Doppler techniques, we studied resistive index values in seven intracerebral arteries in a cohort of very preterm infants in **chapter 3**. With current techniques and adequate ultrasound settings, it is possible to visualize intracranial vessels with a diameter of about 200 micron and flow around 2 cm/sec. Therefore visualization of preterm cerebral microcirculation could be feasible with the use of CUS Doppler. To assess whether visualization and velocity measurements of preterm cerebral perfusion using Doppler techniques are accurate, we describe an in vitro experiment using a microvessel flow phantom in **chapter 4**.

The second part of this thesis focuses on focal brain lesions in critically ill term and preterm neonates, which are probably still under-recognized: cerebellar hemorrhage and perforator stroke. Furthermore, the clinical feasibility and the ability of dedicated serial CUS and MRI to detect various types of preterm brain injury are compared.

Chapter 5 describes the clinical presentation, risk factors and imaging findings of neonatal perforator stroke, followed by the clinical presentation of preterm cerebellar hemorrhage in **chapter 6**. The majority of the brain lesions described in chapter 6 and 7 were initially diagnosed using serial CUS. However, CUS may be considered inferior to MRI for detection of brain lesions. In **chapter 7** detection ability and clinical feasibility of serial dedicated CUS and early MRI are compared in a large prospective cohort study involving very preterm infants. With the use of advanced imaging techniques small lesions such as perforator strokes and small cerebellar hemorrhages can be detected, which raises the question what neurodevelopmental sequelae can be expected. **Chapter 8** focuses on outcome of neonatal perforator strokes in childhood.

In **chapter 9** the main findings and conclusions of this thesis are discussed, as well as suggestions for future research.

References

1. WHO. WHO: Recommended definitions, terminology and format for statistical tables related to perinatal period and use of a new certificate for cause of perinatal deaths. *Acta Obstetricia Et Gynecologica Scandinavica*. 1977;56:247-253.
2. Blencowe H, Cousens S, Oestergaard MZ, Chou D, Moller AB, Narwal R, et al. National, regional, and worldwide estimates of preterm birth rates in the year 2010 with time trends since 1990 for selected countries: A systematic analysis and implications. *Lancet*. 2012;379:2162-2172.
3. Blencowe H CS, Chou D, Oestergaard M, Say L, Moller AB, Kinney M, Lawn J; Born Too Soon Pre-term Birth Action Group. Born too soon: The global epidemiology of 15 million preterm births. *Reprod Health* 2013 10:S2.
4. Nederland SPR. *Grote lijnen 1999-2012* Utrecht Stichting Perinatale Registratie Nederland 2013
5. Liem KD, Greisen G. Monitoring of cerebral haemodynamics in newborn infants. *Early Human Development*. 2010;86:155-158.
6. Khwaja O, Volpe JJ. Pathogenesis of cerebral white matter injury of prematurity. *Archives of Disease in Childhood-Fetal and Neonatal Edition*. 2008;93:F153-F161.
7. Deng WB. Neurobiology of injury to the developing brain. *Nature Reviews Neurology*. 2010;6:328-336.
8. Volpe JJ. Brain injury in premature infants: A complex amalgam of destructive and developmental disturbances. *Lancet Neurology*. 2009;8:110-124.
9. Volpe JJ. Neuhauser,edward b. Lecture - current concepts of brain injury in the premature-infant. *American Journal of Roentgenology*. 1989;153:243-251.
10. Volpe JJ. Hypoxic-ischemic encephalopathy *Neurology of the newborn* Philadelphia WB Saunders Company 2001
11. Krishnamoorthy KS, Fernandez RA, Momose KJ, Delong GR, Moylan FMB, Todres ID, et al. Evaluation of neonatal intracranial hemorrhage by computerized tomography. *Pediatrics*. 1977;59:165-172.
12. Burstein J, Papile L, Burstein R. Subependymal germinal matrix and intraventricular hemorrhage in premature-infants - diagnosis by ct. *American Journal of Roentgenology*. 1977;128:971-976.
13. Papile LA, Burstein J, Burstein R, Koffler H. Incidence and evolution of subependymal and intra-ventricular hemorrhage - study of infants with birth weights less than 1,500 gm. *Journal of Pediatrics*. 1978;92:529-534.
14. Kirks DR, Maravilla KR, Maravilla AM. Craniocerebral computed tomography in neonate. *Computerized Tomography*. 1978;2:207-220.
15. Pape KE, Cusick G, Houang MTW, Reynolds EOR, Blackwell RJ, Sherwood A, et al. Ultrasound detection of brain-damage in preterm infants. *Lancet*. 1979;1:1261-1264.
16. Dewbury KC, Aluwihare APR. Anterior fontanelle as an ultrasound window for study of the brain - preliminary-report. *British Journal of Radiology*. 1980;53:81-84.
17. Steggerda SJ, Leijser LM, Walther FJ, van Wezel-Meijler G. Neonatal cranial ultrasonography: How to optimize its performance. *Early Human Development*. 2009;85:93-99.
18. Enriquez G, Correa F, Aso C, Carreno JC, Gonzalez R, Padilla NF, et al. Mastoid fontanelle approach for sonographic imaging of the neonatal brain. *Pediatric Radiology*. 2006;36:532-540.
19. Di Salvo DN. A new view of the neonatal brain: Clinical utility of supplemental neurologic us imaging windows. *Radiographics*. 2001;21:943-955.
20. Luna JA, Goldstein RB. Sonographic visualization of neonatal posterior fossa abnormalities through the posterolateral fontanelle. *AJR Am J Roentgenol*. 2000;174:561-567.

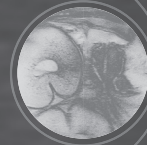
21. Raets MMA, Sol JJ, Govaert P, Lequin MH, Reiss IKM, Kroon AA, et al. Serial cranial us for detection of cerebral sinovenous thrombosis in preterm infants. *Radiology*. 2013;269:879-886.
22. Raets MMA GP, Goos TG, Reiss IKM, de Jonge RCJ, Dudink J. Preterm cerebral microcirculation assessed with colour doppler: A pilot study. *J Pediatr Neuroradiol*. 2014;3:155-160.
23. Widjaja E, Shroff M, Blaser S, Laughlin S, Raybaud C. 2d time-of-flight mr venography in neonates: Anatomy and pitfalls. *AJNR Am J Neuroradiol*. 2006;27:1913-1918.
24. Cowan F, Eriksen M, Thoresen M. An evaluation of the plethysmographic method of measuring cranial blood flow in the new-born infant. *J Physiol*. 1983;335:41-50.
25. Counsell SJ, Tranter SL, Rutherford MA. Magnetic resonance imaging of brain injury in the high-risk term infant. *Seminars in Perinatology*. 2010;34:67-78.
26. Hintz SR, Barnes PD, Bulas D, Slovis TL, Finer NN, Wrage LA, et al. Neuroimaging and neurodevelopmental outcome in extremely preterm infants. *Pediatrics*. 2015;135:E32-E42.
27. Woodward LJ, Anderson PJ, Austin NC, Howard K, Inder TE. Neonatal mri to predict neurodevelopmental outcomes in preterm infants. *New England Journal of Medicine*. 2006;355:685-694.
28. Woodward LJ, Clark CAC, Bora S, Inder TE. Neonatal white matter abnormalities an important predictor of neurocognitive outcome for very preterm children. *Plos One*. 2012;7
29. Counsell SJ, Rutherford MA, Cowan FM, Edwards AD. Magnetic resonance imaging of preterm brain injury. *Archives of Disease in Childhood*. 2003;88:269-274.
30. Ecury-Goossen GM, Camfferman FA, Leijser LM, Govaert P, Dudink J. State of the art cranial ultrasound imaging in neonates. *J Vis Exp*. 2015:e52238.
31. Nordell A, Lundh M, Horsch S, Hallberg B, Aden U, Nordell B, et al. The acoustic hood: A patient-independent device improving acoustic noise protection during neonatal magnetic resonance imaging. *Acta Paediatrica*. 2009;98:1278-1283.
32. Price DL, De Wilde JP, Papadaki AM, Curran JS, Kitney RI. Investigation of acoustic noise on 15 mri scanners from 0.2 t to 3 t. *J Magn Reson Imaging*. 2001;13:288-293.
33. Tkach JA, Li Y, Pratt RG, Baroch KA, Loew W, Daniels BR, et al. Characterization of acoustic noise in a neonatal intensive care unit mri system. *Pediatric Radiology*. 2014;44:1011-1019.
34. Houston LE, Odibo AO, Macones GA. The safety of obstetrical ultrasound: A review. *Prenat Diagn*. 2009;29:1204-1212.
35. Plaisier A, Raets MM, van der Starre C, Feijen-Roon M, Govaert P, Lequin MH, et al. Safety of routine early mri in preterm infants. *Pediatric Radiology*. 2012;42:1205-1211.
36. US Department of Health and Human Services FaDA, Center for Devices and Radiological Health. Criteria for significant risk investigations of magnetic resonance diagnostic devices—guidance for industry and food and drug administration staff 2014
37. Tocchio S, Kline-Fath B, Kanal E, Schmithorst VJ, Panigrahy A. Mri evaluation and safety in the developing brain. *Seminars in Perinatology*. 2015;39:73-104.
38. Plaisier A, Raets MM, Ecury-Goossen GM, Govaert P, Feijen-Roon M, Reiss IK, et al. Serial cranial ultrasonography or early mri for detecting preterm brain injury? *Arch Dis Child Fetal Neonatal Ed*. 2015;100:F293-300.
39. Chang CH, Chang FM, Yu CH, Ko HC, Chen HY. Assessment of fetal cerebellar volume using three-dimensional ultrasound. *Ultrasound in Medicine and Biology*. 2000;26:981-988.
40. Dobbing J, Sands J. Quantitative growth and development of human brain. *Archives of Disease in Childhood*. 1973;757-767.
41. Volpe JJ. Cerebellum of the premature infant: Rapidly developing, vulnerable, clinically important. *Journal of Child Neurology*. 2009;24:1085-1104.

42. Donat JF, Okazaki H, Kleinberg F. Cerebellar hemorrhages in newborn-infants. *American Journal of Diseases of Children*. 1979;133:441-441.
43. Schreiber MS. Posterior fossa (cerebellar) haematoma in the new-born. *Med J Aust*. 1963;2:713-715.
44. Miall LS, Cornette LG, Tanner SF, Arthur RJ, Levene MI. Posterior fossa abnormalities seen on magnetic resonance brain imaging in a cohort of newborn infants. *J Perinatol*. 2003;23:396-403.
45. Steggerda SJ, Leijser LM, Wiggers-de Bruine FT, van der Grond J, Walther FJ, van Wezel-Meijler G. Cerebellar injury in preterm infants: Incidence and findings on us and mr images. *Radiology*. 2009;252:190-199.
46. Limperopoulos C, Benson CB, Bassan H, Disalvo DN, Kinnamon DD, Moore M, et al. Cerebellar hemorrhage in the preterm infant: Ultrasonographic findings and risk factors. *Pediatrics*. 2005;116:717-724.
47. Limperopoulos C, Robertson RL, Sullivan NR, Bassan H, du Plessis AJ. Cerebellar injury in term infants: Clinical characteristics, magnetic resonance imaging findings, and outcome. *Pediatric Neurology*. 2009;41:1-8.
48. Merill J.D. PRE, Fell S.C., Barkovich A.J., Goldstein R.B. A new pattern of cerebellar hemorrhages in preterm infants. . *Pediatrics* 1998;102 E62
49. Muller H, Beedgen B, Schenk JP, Troger J, Linderkamp O. Intracerebellar hemorrhage in premature infants: Sonographic detection and outcome. *J Perinat Med*. 2007;35:67-70.
50. Limperopoulos C, Bassan H, Gauvreau K, Robertson RL, Sullivan NR, Benson CB, et al. Does cerebellar injury in premature infants contribute to the high prevalence of long-term cognitive, learning, and behavioral disability in survivors? *Pediatrics*. 2007;120:584-593.
51. Bodensteiner JB, Johnsen SD. Cerebellar injury in the extremely premature infant: Newly recognized but relatively common outcome. *Journal of Child Neurology*. 2005;20:139-142.
52. Johnsen SD, Bodensteiner JB, Lotze TE. Frequency and nature of cerebellar injury in the extremely premature survivor with cerebral palsy. *Journal of Child Neurology*. 2005;20:60-64.
53. Nelson KB, Lynch JK. Stroke in newborn infants. *Lancet Neurology*. 2004;3:150-158.
54. Lee J, Croen LA, Backstrand KH, Yoshida CK, Henning LH, Lindan C, et al. Maternal and infant characteristics associated with perinatal arterial stroke in the infant. *Jama-Journal of the American Medical Association*. 2005;293:723-729.
55. Chabrier S, Husson B, Dinomais M, Landrieu P, Tich SNT. New insights (and new interrogations) in perinatal arterial ischemic stroke. *Thrombosis Research*. 2011;127:13-22.
56. Estan J, Hope P. Unilateral neonatal cerebral infarction in full term infants. *Archives of Disease in Childhood*. 1997;76:F88-F93.
57. Benders MJNL, Groenendaal F, De Vries LS. Preterm arterial ischemic stroke. *Seminars in Fetal & Neonatal Medicine*. 2009;14:272-277.
58. Raju TNK, Nelson KB, Ferriero D, Lynch JK. Ischemic perinatal stroke: Summary of a workshop sponsored by the national institute of child health and human development and the national institute of neurological disorders and stroke. *Pediatrics*. 2007;120:609-616.
59. Kirton A, deVeber G. Advances in perinatal ischemic stroke. *Pediatric Neurology*. 2009;40:205-214.
60. Kirton A, Deveber G, Pontigon AM, Macgregor D, Shroff M. Presumed perinatal ischemic stroke: Vascular classification predicts outcomes. *Annals of Neurology*. 2008;63:436-443.
61. Abels L, Lequin M, Govaert P. Sonographic templates of newborn perforator stroke. *Pediatric Radiology*. 2006;36:663-669.
62. Berfelo FJ, Kersbergen KJ, van Ommen CH, Govaert P, van Straaten HLM, Poll-The BT, et al. Neonatal cerebral sinovenous thrombosis from symptom to outcome. *Stroke*. 2010;41:1382-1388.

63. deVeber G, Andrew M, Adams C, Bjornson B, Booth F, Buckley DJ, et al. Cerebral sinovenous thrombosis in children. *New England Journal of Medicine*. 2001;345:417-423.
64. Kersbergen KJ, Groenendaal F, Benders MJNL, van Straaten HLM, Niwa T, Nieuvelstein RAJ, et al. The spectrum of associated brain lesions in cerebral sinovenous thrombosis: Relation to gestational age and outcome. *Archives of Disease in Childhood-Fetal and Neonatal Edition*. 2011;96:F404-F409.
65. van der Aa NE, Benders MJNL, Groenendaal F, de Vries LS. Neonatal stroke: A review of the current evidence on epidemiology, pathogenesis, diagnostics and therapeutic options. *Acta Paediatrica*. 2014;103:356-364.
66. Fitzgerald KC, Williams LS, Garg BP, Carvalho KS, Golomb MR. Cerebral sinovenous thrombosis in the neonate. *Archives of Neurology*. 2006;63:405-409.
67. Moharir MD, Shroff M, Pontigon AM, Askalan R, Yau I, MacGregor D, et al. A prospective outcome study of neonatal cerebral sinovenous thrombosis. *Journal of Child Neurology*. 2011;26:1137-1144.
68. Kersbergen KJ, de Vries LS, Leijten FS, Braun KP, Nieuvelstein RA, Groenendaal F, et al. Neonatal thalamic hemorrhage is strongly associated with electrical status epilepticus in slow wave sleep. *Epilepsia*. 2013;54:733-740.
69. Blumenfeld H. From molecules to networks: Cortical/subcortical interactions in the pathophysiology of idiopathic generalized epilepsy. *Epilepsia*. 2003;44 Suppl 2:7-15.

CHAPTER 2

State of the art cranial ultrasound imaging in neonates



G.M. Ecury-Goossen, F.A. Camfferman, L.M. Leijser, P. Govaert, J. Dudink.

J Vis Exp. 2015;(96):e52238.

Abstract

Cranial ultrasound (CUS) is a reputable tool for brain imaging in critically ill neonates. It is safe, relatively cheap and easy to use, even when a patient is unstable. In addition it is radiation-free and allows serial imaging. CUS possibilities have steadily expanded. However, in many neonatal intensive care units, these possibilities are not optimally used. We present a comprehensive approach for neonatal CUS, focusing on optimal settings, different probes, multiple acoustic windows and Doppler techniques. This approach is suited for both routine clinical practice and research purposes. In a live demonstration, we show how this technique is performed in the neonatal intensive care unit. Using optimal settings and probes allows for better imaging quality and improves the diagnostic value of CUS in experienced hands. Traditionally, images are obtained through the anterior fontanel. Use of supplemental acoustic windows (lambdoid, mastoid, and lateral fontanel) improves detection of brain injury. Adding Doppler studies allows screening of patency of large intracranial arteries and veins. Flow velocities and indices can be obtained. Doppler CUS offers the possibility of detecting cerebral sinovenous thrombosis at an early stage, creating a window for therapeutic intervention prior to thrombosis-induced tissue damage. Equipment, data storage and safety aspects are also addressed.

Introduction

Since its clinical introduction in the late 1970's cranial ultrasound (CUS) has been widely used for detecting congenital anomalies and acquired brain lesions during the neonatal period. In many neonatal intensive care units (NICUs), CUS has become indispensable in the care for critically ill neonates. Major advantages are its relatively low cost and the fact that it can be performed at bedside, even when a patient is unstable. In addition it is radiation-free and allows for serial imaging. Another technique often used for neuroimaging in critically ill neonates is magnetic resonance imaging (MRI). MRI provides excellent image quality, but its clinical use in NICU's is currently limited because of logistic and safety issues.¹

Over time, quality of CUS has drastically improved, with advancing technique leading to higher resolution, faster image processing and digital display and back-up. Important brain structures can be adequately visualized using optimal settings. Traditionally, images are obtained through the anterior fontanel. This approach is less suitable for evaluation of infratentorial structures because they are located far away from the transducer and the highly echoic tentorium impedes their assessment. Use of high-frequency linear transducers through alternative acoustic windows and adapted settings also provides access to these brain regions. Examples of these supplemental acoustic windows are the lambdoid (posterior), mastoid and lateral (temporal) fontanels. So far, however, only few NICUs use these additional acoustic windows routinely.²⁻⁵ Doppler techniques can be used for screening patency of intracranial vessels. Flow velocities and indices in cerebral arteries can also be obtained. Some manufacturers now provide hardware to visualize flow around 2 cm/sec (Raets, *et al.*, unpublished data). Small vessels are well displayed: medullary trunks and channels, subependymal veins tributary to the thalamostriate veins, and perforator arteries.

We present our approach of neonatal CUS, focusing on the use of different transducers, multiple acoustic windows and Doppler techniques. Neonatologists and radiologists use this approach in daily clinical practice but is also suitable for research purposes. In the practical part of the video we demonstrate bedside use in the NICU.

Protocol

This protocol follows the guidelines of the local human research ethics committee.

1. General considerations

Note: General considerations regarding equipment, data storage and safety are addressed in the Discussion.

- 1.1) Obtain images using a high-resolution, real-time, mobile 2D ultrasound machine with multiple transducers with a band of frequencies (see Discussion). Typically, obtain images of good quality using a probe with a frequency of 7.5 to 8.5 MHz.

2. Preparation of the CUS exam

- 2.1) Schedule the CUS examination so that it does not coincide with other procedures such as blood sampling.
- 2.2) Ensure that a health care worker or a parent is available to support and/or comfort the neonate during the examination, using strategies such as those according to the principles of Newborn Individualized Developmental Care and Assessment Program.⁶

3. Examination through anterior fontanel

- 3.1) Install the ultrasound machine along the incubator or cot.
- 3.2) Apply transducer gel to the probe to ensure good contact between the probe and the skin. Consider warming the gel before use.
- 3.3) Start imaging through the anterior fontanel with a convex probe in B-mode. Place the probe in the middle of the fontanel with the marker on the probe turned to the right side of the neonate. The left side of the brain will then be displayed on the right side of the monitor.

Note: Imaging through the anterior fontanel can be performed with the neonate in any position.³ For research purposes it may be necessary to strive for a standard head position.

- 3.3.1) Record images in at least five coronal and five sagittal planes. In the first image adjust depth, gain and time gain compensation settings to produce an image filling the sector, containing the cranial contours, avoiding too bright or dark images and aiming for an equilibrium between reflections from nearby and deeper structures.

3.3.2) *Coronal planes*

Note: Try to obtain perfectly symmetrical images. When lesions near the frontal lobe convexity are suspected, consider recording specific oblique coronal sections, so that one hemisphere is displayed in better detail (Figure 1).

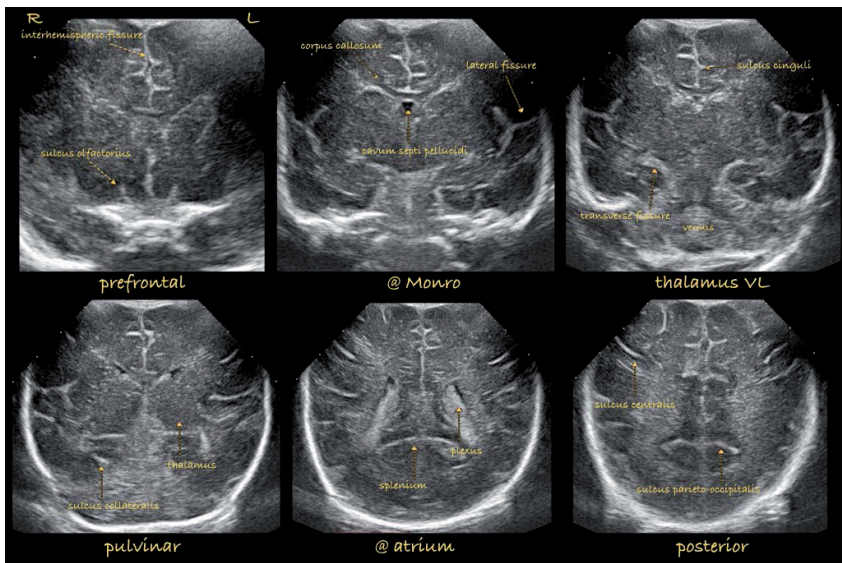


Figure 1. Coronal sections

Imaging through anterior fontanel at standard coronal planes.

Abbreviations:

L = left

R = right

VL = ventrolateral nuclei of thalamus

- 3.3.2.1) For the coronal prefrontal image, angle the probe forwards to visualize the frontal lobes, anterior to the frontal horns of the lateral ventricles at the level of the olfactory sulci.
- 3.3.2.2) For the coronal image at the level of Monro, angle the probe to visualize the coronal section anterior to the tela choroidea to depict the frontal horns of the

lateral ventricles, cavum septi pellucidi, corpus callosum, sulcus cinguli. Note the echogenicity of parts of the basal ganglia.

- 3.3.2.3) For the coronal image at the level of thalamus, angle the probe backwards to identify the lateral fissures, tela choroidea in the roof of the third ventricle and temporal lobes. Note the echogenicity of the thalamus (especially ventrolateral nuclei) in relation to the basal ganglia. Note that network injury in pulvinar may be visualized in an extra coronal section just in front of the atria.
- 3.3.2.4) For the coronal image at the level of atria, visualize the lateral ventricles at the level of the choroid plexus. Identify the temporal lobes and cerebellar hemispheres. Note the echogenicity of periventricular white matter compared to choroid plexus. Compare optic radiation with the normal hyperechoic areas above and lateral to the atria in preterm neonates.
- 3.3.2.5) For the coronal parieto-occipital image, angle the probe backwards to the level of the parieto-occipital sulcus to identify the parietal and occipital lobes.

3.3.3) *Sagittal planes*

- 3.3.3.1) Rotate the probe 90° with the marker on the probe facing towards the neonate's face. The anterior part of the brain will be displayed on the left side of the monitor. Record images at the level of the following structures (Figure 2).
- 3.3.3.2) For the midsagittal image, visualize the corpus callosum, cavum septi pellucidi (CSP), third and fourth ventricle, vermis, cisterna magna, pons and mesencephalon. Note the presence of cavum Vergae and cavum veli interpositi.⁷
- 3.3.3.3) For the parasagittal image through one gangliothalamic ovoid (e.g., the right), angle the probe sideways for a parasagittal view through the lateral ventricle. Identify the choroid plexus and note the echogenicity of thalamus and basal ganglia. The scanned side for parasagittal planes should be appropriately indicated with text tools.
- 3.3.3.4) For the parasagittal insular image, angle the probe further lateral through the insula. Identify the lateral fissure and frontal-, temporal-, parietal- and occipital lobes.
- 3.3.3.5) Repeat parasagittal images for the contralateral side (i.e., the left).

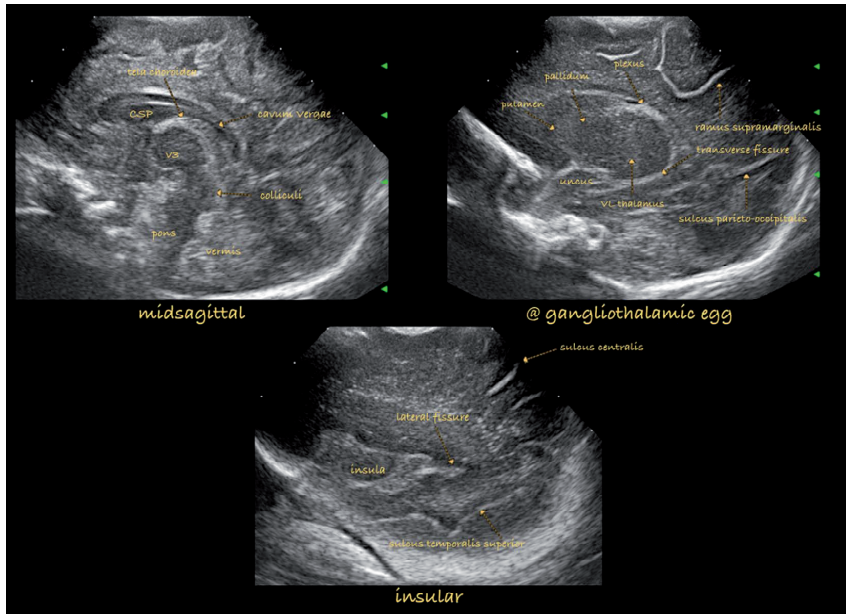


Figure 2. (Para)sagittal sections

Images through anterior fontanel at standard (para)sagittal sections.

Abbreviations:

CSP = cavum septi pellucidum

V3 = third ventricle

3.3.4) Color Doppler

- 3.3.4.1) Continue imaging through the anterior fontanel with a convex probe using color Doppler. Consider evaluating flow velocities in cerebral arteries and veins and obtaining derived indices.

Note: Resistive index (RI) is defined as peak systolic velocity – end diastolic velocity / peak systolic velocity. RI is angle-independent, absolute velocity values are not.^{8–10} RI is not similar in arteries of different caliber. Serial measurements are only useful if performed in the exact same location of the same vessel.

- 3.3.5) Record images in coronal planes of the following vessels (Figure 3):

- 3.3.5.1) Visualize the transverse sinuses at the level of the cerebellum. If only one or none the transverse sinuses is visualized, try lowering the pulse repetition frequency (PRF). If then still only one or none of the transverse sinuses can be

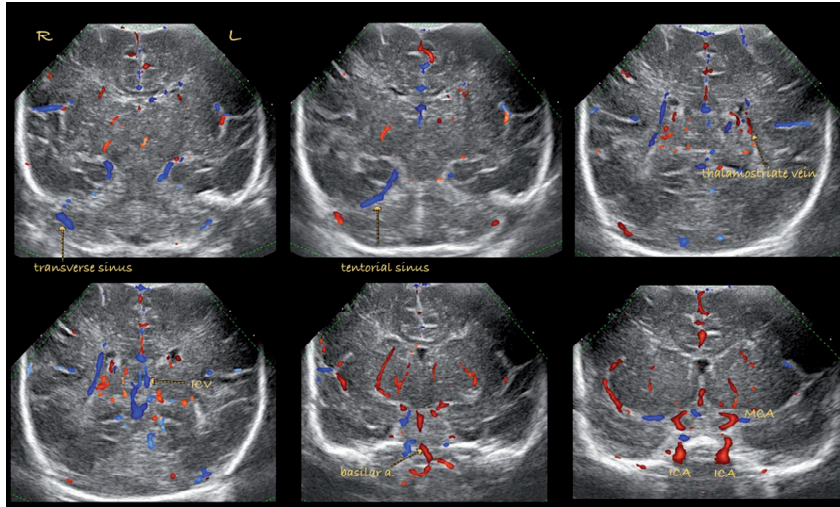


Figure 3. Coronal Doppler

Coronal color Doppler images through anterior fontanel.

Abbreviations:

Basilar a. = basilar artery

ICA = internal carotid artery

ICV = internal carotid vein

L = left

MCA = middle cerebral artery

R = right

identified through the anterior fontanel, use a high frequency linear probe for visualization through the mastoid fontanel (see section 4.4.2).

- 3.3.5.2) Visualize the circle of Willis with internal carotid arteries, middle cerebral arteries and anterior cerebral arteries at the level of the frontal horns of the lateral ventricles. Distinguishing the left and right anterior cerebral arteries is often challenging, but is usually unnecessary. Identify the striatal candelabra of arteries.
- 3.3.5.3) Angle the probe backwards to visualize the basilar artery with adjacent jugular veins.
- 3.3.5.4) Angle even more backwards to visualize the internal cerebral and thalamostriate veins.
- 3.3.6) Record an image in the sagittal plane of one anterior cerebral artery (Figure 4). Assess flow velocity and RI at a specific part of this vessel (usually below

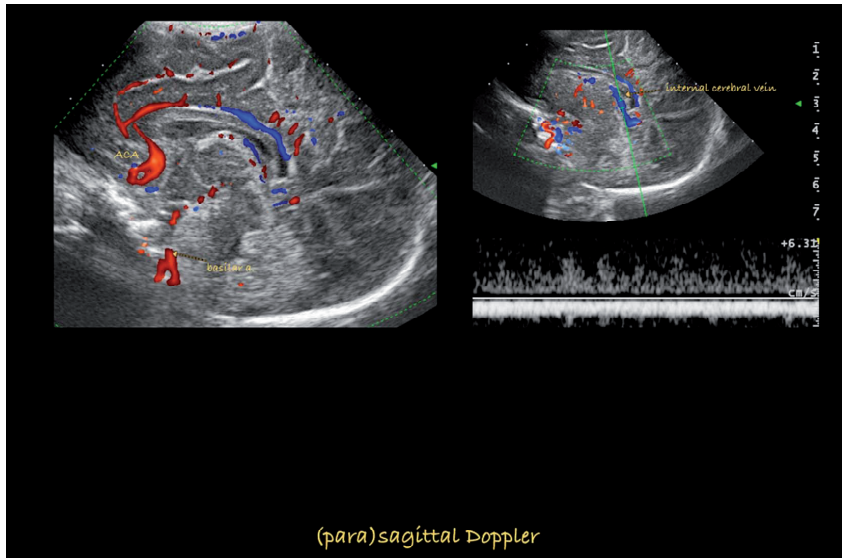


Figure 4. (Para)sagittal Doppler
(Para)sagittal color Doppler images through anterior fontanel.

Abbreviations:

ACA = anterior cerebral artery

Basilar a. = basilar artery

the genu of the corpus callosum). Near the midline velocities in the internal cerebral vein can be readily measured.

- 3.3.7) Using a high frequency linear probe in a coronal plane in the anterior fontanel, identify the superior sagittal sinus. If this should fail, reduce the amount of pressure applied with the probe to the fontanel.

Note: The linear probe can be used for detailed visualization of superficial structures (meninges, arachnoid and subdural space, cortex). Tangential vessels are in the subarachnoid space. Ideally, Doppler imaging as described in the previous steps will be performed during the first CUS examination of the neonate. During follow-up examination some of the steps may be skipped. In case of suspected cerebral sinovenous thrombosis Doppler imaging as described in steps 3.3.5.1, 3.3.7 and 4.4.2 should be performed.

4. Examination through alternative acoustic windows

- 4.1) Next, continue examination through alternative acoustic windows.

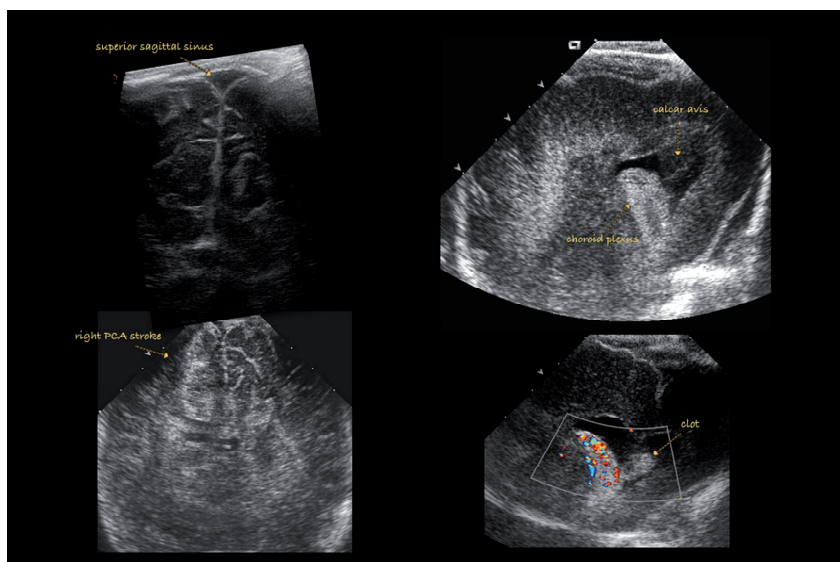


Figure 5. Lambdoid view
Imaging through lambdoid fontanel.
Abbreviations:
PCA = posterior cerebral artery

- 4.2) Consider recording images through the lambdoid (posterior) fontanel using a convex probe (Figure 5). The posterior fontanel is located at the junction of the sagittal and lambdoid sutures.^{3, 11} Image through the posterior fontanel by placing the neonate in the lateral decubitus position.

Note: In many premature infants satisfactory images may also be obtained through the posterior aspect of the sagittal suture with the infant in a supine position.³

- 4.2.1) Position the probe in the middle of the posterior fontanel for a sagittal view. Angle the probe slightly off midline to identify the body of the lateral ventricle and its occipital horn. Turn the probe roughly 90° to obtain a coronal view. Identify the occipital horns of the lateral ventricles.
- 4.3) Consider recording images through the lateral (temporal) window using a convex or linear probe above the ear (Figure 6).

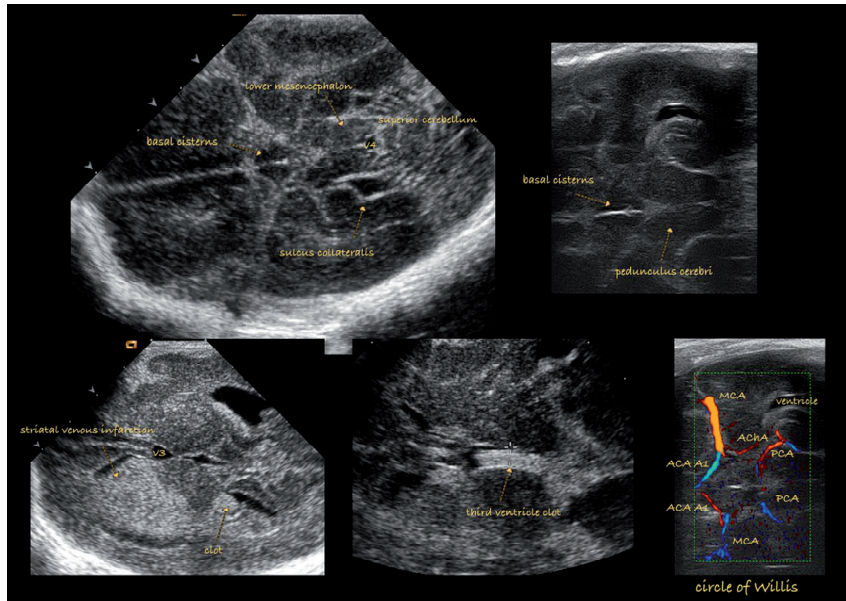


Figure 6. Temporal (lateral) view
Imaging through lateral fontanel.

Abbreviations:

ACA A1 = A1 segment of anterior cerebral artery

AChA = anterior choroidal artery

MCA = middle cerebral artery

PCA = posterior cerebral artery

V3 = third ventricle

V4 = fourth ventricle

- 4.3.1) If necessary, obtain images through the lateral window to allow a detailed view of the brainstem.¹² Place the probe horizontally above and slightly in front of the ear. Move the probe until the cerebral peduncles are visualized.

Note: Other structures that can be identified are the third ventricle, aqueduct and temporal lobes. Using color Doppler, the circle of Willis can be visualized.

- 4.4) Record images through the mastoid fontanel (Figure 7). The mastoid fontanel is located behind the ear, at the junction of the temporal, parietal and occipital bones.⁴ Image through the mastoid fontanel by placing the neonate in a lateral decubitus position.³

Note: In our experience, neonates often show signs of discomfort when images through the mastoid fontanel are obtained. Therefore, it would be best to do

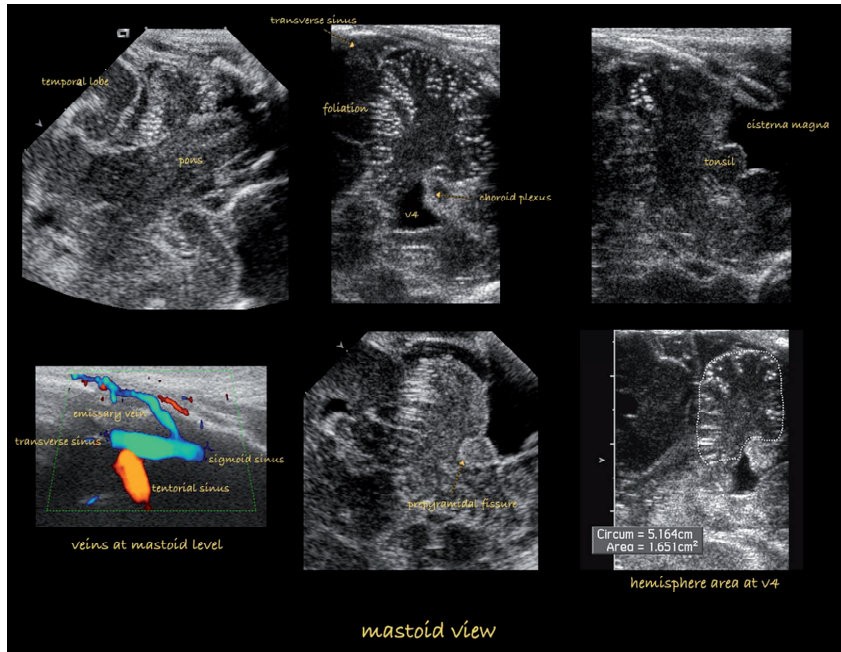


Figure 7. Mastoid view

Imaging through mastoid fontanel.

Abbreviations:

V4 = fourth ventricle

this after imaging through the anterior fontanel and other acoustic windows. We hypothesize that this discomfort could be caused by the mechanism of auditory response to pulses of radiofrequency energy.¹³

- 4.4.1) Image through mastoid fontanel using a convex probe. Place the probe parallel to the ear to obtain a coronal view. Sweep the probe back and forth to identify the cerebellar hemispheres, vermis, third and fourth ventricle, pons and cisterna magna. In small preterms the contralateral cerebellar hemisphere may be well depicted.
- 4.4.2) Image through mastoid fontanel using a linear probe. If (one of) the transverse sinuses cannot be identified through the anterior fontanel, use a high frequency linear probe for visualization through the mastoid fontanel. Place the probe parallel to the ear lobe to obtain a coronal view.
 - 4.4.2.1) Identify the cerebellar hemisphere and fourth ventricle. Using color Doppler, identify the transverse and sigmoid sinus, tentorial sinus and emissary veins.

- 4.5) Consider additional visualization of the posterior fossa through foramen magnum.¹⁴

Representative results

Examples of imaging made according to the described protocol are presented in Figures 1–7. Images should be carefully interpreted by an experienced observer. Symmetrical imaging is necessary for adequate interpretation of coronal images made through the anterior fontanel (Figure 1). Any suspected lesion should be visualized in both a coronal and (mid)sagittal plane or by visualization through an acoustic window other than the anterior fontanel. Use Color Doppler for visualization of intracerebral vessels (Figures 3, 4, 6 and 7). Some examples of intracerebral lesions are shown in Figures 5 (right posterior cerebral artery stroke, clot in lateral ventricle) and 6 (striatal venous infraction, third ventricle clot). Reliable measurement using linear, elliptoid and free tracing tools are part of routine imaging (Figure 7). Ventricular measurements such as ventricular index, anterior horn width and thalamo-occipital distance are used in clinical practice to monitor ventricular size.

Discussion

We describe and demonstrate a state-of-the-art approach for neonatal Doppler CUS. In experienced hands, this is an excellent tool for safe, serial bedside neonatal brain imaging. In many NICUs the described possibilities are not optimally used. Adding Doppler studies allows for screening of patency of intracranial arteries and veins. Flow velocities can be evaluated and indices obtained. Doppler CUS permits detection of cerebral sinovenous thrombosis at an early stage in the fragile transverse to sigmoid sinus angle, allowing therapeutic intervention prior to stroke.² Use of supplemental acoustic windows enhances detection of brain injury.

Another much used technique for neuroimaging in critically ill neonates is MRI. MRI provides excellent image quality and is considered superior to CUS in identifying cerebellar lesions and white matter injury.¹⁵ However, MRI is expensive and its clinical use in NICUs is limited because of logistic and safety issues.¹ CUS on the other hand is relatively cheap, directly available and allows serial bedside imaging. A local protocol for sequential CUS imaging is desirable. The use of supplemental acoustic windows, color Doppler imaging, higher transducer frequencies and careful interpretation of images by an experienced observer results in high accuracy to identify brain lesions (Plaisier, *et al.*, unpublished data).

In short, CUS is a reputable tool for neonatal brain imaging. For optimal use of the technique, there are aspects regarding equipment, data storage and safety that need to be addressed. Make sure special settings for the neonatal brain are programmed on the ultrasound machine. Use multiple transducers with a band of frequencies. Consider which probe is most suitable for the area of interest. In general, images of good quality can be obtained using a probe with a frequency of 7.5 to 8.5 MHz. A higher frequency results in loss of penetration. A lower frequency allows better penetration and consequently a better view of deeper structures, such as deep gray matter. The drawback of a lower transducer frequency is loss of resolution. This can be resolved by adapting the focus or using multiple focus points. The ultrasound beam has the narrowest width at the depth of the focus point. Adapting the focus point therefore improves resolution, allowing a more detailed view of the region of interest. Using multiple focus points allows better visualization of the area between these points. For standard CUS, the focus point is preferably aimed at the ventricular or periventricular areas.¹⁶ Multiple focus points may cause artefacts. Consider which probe size is most suitable for imaging. Probes are available in different shapes and sizes. Ideally, the footprint should be small enough to fit in the anterior fontanel, necessitating a convex scanhead. In the smallest preterm infants, only a phased array probe may be small enough to fit in the anterior fontanel: in this probe the ultrasound beam diverges from one point. Phased array convex probes produce pie-shaped (sector) images. In a linear array transducer, crystal elements are arranged parallel to each other, producing a rectangular image with high image quality. However, the high frequency results in loss of penetration and because of its large size the linear array transducer will not optimally fit in the anterior fontanel.

Acquiring images of good quality not only depends on the quality of the equipment used, but also on the skills of the examiner. Make sure operators are properly trained in neonatal CUS. Operators should be familiar with functions like gain, time gain compensation, dynamic range, speckle reduction filters.

Make sure qualified technical personnel is available to service equipment. Probes contain delicate components, which can easily be damaged if not handled with care. Make a conscious effort to protect equipment during everyday use. Consider how to store the obtained images. They can be digitally stored or printed and stored with the patient's file.

One should be aware of the potential risks and burden of CUS for critically ill neonates. The extra handling involved in the examination and applying pressure and cold gel to the fontanel(s) could lead to respiratory instability. Also, there is a potential risk of dislocating tubes or intravenous devices, of introducing micro-organisms from equip-

ment that is not appropriately cleaned or from the examiner, and of possible hazardous effects of ultrasound waves.¹⁷ These matters can be prevented or reduced with fairly simple precautions. As mentioned earlier, the infant should be supported by a health care worker or parent according to the principles of Newborn Individualized Developmental Care and Assessment Program.⁶ While handling the probe, keep the applied pressure to a minimum. Cold gel can be warmed before the examination. Ultrasound equipment should be regularly cleaned. After each examination the probe should be wiped clean. Consult with the manufacturer whether probes are suited to be wiped clean with disinfectant.

At tissue level, ultrasound energy is converted into heat which may increase local temperature. The amount of energy absorbed depends on tissue type, duration of exposure and ultrasound mode or route. Doppler imaging, though, has higher output potential compared to standard B-mode imaging, because of its intensity and the small area of tissue being examined.¹⁸ Therefore, keep the duration of exposure to a minimum, especially in Doppler imaging. Regulatory bodies such as the American Institute of Ultrasound in Medicine (AIUM), the British Medical Ultrasound Society (BMUS), European Federation of Societies for Ultrasound in Medicine and Biology (EFSUMB), and World Federation for Ultrasound in Medicine and Biology (WFUMB), have published guidelines on mechanical and thermal indices for diagnostic ultrasound. Thermal and mechanical indices less than one are generally accepted as safe.¹⁸ Standard settings should be kept within the range indicated in these guidelines and when adjusting settings during examination one should make sure to adhere to these guidelines, especially during color Doppler examination. Make sure to turn the Doppler mode off and switch back to normal imaging mode as soon as the Doppler examination is completed. To date there is no evidence of adverse effects of ultrasound examination in neonates. There have been reports of a mildly increased risk of delayed speech, left handedness in boys and intrauterine growth restriction after fetal exposure to ultrasound.¹⁸ A recent systematic review found that ultrasonography during pregnancy was not associated with adverse perinatal or childhood outcome.¹⁹ However, in most of the reviewed studies ultrasound machines were used with less output potential than currently available.¹⁸

Keeping the aforementioned safety issues in mind, further advances in ultrasound technology will lead to improvement of image quality and will expand the possibilities of CUS imaging. Examples include portable handheld devices, wireless transducers, 3D imaging, functional ultrasonography and ShearWave Elastography.

In conclusion, Doppler CUS is an excellent, relatively inexpensive tool for serial neonatal bedside neuroimaging in experienced hands. Optimal use of currently available equip-

ment and techniques provides better imaging quality and improves diagnostic value of CUS.

Acknowledgments

We thank the nurses (appearing on film) for supporting the neonates.

We thank J. Hagoort, MA, linguist, Department of Pediatric Surgery, Erasmus MC-Sophia Children’s Hospital, Rotterdam, the Netherlands, for reading and correcting the manuscript.

Materials

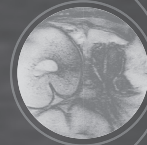
Name of Material/ Equipment	Company	Comments/Description
MyLab 70	Esaote (Genoa, Italy)	Ultrasound system

References

1. Plaisier A, Raets MMA, van der Starre C, Feijen-Roon M, Govaert P, Lequin MH, et al. Safety of routine early mri in preterm infants. *Pediatric Radiology*. 2012;42:1205-1211.
2. Raets MMA, Sol JJ, Govaert P, Lequin MH, Reiss IKM, Kroon AA, et al. Serial cranial us for detection of cerebral sinovenous thrombosis in preterm infants. *Radiology*. 2013;269:879-886.
3. Di Salvo DN. A new view of the neonatal brain: Clinical utility of supplemental neurologic us imaging windows. *Radiographics*. 2001;21:943-955.
4. Enriquez G, Correa F, Aso C, Carreno JC, Gonzalez R, Padilla NF, et al. Mastoid fontanelle approach for sonographic imaging of the neonatal brain. *Pediatric Radiology*. 2006;36:532-540.
5. Luna JA, Goldstein RB. Sonographic visualization of neonatal posterior fossa abnormalities through the posterolateral fontanelle. *AJR Am J Roentgenol*. 2000;174:561-567.
6. Als H, Lawhon G, Brown E, Gibes R, Duffy FH, Mcanulty G, et al. Individualized behavioral and environmental care for the very-low-birth-weight preterm infant at high-risk for bronchopulmonary dysplasia - neonatal intensive-care unit and developmental outcome. *Pediatrics*. 1986;78:1123-1132.
7. Govaert P, de Vries LS. *An atlas of neonatal brain sonography, 2nd edition*. London: Mac Keith Press 2010.
8. Gray PH, Griffin EA, Drumm JE, Fitzgerald DE, Duignan NM. Continuous wave doppler ultrasound in evaluation of cerebral blood-flow in neonates. *Archives of Disease in Childhood*. 1983;58:677-681.
9. Seibert JJ, Mccowan TC, Chadduck WM, Adametz JR, Glasier CM, Williamson SL, et al. Duplex pulsed doppler ultrasonography versus intracranial-pressure in the neonate - clinical and experimental studies. *Radiology*. 1989;171:155-159.
10. Volpe JJ, Perlman JM, Hill A, Mcmenamin JB. Cerebral blood-flow velocity in the human newborn - the value of its determination. *Pediatrics*. 1982;70:147-152.
11. Correa F, Enriquez G, Rossello J, Lucaya J, Piqueras J, Aso C, et al. Posterior fontanelle sonography: An acoustic window into the neonatal brain. *American Journal of Neuroradiology*. 2004;25:1274-1282.
12. Helmke K, Winkler P, Kock C. Sonographic examination of the brain stem area in infants. An echographic and anatomic analysis. *Pediatric Radiology*. 1987;17:1-6.
13. Elder JA, Chou CK. Auditory response to pulsed radiofrequency energy. *Bioelectromagnetics*. 2003;Suppl 6:S162-173.
14. Brennan CM, Taylor GA. Sonographic imaging of the posterior fossa utilizing the foramen magnum. *Pediatric Radiology*. 2010;40:1411-1416.
15. Rutherford MA, Supramaniam V, Ederies A, Chew A, Bassi L, Groppo M, et al. Magnetic resonance imaging of white matter diseases of prematurity. *Neuroradiology*. 2010;52:505-521.
16. van Wezel-Meijler G, Steggerda SJ, Leijser LM. Cranial ultrasonography in neonates: Role and limitations. *Seminars in Perinatology*. 2010;34:28-38.
17. Leijser LM, de Vries LS, Cowan FM. Using cerebral ultrasound effectively in the newborn infant. *Early Human Development*. 2006;82:827-835.
18. Houston LE, Odibo AO, Macones GA. The safety of obstetrical ultrasound: A review. *Prenatal Diagnosis*. 2009;29:1204-1212.
19. Torloni MR, Vedmedovska N, Meriardi M, Betran AP, Allen T, Gonzalez R, et al. Safety of ultrasonography in pregnancy: Who systematic review of the literature and meta-analysis. *Ultrasound in Obstetrics & Gynecology*. 2009;33:599-608.

CHAPTER 3

Resistive index of cerebral arteries in very preterm infants: values throughout stay in the Neonatal Intensive Care Unit and impact of patent ductus arteriosus



G.M. Ecury-Goossen, M.M.A. Raets, F.A. Camfferman, H.J. Vos, J. van Rosmalen,
I.K.M. Reiss, P. Govaert, J. Dudink.

Pediatr Radiol 2016;46:1291-1300.

Abstract

Background

Little is known about cerebral artery resistive index (RI) values in infants born extremely preterm.

Objectives

To report RI values in various cerebral arteries in a prospective cohort of preterm infants born at < 29 weeks gestation. We aim to compare RI in these arteries, and to assess the relationship between RI and hemodynamically significant patent ductus arteriosus.

Materials and Methods

Using color Doppler imaging, RI values of internal carotid arteries, basilar artery, anterior cerebral artery, pial and striatal arteries were obtained in the first three days of life and weekly after that until discharge or death. RI measurements from the same subject were compared with the Wilcoxon signed-rank test, between-group comparisons with the Mann-Whitney test.

Results

771 examinations were performed in 235 infants. RI differed between the arteries: vessels with larger diameters showed significantly higher RIs. RI in infants without patent ductus arteriosus was lower than that in infants with hemodynamically significant patent ductus arteriosus (median in anterior cerebral artery 0.75 vs 0.82, $p < 0.001$), though not statistically significant in all arteries. There was no difference in pre- and postligation RI in infants who underwent patent ductus arteriosus ligation.

Conclusion

For accurate follow-up and comparison of cerebral artery RI, the same artery should be examined.

Introduction

Cerebral vascular anatomy and disturbance of cerebral hemodynamics are key factors in pathophysiology of brain injury in preterm infants.¹ As therapeutic options for brain injury in these infants are currently lacking, clinicians focus on prevention through hemodynamic monitoring. Therefore, there is renewed interest in non-invasive methods to evaluate cerebral blood flow. One such method assessing one aspect of cerebral blood flow is measuring resistive index (RI) in cerebral arteries using color Doppler imaging. The internal carotid artery, basilar artery, anterior cerebral artery and lenticulostriate arteries can be easily visualized with color Doppler imaging.² Flow can be evaluated and peak systolic velocity, end-diastolic velocity and RI can thus be obtained. RI is defined as (peak systolic velocity – end-diastolic velocity) / peak systolic velocity.³ In current neonatal clinical practice, RI is typically assessed in the anterior cerebral artery in both term and preterm infants admitted to the Neonatal Intensive Care Unit. Low RI is considered a possible sign of luxury perfusion in term birth asphyxia.³ A patent ductus arteriosus is considered to be the usual cause for elevated RI in preterm infants.³

In previous studies RI of cerebral arteries has been described in healthy term neonates^{4–10}, small groups of clinically stable preterm neonates^{11–15,9,16,17}, and sick infants.^{11,16,18,19,20} These studies included only small numbers of very preterm infants or described RI during a short time frame. Results of previous studies in preterm infants are summarized in Table 1. Nowadays, more infants born at extremely low gestational age are treated. Reference values for RI of cerebral arteries in these infants are lacking.

The purpose of this study is to report RI values in various cerebral arteries in a cohort of preterm infants born at < 29 weeks gestation, measured from the first postnatal day throughout their stay in the Neonatal Intensive Care Unit. Furthermore, we aim to compare RI values between various intracranial arteries, to compare RI values in left versus right-sided arteries, and to assess relationships between RI and the Score for Neonatal Acute Physiology, Perinatal Extension, Version II (SNAPPE-II scores)²¹, gestational age and hemodynamically significant patent ductus arteriosus. We hypothesized that (1) RI will differ depending on the diameter of the artery where it is measured: RI will be higher in larger intracerebral arteries (e.g. internal carotid arteries, anterior cerebral artery and basilar artery) compared to that in smaller intracerebral arteries (e.g. striatal and pial arteries), and (2) that RI will be higher in the presence of a hemodynamically significant patent ductus arteriosus.

Table 1. RI values in previous studies

Study ID	Population	Insonated vessels	RI values
Ando 1985 ¹¹	n = 14 preterm infants without complications, GA 30-35 weeks	ACA	during the first 3 hours after birth 0.878±0.057 at 4-6 hours 0.855±0.045 at 7-12 hours 0.656±0.021
	n = 13 preterm infants with respiratory distress, GA 25-33 weeks		Results presented in figure
	n = 8 preterm infants with SEH or IVH, GA 27-33 weeks		no results shown
Blankenberg 1997 ¹⁹	n = 16 preterm infants, assessed during the first 5-6 days of life, mean GA 26.8 weeks (range 24-31 weeks). 11/16 without PVL or IVH	lenticulostriate arteries	mean RI 0.586±0.091
	5/16 developed PVL and/or IVH		mean RI 0.543±0.087
Calvert 1988 ¹²	n = 29 preterm infants, assessed during the first 72 hours of life, GA 25-32 weeks	Right and left cerebral arteries	GA 26-28 RI 0.91±0.09 GA 29-32 RI 0.86±0.08
Evans 1988 ¹³	n = 27 VLBW infants (< 1500 grams), assessed during first 7 days of life	ACA	mean RI 0.79
		MCA	mean RI 0.81
Lipman 1982 ¹⁴	n = 8 preterm infants with PDA with left- to-right shunt, GA 26-33 weeks (mean 29 weeks)	ACA	mean RI 0.90 before ductal closure, 0.76 after ductal closure
	n = 40 healthy control group, mean GA 31.6 weeks		mean RI 0.79 (range 0.72-0.85)
Mires 1994 ¹⁵	n = 137 uncomplicated preterm infants assessed during first 10 days of life 23/137 GA ≤ 32 weeks 44/137 GA 33-34 weeks 70/137 GA ≥ 35 weeks	ACA and MCA	Results for 3 groups (≤ 32, 33-34 and > 35 weeks) at 1 hour and 12 hours postnatal age, after 24 hours steady state was reached
Pezzati 2002 ⁹	n = 120 healthy neonates, assessed during the first 8 hours of life, GA 24-41 weeks	ACA	GA 24-28 RI 0.75 (0.07)* GA 29-32 RI 0.78 (0.06)* GA 33-37 RI 0.78 (0.07)* GA 38-41 RI 0.80 (0.07)*
		MCA bilaterally	GA 24-28 RI 0.76 (0.07)* GA 29-32 RI 0.80 (0.07)* GA 33-37 RI 0.82 (0.07)* GA 38-41 RI 0.81 (0.87)*

Table 1. RI values in previous studies (continued)

Study ID	Population	Insonated vessels	RI values
Romagnoli 2006 ¹⁷	n = 70 "healthy" preterm infants, assessed during the first month of life, mean GA 31.7 weeks (range 25-35)	ACA	- GA 25-28 weeks
			RI 0.74, 0.71, 0.79, 0.77, 0.76, 0.80 **
			- GA 29-30 weeks
			RI 0.71, 0.75, 0.74, 0.75, 0.78, 0.74 **
			- GA 31-32 weeks
	10/70 GA 25-28 weeks 13/70 GA 29-30 weeks 16/70 GA 31-32 weeks 31/70 GA 33-35 weeks		RI 0.76, 0.74, 0.74, 0.76, 0.78, 0.78 **
			- GA 33-35 weeks
			RI 0.75, 0.75, 0.75, 0.74, 0.76, 0.78 **
			- GA 25-28 weeks
			RI 0.75, 0.70, 0.74, 0.76, 0.79, 0.76 **
		MCA	- GA 29-30 weeks
			RI 0.73, 0.74, 0.77, 0.77, 0.78, 0.79 **
			- GA 31-32 weeks
			RI 0.73, 0.75, 0.77, 0.77, 0.78, 0.79 **
			- GA 33-35 weeks
Seibert 1989 ¹⁶	n = 57 healthy neonates, mean GA 34 weeks n = 285 ill neonates, GA not mentioned	ACA, MCA and ICA bilaterally	RI 0.74, 0.75, 0.73, 0.77, 0.75, 0.74 **
			Mean RI 0.75±0.10 in healthy neonates

*Mean and SD of RI

** 50th percentile of RI values on day 1, 3, 7, 14, 21 and 28 respectively.

Abbreviations:

ACA= anterior cerebral artery, GA= gestational age (in weeks), GMH= germinal matrix hemorrhage, ICA= internal carotid artery, MCA= middle cerebral artery, PDA= patent ductus arteriosus, PVL= periventricular leukomalacia, RI= resistive index, SEH= subependymal hemorrhage, VLBW= very low birthweight

Materials and Methods

The study was approved by the local Medical Ethics Review Board, and written parental consent was obtained. Preterm infants born at < 29 weeks gestation admitted to our Neonatal Intensive Care Unit between May 2010 and January 2013 were eligible for this prospective cohort study. Exclusion criteria were congenital malformation (patent ductus arteriosus was not considered a congenital malformation in this cohort of very preterm infants), parental refusal and uncertain gestational age. Our department is a tertiary Neonatal Intensive Care Unit with an average of 800 Neonatal Intensive Care Unit admissions per year (including 250–300 very preterm infants).

Imaging protocol

Included infants were examined with cranial ultrasound, including color Doppler imaging, according to standard local protocol (on days 0, 1, 2, and 7 after birth and then weekly until discharge or death). Cranial ultrasound was performed by two authors with expertise in neonatal cranial ultrasound (MR with 4 years of experience in cranial ultrasound and PG with 25 years of experience at the end of the study). Most of the data was collected by MR. In her unexpected absence PG performed the Cranial ultrasound.

Images were obtained in a coronal plane through the anterior fontanel, using the 8.5-MHz convex probe of an Esaote MyLab 70 ultrasound machine (Genova, Italy). A coronal rather than sagittal plane was chosen because in one plane indices can be measured in both large arteries (*e.g.* basilar artery) and in smaller arteries (*e.g.* striatal arteries, branches from the middle cerebral artery ascending into putamen). The following intracranial vessels were visualized using color Doppler (see Figure 1): internal carotid artery, basilar artery, anterior cerebral artery, striatal arteries, and pial arteries (mesial interhemispheric frontal branches of the anterior carotid artery). Internal carotid artery and striatal arteries were examined bilaterally. Deviation of protocol occurred on clinical grounds (*e.g.* hemodynamic or respiratory instability). Doppler settings included pulse repetition frequency of 1.5 kHz, Doppler frequency of 5 MHz, gain of 64%, persistence 16 and depth of 76 mm. Mechanical and thermal indices were kept below 1. RI was manually assessed in the aforementioned arteries using pulsed wave Doppler. Mean RI was calculated from average peak systolic velocity and end-diastolic velocity of at least five sequential stable waveforms. One RI assessment per artery was performed on days 0, 1, 2, and 7 after birth and then weekly until discharge or death. RI measurements were performed without knowledge of the clinical condition of the infant. However, it was possible that the observers were aware that ductal ligation had taken place.

Demographic, perinatal and postnatal data, including SNAPPE-II scores [21], were retrieved from medical charts and computerized patient data management system. Patent ductus arteriosus was diagnosed echocardiographically and treated when deemed

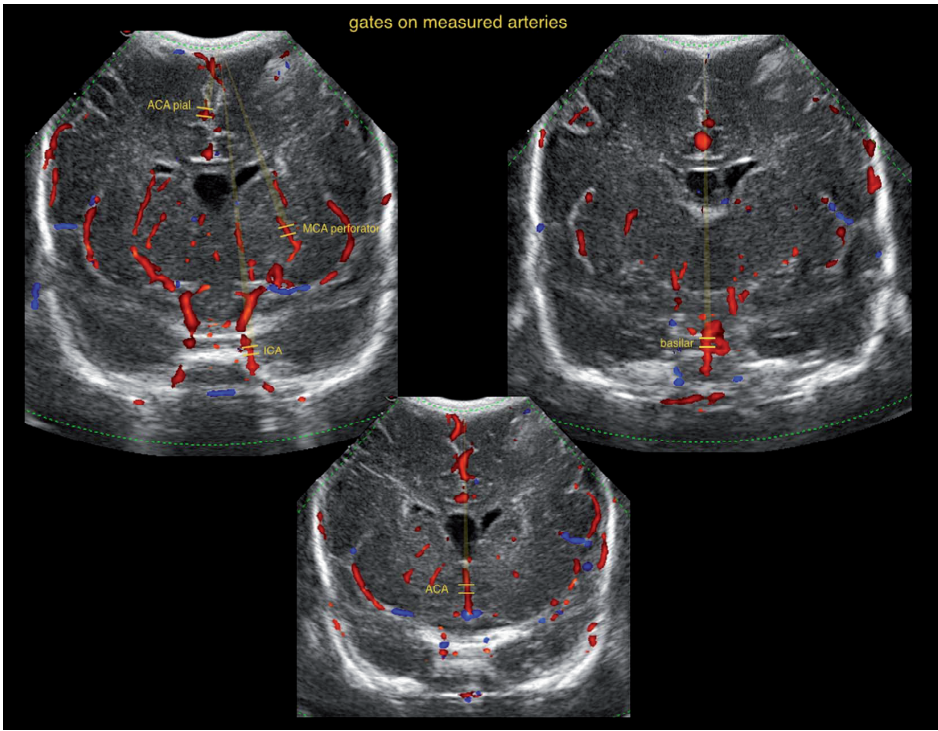


Figure 1. Insonated arteries

Figure legend: Color Doppler cranial ultrasound of a one month old preterm girl, born at 26 weeks of gestation, birth weight 900 grams. She was diagnosed with a hemodynamically significant PDA for which surgical ligation was performed later on. Her course was complicated by *S. Aureus* sepsis.

Coronal images through the anterior fontanel with color Doppler showing various vessels.

Abbreviations:

ACA= anterior cerebral artery

ICA= internal carotid artery

MCA= middle cerebral artery

PDA= patent ductus arteriosus

hemodynamically significant by the investigating cardiologist. Criteria for hemodynamically significant patent ductus arteriosus included ductal size > 2 mm, left atrium to aortic root diameter of > 1.6 , and pulsatile flow pattern of patent ductus arteriosus [22].

Statistical analysis

This study was part of a large prospective cohort study with the primary objective to investigate structural growth and brain maturation with cranial ultrasound in very preterm infants. Due to lack of similar studies, a proper sample size calculation was not possible. From the onset of the current study it was clear that a larger number of

extremely premature infants would be included than in any previous study describing RI in intracranial arteries (see Table 1).

Patient characteristics and RI values were described using medians and (interquartile) ranges for continuous variables, and using percentages for categorical variables. RI values were compared between infants with hemodynamically significant patent ductus arteriosus and those without hemodynamically significant patent ductus arteriosus using the Mann-Whitney test (for independent samples). Pairs of RI measurements in two different arteries from the same subjects were compared with the Wilcoxon signed-rank test (for paired samples). Pairs of pre- and postligation RI values from the same subjects were also compared using the Wilcoxon signed-rank test. Multivariable linear regression analysis was used to assess the relationship between the independent variables SNAPPE-II score, presence of (hemodynamically significant) patent ductus arteriosus, gestational age and sex and the continuous dependent variable RI. A separate linear regression analysis was performed for each artery. Assessment of the distribution of the residuals in the linear regression analyses was performed using histograms and the Shapiro-Wilk test. Statistical significance was assumed if the two-sided p-value was < 0.05 . Statistical analyses were performed using Microsoft Excel and SPSS (version 21 for Windows; IBM, New York, NY).

Results

During the study period, 333 eligible infants were admitted. 98 were excluded (21 congenital malformation, 3 uncertain gestational age, 12 parental refusal, 62 lack of data (because of death soon after birth, absence of both observers, or insufficient image quality)), leaving 235 to be included. Patient characteristics are shown in Table 2. A total of 771 RI examinations were performed in those 235 infants, varying from one to eight (median three) per subject. This variation is explained by the fact that 38 infants (16%) died while admitted to the Neonatal Intensive Care Unit and that infants were transferred to level II hospitals when reaching a corrected age of 30 weeks gestation and intensive care was no longer needed.

RI values measured in seven different intracranial vessels throughout admission in our Neonatal Intensive care Unit are presented in Table 3.

When comparing RI in left and right sided arteries (measured in the same session in the same subject), RI in the left internal carotid artery (median 0.85) was slightly higher than in the right internal carotid artery (median 0.84) ($p = 0.023$, sum of ranks 1824 negative, 3126 positive). There was no statistically significant difference in RI between left (median 0.64) and right (median 0.62) sided striatal arteries ($p = 0.22$, sum of ranks 801 negative, 1153 positive). Results for comparison of RI in the different arteries (measured in the

Table 2. Patient characteristics

	No. (%) or median (range)
Gestational age, weeks	27 (23 6/7 – 28 6/7)
Birth weight, grams	920 (360 – 1610)
Male	129 (55%)
Singleton	160 (68%)
Antenatal steroids (doses)	2 (0-2)
none	19 (8%)
Vaginal delivery	111 (47%)
SGA	37 (16%)
Apgar score 1 minute	6 (0 – 10)
Apgar score 5 minutes	8 (1 – 10)
Umbilical cord pH (n = 203)	7.31 (6.78 – 7.48)
SNAPPE II scores (n = 232)	22 (0 – 104)
Surfactant (doses)	1 (0 – 3)
Mechanical ventilation (days)	6 (0 – 46)
Inotropic support	68 (29%)
PDA (n = 227)	135 (59%)
Hemodynamic significant PDA	111 (49%)
Treatment of PDA	109/111 (98%)
Medication only	80/109 (73%)
Surgical ligation	29/109 (27%)
Number of days admitted to NICU	31 (1-139)

Abbreviations:

PDA= patent ductus arteriosus

NICU= Neonatal Intensive Care Unit

SGA= small for gestational age

SNAPPE II= Score for Neonatal Acute Physiology, Perinatal Extension, Version II

same session in the same subject) are presented in Table 4. RI in larger arteries (internal carotid arteries, anterior cerebral artery, and basilar artery) was consistently higher than RI in the smaller pial and striatal arteries.

Ninety-nine infants were diagnosed with focal brain injury with cranial ultrasound and/or magnetic resonance imaging at some point during their stay in the Neonatal Intensive Care Unit. These focal brain injuries included germinal matrix hemorrhage, intraventricular hemorrhage, periventricular hemorrhagic infarction, cerebellar hemorrhage, perforator stroke and sinovenous thrombosis.

Table 5 presents RI values in infants with and without hemodynamically significant patent ductus arteriosus. Nine infants underwent Doppler examination before and after ductal ligation. In four of these RI in right internal carotid artery was lower after ligation. Similar results were found in the other six insonated vessels.

Table 3. Resistive index values throughout Neonatal Intensive Care Unit stay**A.** RI values for corrected age

Corrected age (weeks)	ICA right	ICA left	ACA	Striatal right	Striatal left	Pial	Basilar
24	0.80 (0.78-0.87)	0.85 (0.79-0.91)	0.78 (0.72-0.84)	0.61 (0.57-0.66)	0.66 (0.59-0.69)	0.74 (0.67-0.81)	0.80 (0.73-0.85)
25	0.85 (0.74-0.89)	0.85 (0.78-0.91)	0.82 (0.75-0.88)	0.64 (0.60-0.70)	0.68 (0.59-0.71)	0.70 (0.65-0.77)	0.79 (0.74-0.88)
26	0.81 (0.74-0.86)	0.83 (0.78-0.89)	0.81 (0.72-0.86)	0.62 (0.59-0.68)	0.66 (0.60-0.72)	0.67 (0.63-0.73)	0.76 (0.73-0.83)
27	0.84 (0.77-0.89)	0.85 (0.79-0.90)	0.81 (0.74-0.87)	0.64 (0.58-0.70)	0.64 (0.60-0.69)	0.70 (0.66-0.76)	0.79 (0.72-0.85)
28	0.83 (0.77-0.89)	0.84 (0.77-0.89)	0.80 (0.74-0.87)	0.64 (0.58-0.70)	0.64 (0.60-0.69)	0.70 (0.65-0.78)	0.79 (0.73-0.85)
29	0.84 (0.77-0.89)	0.83 (0.77-0.89)	0.80 (0.73-0.85)	0.67 (0.60-0.71)	0.67 (0.60-0.71)	0.71 (0.64-0.78)	0.80 (0.73-0.85)
30	0.84 (0.80-0.88)	0.86 (0.82-0.90)	0.81 (0.77-0.86)	0.66 (0.61-0.71)	0.67 (0.63-0.74)	0.71 (0.68-0.76)	0.82 (0.78-0.86)
31	0.87 (0.80-0.91)	0.86 (0.83-0.92)	0.84 (0.75-0.89)	0.68 (0.65-0.70)	0.66 (0.62-0.70)	0.72 (0.66-0.79)	0.75 (0.74-0.82)
32	0.83 (0.77-0.85)	0.85 (0.79-0.87)	0.80 (0.76-0.85)	0.63 (0.58-0.66)	0.64 (0.63-0.69)	0.72 (0.67-0.74)	0.78 (0.67-0.78)
33	0.89 (0.87-0.91)	0.84 (0.84-0.87)	0.89 (0.88-0.93)	0.60 (0.52-0.64)	0.68 (0.59-0.69)	0.87 (0.86-0.87)	0.81 (0.78-0.82)
34	0.81 (0.78-0.82)	0.79 (0.79-0.82)	0.78 (0.75-0.79)	0.48 (0.48-0.58)	0.53 (0.51-0.60)	0.66 (0.57-0.74)	0.72 (0.72-0.74)

B. RI values for postnatal age

Postnatal age (weeks)	ICA right	ICA left	ACA	Striatal right	Striatal left	Pial	Basilar
0	0.83 (0.76-0.88)	0.84 (0.77-0.89)	0.79 (0.73-0.86)	0.62 (0.57-0.69)	0.64 (0.59-0.69)	0.69 (0.64-0.75)	0.78 (0.71-0.85)
1	0.82 (0.76-0.87)	0.82 (0.78-0.90)	0.81 (0.74-0.85)	0.64 (0.59-0.70)	0.65 (0.60-0.69)	0.70 (0.65-0.77)	0.79 (0.72-0.84)
2	0.84 (0.78-0.90)	0.85 (0.79-0.90)	0.84 (0.75-0.88)	0.66 (0.61-0.72)	0.67 (0.63-0.74)	0.74 (0.68-0.77)	0.80 (0.75-0.87)
3	0.85 (0.80-0.87)	0.86 (0.81-0.91)	0.81 (0.74-0.87)	0.67 (0.63-0.71)	0.65 (0.60-0.70)	0.70 (0.66-0.77)	0.78 (0.74-0.81)
4	0.85 (0.81-0.90)	0.86 (0.77-0.89)	0.82 (0.77-0.88)	0.68 (0.64-0.72)	0.70 (0.63-0.75)	0.77 (0.68-0.80)	0.82 (0.75-0.86)
5	0.83 (0.75-0.89)	0.85 (0.78-0.87)	0.82 (0.76-0.88)	0.64 (0.58-0.68)	0.68 (0.65-0.71)	0.73 (0.68-0.81)	0.86 (0.84-0.86)
6	0.83 (0.77-0.89)	0.88 (0.85-0.90)	0.82 (0.78-0.88)	0.67 (0.63-0.68)	0.64 (0.62-0.68)	0.71 (0.64-0.79)	0.79 (0.72-0.81)
7	0.82 (0.79-0.87)	0.86 (0.84-0.89)	0.79 (0.76-0.83)	0.62 (0.53-0.68)	0.66 (0.50-0.68)	0.74 (0.72-0.78)	0.78 (0.75-0.83)

Median (interquartile range)

Abbreviations:

ACA= anterior cerebral artery

ICA= internal carotid artery

RI= resistive index

Table 4. Comparison of Resistive index in different arteries

Comparison	median RI values	p value	sum of ranks	
			negative	positive
RI ICA right > striatal artery right	0.83 vs 0.64	< 0.001	0	4095
RI ICA left > striatal artery left	0.84 vs 0.66	< 0.001	2.5	2554
RI ICA right > pial artery	0.83 vs 0.70	< 0.001	54	2091
RI ICA left > pial artery	0.84 vs 0.70	< 0.001	12	1699
RI ACA > striatal artery right	0.81 vs 0.64	< 0.001	2	3568
RI ACA > striatal artery left	0.81 vs 0.66	< 0.001	3.5	2275
RI ACA > pial artery	0.81 vs 0.70	< 0.001	41	1790
RI basilar > striatal artery right	0.79 vs 0.64	< 0.001	26	2824
RI basilar > striatal artery left	0.79 vs 0.66	< 0.001	7.5	1589
RI basilar > pial artery	0.79 vs 0.70	< 0.001	134	1092
RI basilar > ACA	0.79 vs 0.81	0.126	1371	2033

Abbreviations:

ACA= anterior cerebral artery

ICA= internal carotid artery

RI= resistive index

Table 5. Resistive index values in infants with hemodynamically significant PDA compared to infants without PDA

Artery	No PDA	hs-PDA	p-value	sum of ranks	
				negative	positive
ICA right	0.79 (0.73 – 0.84)	0.81 (0.75 – 0.87)	0.11	2632	3810
ICA left	0.79 (0.75 – 0.84)	0.85 (0.80 – 0.90)	< 0.001	1905	3766
ACA	0.75 (0.70 – 0.81)	0.82 (0.78 – 0.87)	< 0.001	2323	4698
Striatal right	0.63 (0.58 – 0.69)	0.65 (0.61 – 0.70)	0.24	1765	2796
Striatal left	0.62 (0.57 – 0.65)	0.66 (0.59 – 0.72)	0.06	979	1948
Pial	0.67 (0.61 – 0.72)	0.69 (0.66 – 0.76)	0.03	1016	1835
Basilar	0.77 (0.68 – 0.81)	0.78 (0.73 – 0.85)	0.046	1703	2858

Data are medians, numbers in parentheses are interquartile ranges

Abbreviations:

ACA= anterior cerebral artery

hs-PDA= hemodynamically significant patent ductus arteriosus

ICA= internal carotid artery

PDA= patent ductus arteriosus

RI= resistive index

Multivariate analysis showed no significant relation between RI and SNAPPE-II score, gestational age or sex. In the anterior cerebral artery and right internal carotid artery there was a significant association between patent ductus arteriosus and RI, as RI in the anterior cerebral artery was 0.069 (95% CI 0.018 – 0.120) higher for patients with hemodynamically significant patent ductus arteriosus compared to patients without

patent ductus arteriosus, and RI in the right internal cerebral artery was 0.069 (95% CI 0.023 – 0.116) higher for patients with hemodynamically significant patent ductus arteriosus compared to patients without patent ductus arteriosus. There was no significant association between patent ductus arteriosus and RI in the other five arteries. The residuals in these linear regression models did not have a normal distribution. Therefore bootstrapping was performed to calculate standard errors that are robust to violations of the normality assumption, using the accelerated bias-corrected bootstrapping method. Because the results of bootstrapping are almost identical to those without bootstrapping, we present the results without bootstrapping in Table 6.

Table 6. Results linear regression analyses

Artery	Predictor	Coefficient	95% CI		p-value
			Lower bound	Upper bound	
RI ACA	PDA				.030
	<i>no PDA</i>	-.069	-.120	-.018	.008
	<i>PDA, nhs</i>	-.037	-.118	.044	.372
	<i>hs-PDA</i>	Reference			
	SNAPPE score	.001	.000	.003	.080
	GA in weeks	-.006	-.013	.025	.544
	male sex	-.004	-.053	.043	.051
RI ICA right	PDA				.014
	<i>no PDA</i>	-.069	-.116	-.023	.004
	<i>PDA, nhs</i>	-.030	-.101	.041	.398
	<i>hs-PDA</i>	Reference			
	SNAPPE score	.001	.000	.002	.144
	GA in weeks	.007	-.010	.025	.409
	male sex	-.034	-.077	.008	.115
RI ICA left	PDA				.152
	<i>no PDA</i>	-.047	-.096	.003	.063
	<i>PDA, nhs</i>	-.001	-.075	.072	.968
	<i>hs-PDA</i>	Reference			
	SNAPPE score	.001	-.001	.002	.201
	GA in weeks	.002	-.017	.021	.817
	male sex	-.021	-.066	.024	.352
RI striatal artery right	PDA				.152
	<i>no PDA</i>	-.033	-.074	.008	.115
	<i>PDA, nhs</i>	-.050	-.114	.014	.123
	<i>hs-PDA</i>	Reference			
	SNAPPE score	.000	-.001	.002	.659
	GA in weeks	.000	-.015	.015	.962
	male sex	-.005	-.044	.034	.796

Table 6. Results linear regression analyses (continued)

Artery	Predictor	Coefficient	95% CI		p-value
			Lower bound	Upper bound	
RI striatal artery left	PDA				.84
	<i>no PDA</i>	.009	-.027	.044	.633
	<i>PDA, nhs</i>	-.006	-.064	.051	.833
	<i>hs-PDA</i>	Reference			
	SNAPPE score	.000	-.001	.002	.380
	GA in weeks	-.002	-.016	.012	.816
	male sex	-.010	-.044	.024	.561
RI pial artery	PDA				.249
	<i>no PDA</i>	-.050	-.115	.014	.125
	<i>PDA, nhs</i>	-.053	-.146	.039	.254
	<i>hs-PDA</i>	Reference			
	SNAPPE score	.001	-.001	.003	.369
	GA in weeks	.000	-.025	.024	.976
	male sex	-.008	-.068	.052	.788
RI basilar artery	PDA				.323
	<i>no PDA</i>	-.045	-.105	.015	.138
	<i>PDA, nhs</i>	-.028	-.113	.057	.511
	<i>hs-PDA</i>	Reference			
	SNAPPE score	.002	.000	.003	.094
	GA in weeks	.009	-.013	.031	.431
	male sex	-.002	-.055	.051	.937

Abbreviations:

ACA= anterior cerebral artery

ICA= internal carotid artery

GA= gestational age

hs-PDA= hemodynamically significant patent ductus arteriosus

PDA= patent ductus arteriosus

PDA, nhs= patent ductus arteriosus, not hemodynamically significant

RI= resistive index

SNAPPE= Score for Neonatal Acute Physiology, Perinatal Extension

Discussion

To our knowledge, this is the first study reporting prospective serial cerebral artery RI measurements in such a large cohort of preterm infants born at < 29 weeks gestation. We found that RI differed between arteries examined: large arteries showed significantly higher RIs than smaller arteries. Thus, when serially assessing RI, measurements must be made in the same artery to ensure valid comparison. Infants without patent ductus arteriosus had slightly lower RI than infants with hemodynamically significant patent ductus arteriosus, but this difference did not reach statistical significance in all arteries.

In infants who underwent ductal ligation, pre- and postligation RI did not differ. We found no significant relation between RI and SNAPPE-II score, gestational age, or sex.

In previous work, RI in internal carotid artery was higher than in anterior cerebral artery and middle cerebral artery¹⁶ and lower in lenticulostriate arteries in comparison to internal carotid artery, anterior cerebral artery and basilar artery.²³ However, in these studies exact RI values and statistical significance were not reported. Our study shows that RI is related to the diameter of the insonated artery: RI was higher in larger arteries. There was a considerable intersubject difference in RI between the larger internal carotid arteries, anterior cerebral artery and basilar artery on one hand and the smaller pial and striatal arteries on the other hand.²⁴ This difference can be explained by differences in peak systolic velocity and end-diastolic velocity between the greater and smaller cerebral arteries; in lenticulostriate arteries velocities are lower than in the great cerebral arteries, but the diastolic component is proportionally higher.² For accurate follow-up and comparison of RI, it is essential to serially assess the same artery at roughly the same level of its course. With current Doppler ultrasound techniques it is not possible to reliably measure the diameter of large intracerebral arteries in extremely preterm infants. Because of this inaccuracy we did not determine the diameter of the assessed arteries and diameter of the arteries was not included in the linear regression analysis.

In previous studies, there was no difference in RI between right and left-sided arteries.^{9,16} We did not find significant differences in RI between left and right striatal arteries in the same subject. However, a slightly higher RI was found in left internal carotid artery compared to right. This small difference, although statistically significant, seems clinically irrelevant. It could be a consequence of measurement variability. It may possibly be explained by a ductal steal phenomenon, as the duct is situated proximal to the left common carotid artery (and subsequently the left internal carotid artery) and more distal from the brachiocephalic trunk (and thus the right internal carotid artery). The higher RI in the left internal carotid artery could be explained by decreased EDV, which could render the left hemisphere more prone to intracerebral lesions, such as stroke or venous infarcts. For example, it has been described that the left hemisphere is preferentially affected in infants with perinatal arterial ischemic stroke.²⁵ However, stroke is often caused by embolism and it is not straightforward that arteries with higher RI would be preferentially affected by an embolus. In this study we did not examine the relationship between RI and focal brain injury.

In earlier work, RI in healthy term and preterm infants was inversely related to gestational age. However, differences due to gestational age were not statistically significant with regression analysis.¹⁶ In a study of 120 healthy preterm and term infants in the first 8 hours of life, RI in both anterior cerebral artery and middle cerebral artery increased

significantly with increasing gestational age.⁹ In our cohort of preterm infants born at < 29 weeks gestation, RI was not related to gestational age. This is probably explained by the narrower age range (*i.e.* 24–29 weeks gestation) compared to the aforementioned studies. There was no significant relation between RI and SNAPPE-II score or sex. To our knowledge, there are no studies on the association between RI and SNAPPE-II score.

In previous work, presence of patent ductus arteriosus was associated with higher RI, ascribed to decreased diastolic flow.¹⁴ Therefore, it was concluded that cerebral perfusion is affected by patent ductus arteriosus. In the present study, infants without patent ductus arteriosus had lower RI values than infants with echocardiographic hemodynamically significant patent ductus arteriosus, but this difference was small and statistically significant in some, but not all of the insonated arteries. Also, RI values in these two groups were overlapping for all arteries. This seems to implicate that high RI values in cerebral arteries are not always indicative of the presence of echocardiographic hemodynamically significant patent ductus arteriosus in very preterm infants. Another possible explanation is that the presence of echocardiographic hemodynamically significant patent ductus arteriosus may not always significantly affect cerebral perfusion, especially in the smaller cerebral arteries such as striatal arteries.

In our cohort, nine infants with echocardiographic hemodynamically significant patent ductus arteriosus underwent Doppler examination before and after ductal ligation. RI was not significantly different after ligation in any of the insonated vessels. In some infants RI was lower after ligation, in others it was higher. Two previous studies showed a significant drop in RI after ductal closure^{14,26}, due to increase of end-diastolic velocity. Sample sizes were small in both studies, eight and seven infants respectively.

In our experience, measurement of RI is relatively easy and not time-consuming. Absolute velocity measurements are difficult to compare, as they depend on the angle of the probe to the intracerebral vessel.¹⁶ RI value is not affected by changes in probe angle placement, because values for both peak systolic velocity and end-diastolic velocity will be affected similarly.^{7,16} It has been shown that assessment of RI is reproducible and interobserver reliability is high.² However, there are some pitfalls. Measurement of RI is non-continuous and represents a snapshot in time. As mentioned before, RI is related to the caliber of the insonated artery. For purposes of comparison and follow-up we therefore recommend to serially assess RI in the same artery at roughly the same level of its course. One should be aware that RI is an index, and will not change when both peak systolic velocity and end-diastolic velocity are similarly affected. For example, RI may be normal in a critical situation, such as low blood flow. RI will be abnormal only when either peak systolic velocity or end-diastolic velocity is predominantly affected.

For further understanding of the relation between systemic arterial blood pressure and intracerebral blood flow, cerebral oxygenation and functional state, it would be valuable to simultaneously monitor RI combined with invasive arterial blood pressure measurement, regional cerebral saturation and fractional tissue oxygen extraction using near infrared spectroscopy, evaluation of microcirculation²⁷ and electroencephalogram. Future research may gain insight into the relationship between RI and evolution of both unilateral and bilateral focal brain injury in very preterm infants.

Our report has limitations inherent to its design and local logistics. Because infants were transferred to level II hospitals when reaching a corrected age of 30 weeks gestation and when intensive care was no longer needed, the number of times RI was measured varied from one to eight times per subject. Not all seven arteries were examined in every session, for example when infants showed respiratory instability. One limitation is potential selection bias: as the patients that died soon after birth could not be included in this study, RI values in these patients are missing. Although the observers performed the RI measurements without knowledge of the clinical condition of the child, it is possible that they were aware that ductal ligation had taken place. Hence, the observers were not always blinded. We realize that physiological variables such as PCO_2 and treatments such as inotropics and blood transfusions could affect cerebral blood flow and consequently RI. However, as measurement of variables such as PCO_2 at the time of cranial ultrasound would imply additional blood sampling, we choose not to include these in this study. We did not assess the effect of fontanel pressure on RI. All measurements were made while fontanel pressure was kept to a minimum by applying a generous amount of gel, and low pressure was confirmed by visualizing flow through the superior sagittal sinus as a routine.

Conclusion

We present serial RI values in seven intracranial arteries in a cohort of 235 very preterm infants born at < 29 weeks of gestation. RI differs depending on the caliber of the examined artery: larger vessels showed significantly higher RIs than smaller vessels. Therefore, for accurate follow-up and comparison of RI of cerebral arteries in these infants, it is important to examine the same artery at roughly the same level of its course. Infants without patent ductus arteriosus had slightly lower RI than infants with hemodynamically significant patent ductus arteriosus, but this difference did not reach statistical significance in all arteries. In infants who underwent ductal ligation, pre- and postligation RI did not differ.

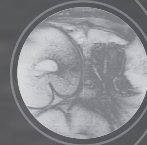
References

1. Liem KD, Greisen G. Monitoring of cerebral haemodynamics in newborn infants. *Early Hum Dev.* 2010;86:155-8.
2. Couture A.P. VC. Transfontaneller Doppler Imaging in Neonates. Berlin Heidelberg: Springer-Verlag 2001.
3. Lowe LH, Bailey Z. State-of-the-art cranial sonography: Part 1, modern techniques and image interpretation. *AJR Am J Roentgenol.* 2011;196:1028-33.
4. Allison JW, Faddis LA, Kinder DL, Roberson PK, Glasier CM, Seibert JJ. Intracranial resistive index (RI) values in normal term infants during the first day of life. *Pediatr Radiol.* 2000;30:618-20.
5. Ando Y, Takashima S, Takeshita K. Postnatal changes of cerebral blood flow velocity in normal term neonates. *Brain Dev.* 1983;5:525-8.
6. Archer LN, Evans DH, Levene MI. Doppler ultrasound examination of the anterior cerebral arteries of normal newborn infants: the effect of postnatal age. *Early Hum Dev.* 1985;10:255-60.
7. Gray PH, Griffin EA, Drumm JE, Fitzgerald DE, Duignan NM. Continuous wave Doppler ultrasound in evaluation of cerebral blood flow in neonates. *Arch Dis Child.* 1983;58:677-81.
8. Fenton AC, Shortland DB, Papathoma E, Evans DH, Levene MI. Normal range for blood flow velocity in cerebral arteries of newly born term infants. *Early Hum Dev.* 1990;22:73-9.
9. Pezzati M, Dani C, Biadaoli R, Filippi L, Biagiotti R, Giani T, Rubaltelli FF. Early postnatal doppler assessment of cerebral blood flow velocity in healthy preterm and term infants. *Dev Med Child Neurol.* 2002;44:745-52.
10. Meerman RJ, van Bel F, van Zwieten PH, Oepkes D, den Ouden L. Fetal and neonatal cerebral blood velocity in the normal fetus and neonate: a longitudinal Doppler ultrasound study. *Early Hum Dev.* 1990;24:209-17.
11. Ando Y, Takashima S, Takeshita K. Cerebral blood flow velocity in preterm neonates. *Brain Dev.* 1985;7:385-91.
12. Calvert SA, Ohlsson A, Hosking MC, Erskine L, Fong K, Shennan AT. Serial measurements of cerebral blood flow velocity in preterm infants during the first 72 hours of life. *Acta Paediatr Scand.* 1988;77:625-31.
13. Evans DH, Levene MI, Shortland DB, Archer LN. Resistance index, blood flow velocity, and resistance-area product in the cerebral arteries of very low birth weight infants during the first week of life. *Ultrasound Med Biol.* 1988;14:103-10.
14. Lipman B, Serwer GA, Brazy JE. Abnormal cerebral hemodynamics in preterm infants with patent ductus arteriosus. *Pediatrics.* 1982;69:778-81.
15. Mires GJ, Patel NB, Forsyth JS, Howie PW. Neonatal cerebral Doppler flow velocity waveforms in the uncomplicated pre-term infant: reference values. *Early Hum Dev.* 1994;36:205-12.
16. Seibert JJ, McCowan TC, Chadduck WM, Adametz JR, Glasier CM, Williamson SL, et al. Duplex pulsed Doppler US versus intracranial pressure in the neonate: clinical and experimental studies. *Radiology.* 1989;171:155-9.
17. Romagnoli C, Giannantonio C, De Carolis MP, Gallini F, Zecca E, Papacci P. Neonatal color Doppler US study: normal values of cerebral blood flow velocities in preterm infants in the first month of life. *Ultrasound Med Biol.* 2006;32:321-31.
18. Ando Y, Takashima S, Takeshita K. Cerebral blood flow velocities in postasphyxial term neonates. *Brain Dev.* 1983;5:529-32.
19. Blankenberg FG, Loh NN, Norbash AM, Craychee JA, Spielman DM, Person BL, Berg CA, Enzmann DR. Impaired cerebrovascular autoregulation after hypoxic-ischemic injury in extremely

- low-birth-weight neonates: detection with power and pulsed wave Doppler US. *Radiology*. 1997;205:563-8.
20. van Bel F, van de Bor M, Stijnen T, Baan J, Ruys JH. Cerebral blood flow velocity pattern in healthy and asphyxiated newborns: a controlled study. *Eur J Pediatr*. 1987;146:461-7.
21. Richardson DK, Corcoran JD, Escobar GJ, Lee SK. SNAP-II and SNAPPE-II: Simplified newborn illness severity and mortality risk scores. *J Pediatr*. 2001;138:92-100.
22. Tavera MC, Bassareo PP, Biddau R, Montis S, Neroni P, Tumbarello R. Role of echocardiography on the evaluation of patent ductus arteriosus in newborns. *J Matern Fetal Neonatal Med*. 2009;22 Suppl 3:10-3.
23. Couture A, Veyrac C, Baud C, Saguintaah M, Ferran JL. Advanced cranial ultrasound: transfontanellar Doppler imaging in neonates. *Eur Radiol*. 2001;11:2399-410.
24. van den Bergh R, van der Eecken H. Anatomy and embryology of cerebral circulation *Prog Brain Res*. 1968;30:1-25.
25. Benders MJ, Groenendaal F, De Vries LS. Preterm arterial ischemic stroke. *Semin Fetal Neonatal Med*. 2009;14:272-7.
26. Saliba EM, Chantepie A, Gold F, Marchand M, Pourcelot L, Laugier J. Intraoperative measurements of cerebral haemodynamics during ductus arteriosus ligation in preterm infants. *Eur J Pediatr*. 1991;150:362-5.
27. Raets MMA, Govaert P, Goos TG, Reiss IKM, de Jonge RCJ, Dudink J. Preterm cerebral microcirculation assessed with colour Doppler: a pilot study. *J Pediatr Neuroradiol*. 2014;3:155-60.

CHAPTER 4

Calibrating Doppler imaging of preterm intracerebral circulation using a microvessel flow phantom



F.A. Camfferman, G.M. Ecury-Goossen, J.E. La Roche, N. de Jong, W. van 't Leven, H.J. Vos, M.D. Verweij, K. Nasserinejad, F. Cools, P. Govaert, J. Dudink.

Front Hum Neurosci. 2015;8:1068.

Abstract

Introduction

Preterm infants are born during critical stages of brain development, in which the adaptive capacity of the fetus to extra-uterine environment is limited. Inadequate brain perfusion has been directly linked to preterm brain damage. Advanced high-frequency ultrasound probes and processing algorithms allow visualization of microvessels and depiction of regional variation. To assess whether visualization and flow velocity estimates of preterm cerebral perfusion using Doppler techniques is accurate, we conducted an in vitro experiment using a microvessel flow phantom.

Materials and Methods

An in-house developed flow phantom containing two microvessels (inner diameter 200 and 700 microns) with attached syringe pumps, filled with blood-mimicking fluid, was used to generate non-pulsatile perfusion of variable flow. Measurements were performed using an Esaote MyLab70 scanner.

Results

Microvessel mimicking catheters with velocities as low as 1 cm/sec were adequately visualized with a linear ultrasound probe. With a convex probe velocities < 2 cm/sec could not be depicted. Within settings, velocity and diameter measurements were highly reproducible (intra class correlation 0.997 (95% CI 0.996–0.998) and 0.914 (0.864–0.946)). Overall, mean velocity was overestimated up to 3-fold, especially in high velocity ranges. Significant differences were seen in velocity measurements when using steer angle correction and in vessel diameter estimation ($p < 0.05$).

Conclusion

Visualization of microvessel size catheters mimicking small brain vessels is feasible. Reproducible velocity and diameter results can be obtained, although important overestimation of the values is observed. Before velocity estimates of microcirculation can find its use in clinical practice, calibration of the ultrasound machine for any specific Doppler purpose is essential. The ultimate goal is to develop a sonographic tool that can be used for objective study of regional perfusion in routine practice.

Introduction

Central to normal human brain development and function is maintenance of adequate blood flow and oxygenation. This requires complex regulatory mechanisms, which at the early stages of human development, exist in a vulnerable equilibrium and are notoriously difficult to monitor. Severe neonatal conditions, such as prematurity, birth trauma, infections and congenital malformations, often compromise brain perfusion during this critical period of brain development and will grow into an avalanche of neurodevelopmental problems, including cognitive deficits, motor disability and psychiatric diseases^{1, 2} with ensuing lifelong burdens for the growing individuals and their families, and a major socio-economic impact for the health care system and the whole of society.³

Brain injury as a complication of preterm birth is directly or indirectly linked to low brain perfusion and oxygenation.^{4, 5} Although little is known about the ability of the preterm to regulate cerebral blood flow (CBF) in response to changes in perfusion pressure, there is some evidence that the autoregulatory range is limited compared with that of adults and absent in sick infants.⁶ Muscular walls are even absent in fragile medullary channels of the preterm brain, suggesting that some functional tools for autoregulation are not present yet.⁷ Consequently, extremes of systemic perfusion are transmitted unaltered to brain tissue. It is still a challenge to study neonatal organ and brain blood perfusion systematically. A reliable, objective, repeatable, safe and bedside method to characterize neonatal blood perfusion is needed.

Alternative methods to approximate blood flow, like blood pressure, diuresis, heart rate and limb oxygen saturation are extensively used, but are notoriously poor surrogates of neonatal brain perfusion. Standard techniques for adult brain studies are undesirable or very difficult to apply in the neonate. CBF measured with radioactive Xenon or jugular occlusion plethysmography, are disruptive to the infant and cannot be repeated frequently. MRI perfusion scans (such as arterial spin labeling) are not suited for (repeated) monitoring and require transport of often critically ill and clinically unstable infants to the radiology ward.⁸ Now tissue oxygen delivery can be studied using optical near infrared spectroscopy (NIRS), a bedside and safe technique, which allows continuous monitoring. However, NIRS is not quantitative and only provides indirect information about blood flow in regions that cannot be precisely pinpointed. Although trends in CBF may be inferred from changes in cerebral oxygenation and/or blood volume, NIRS does not allow a direct measure of CBF.^{9, 10}

EEG monitoring, like NIRS, is a safe and bedside neuro monitoring tool, which gained renewed interest of clinicians and researchers because of improved hardware and soft-

ware in recent years. However changes in EEG signal reflect large neuronal electrophysiological changes in a late and often irreversible stage of brain injury evolution.¹¹

Brain ultrasound is a widely used non-invasive and bedside tool for evaluation of neonatal brain anatomy and detection of brain injury. Color Doppler has already found a limited application in the analysis of patent ductus arteriosus and birth asphyxia. Indices like Pulsatility Index and Resistance Index have been developed and used as proxies for flow.^{12, 13} Recent advances in ultrasound technique have made visualization of small diameter vessels (microcirculation) possible.¹⁴ Yet, conventional pulsed wave Doppler (PW) is regularly used for absolute flow velocity measurements. Triplex mode imaging is used in current daily practice, in which flow information is overlaid to an anatomical B-mode image, and absolute flow velocities are measured in the PW Doppler panel.¹⁵ Flow information is visualized either in color flow mode (CD) or power Doppler (PD). In CD the color indicates average velocity in the vessel, which is sensitive to the angle of the vessel. In PD the color indicates the total amount of Doppler energy in the echo from the vessel, which is not sensitive to the angle. The general effect is that PD should be able to detect lower flow velocities and smaller vessels, at the cost of loss of quantitative velocity information. Moreover, the additional method directional power Doppler gives the power Doppler, but estimates the direction of the flow and colors it subsequently.

Although there is no general consensus on the definition of 'microcirculation' in the preterm brain, it is often defined as arteriolar and venular flow. Extrapolating from descriptions of vessel anatomy in fetuses, the diameter of microvessels visualized with Doppler in cerebral white matter of a preterm infant between 24 and 30 weeks is expected to be between 50 and 100 microns.^{7, 16} The large arteries of the circle of Willis of 24 week old fetuses have diameters around 400 to 500 microns.¹⁷ High-frequency linear probes permit visualization of vessels with a diameter below 200 micron. Therefore, visualization of the brain microcirculation of the preterm infant is feasible, making this a potential tool for in-vivo, safe, bedside, repeatable measurement of CBF. Still, one of the challenges of ultrasound is that the vessel caliber cannot be accurately measured, so that flow cannot be estimated.^{18, 19}

Models using a flow phantom and advanced (power) Doppler technique may be of use to objectively quantify regional flow variation. To mimic preterm brain tissue, this model should depict very small vessel sizes (about 200 micron) and very low flow (< 2 cm/ sec).

As far as we know, no studies are reported to assess the accuracy of current PW, CD, and directional PD techniques in the visualization of microperfusion. Our aim was to evaluate if velocity measurements of microvessels are reproducible and accurate using sensitive modern ultrasound techniques. The second aim was to determine which Doppler tech-

nique (color versus power Doppler, type of probe) is best used to visualize these small vessels. To this purpose, we set up an in vitro experiment using a microvessel flow phantom designed to mimic preterm cerebral perfusion. We hypothesized that current ultrasound technique is sufficiently accurate to estimate flow in preterm brain microvessels.

Material and Methods

Microvessel flow phantom

The flow phantom (figure 1) consisted of an acrylic container filled with agar-based tissue-mimicking material, built according to Teirlinck et al.²⁰ The tissue-mimicking material contained two vessels made of polyethylene terephthalate glycol-modified (Paradigm Optics, Vancouver, WA, USA) with an inner diameter of 200 microns each, and three silicone vessels (ERIKS bv, Alkmaar, the Netherlands) with an inner diameter of 700, 1000 and 2000 microns respectively. The blood-mimicking fluid (BMF) used to run through the vessels was based on the recipe by Ramnarine et al.²¹ However, our BMF contains half the amount of dextran and glycerol compared to the original recipe. This

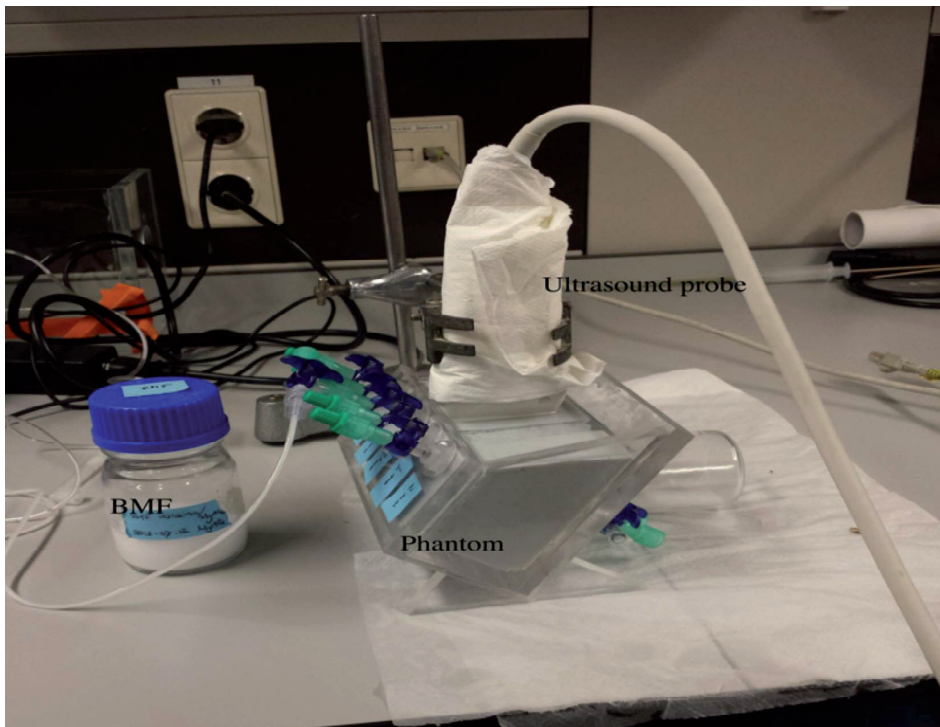


Figure 1. The test setting.

Flow phantom with a fixed ultrasound probe. BMF – Blood Mimicking Fluid

reduces the viscosity of the fluid, which is necessary to prevent blockage of the small vessels used in this study.

We intended to simulate the internal cerebral veins (ICV) and intracerebral medullary veins of very preterm infants using this microvessel flow phantom. Based on measurements performed in daily clinical practice the distance from the anterior fontanel to the ICV is 2.5 to 5 cm, and intracerebral medullary veins are located at a depth of 2 cm. Blood flow velocity in the ICV is about 5 cm/s and in medullary veins this lies around 1 cm/sec.^{22, 23} ICV diameter is estimated to be 500 microns in these neonates, while the diameter of the intracerebral medullary veins is around 100 microns.⁷ Since capillaries for the flow phantom with a diameter of 100 and 500 micron were not available, we used the 200 and 700 micron vessels for this study.

Test setting

To generate steady flow through the capillaries we used a calibrated syringe pump (Harvard Apparatus Pump 11 Elite, Instech Laboratories, Plymouth Meeting, USA) to infuse BMF at velocities ranging from 1 to 10 cm/s. This pump can produce regular flows as low as 1.28 pL/minute. To calibrate the syringe pump, we calculated expected BMF volume based on pump speed and duration of the experiment and compared this with the volume of BMF collected at the flow phantom outlet. Recording time was started at the first drop.

For each vessel size, flow settings ($\mu\text{L/s}$) were calculated according to the following equation:

$$Q = (V_{\text{avg}} \times \pi r^2) * 10^9 \quad (\text{Eq. 1}).$$

Q is flow in $\mu\text{L/s}$, V_{avg} is average velocity in m/s and r is the radius of the vessel in m.

Measurements were obtained using an Esaote system (Mylab 70, Genova, Italy) with a linear (Esaote LA 435 Linear Array Ultrasound Probe, 6.0–18.0 MHz) and convex probe (Esaote CA123 Convex Array Ultrasound Probe, 3.3–9.0 MHz). A standard ultrasound preset was used, identical to the preset used for imaging in daily clinical practice. This standard preset was optimized for neonatal preterm microvessel visualization prior to a large local prospective cohort study. The aim of that study was to explore the feasibility of color Doppler for monitoring of cerebral perfusion in very preterm infants at the level of microvessels (unpublished data of Raets *et al* - Preterm cerebral microcirculation assessed with colour Doppler: A pilot study). According to Ten Cate *et al*²⁴ the Esaote Ultrasound machine, as used in this experiment, proved to be more suitable for micro-circulation imaging in comparison to the other ultrasound brands. This is most probably

Table 1. Ultrasound settings used in this study

Doppler Mode	Probe	Frequency [MHz]	Gain [%]	PRF [kHz]	PRS	PRC	Wall Filter
PWD	Linear	5.9	53 – 60	0.5 – 10	-	6	100 Hz
	Convex	6.3	50 – 56	0.75 – 2	-	6	65 Hz
CD	Linear	7.7	50	0.37	16	M/2	1
	Convex	5	64	1.5	16	H/2	2
Directional PD	Linear	7.7	50	1 – 2.5	3, 4	M/2, H/2	2, 3
	Convex	5	64	1 – 2	3, 4, 6	L/2, M/2	2, 4

PWD – Pulsed wave Doppler, CD – Colour Doppler mode, PD – Power Doppler, PRF – Pulse repetition frequency, PRS – Persistence, PRC – Processing.

mainly caused by fundamental differences in processing the Doppler signal or internal settings inaccessible to users. Settings used in this study are summarized in Table 1. For the linear probe, settings included a transmit frequency of 7.7 MHz in flow visualization and 5.9 MHz in PW Doppler, a gain of 50% and an imaging depth of 30 mm. For the convex probe, settings included a transmit frequency of 5 MHz in flow visualization and 6.3 MHz in PW Doppler, a gain of 54% and imaging depth of 76 mm. Thermal and mechanical indices were always kept below 1.0.

The syringe pump was set to generate non-pulsatile perfusion of predefined volumes for each of the vessels (see above). Using the convex and linear probes, peak flow velocity and diameter of the capillaries was measured at 2 cm depth. Detection and diameter sizing measurements were performed using color flow mode (CD) and directional power Doppler mode (PD). To obtain diameter measurements, a Doppler image was frozen, and diameter was estimated using a manual caliber measurement. Velocity measurements were performed in the PW Doppler panel by manually putting a marker at the extreme bound of the PW profile. Since the flow was non-pulsatile, this extreme bound was persistent over the entire measurement period (1 or more seconds) and easily identifiable. When enabled, the steering angle was aligned parallel to the capillary. The velocity measurements were repeated three times at each predefined velocity. In order to minimize bias a single observer obtained the measurements in the presence of a second observer.

In order to prevent motion artifacts the probes were fixed using a tripod. With set flow velocities of 5 cm/s and above a pulsatile flow pattern was witnessed. This disturbance vanished when using a 10 ml low friction glass syringe (GASTIGHT #1010, Hamilton Company, Bonaduz, Switzerland) or a 60 mL plastic syringe instead of a 10 mL plastic syringe. Therefore, for all set flow velocities of 5 cm/s and more we used the glass syringe.

Statistical analysis

To assess the reproducibility of the velocity measurements and whether velocity measured with the ultrasound corresponded with the actual set velocity, one-way random intra-class correlation (ICC) coefficient was computed with single measures. Based on bootstrap sampling, the 95% confidence interval for ICC coefficient was calculated. To compare the measured diameter with the actual diameter of the capillaries we used the Student's one sample t-test. Statistically significant was assumed if two-sided p value was < 0.05 . All statistical analyses were performed in R (version 3.1.1; R Foundation for Statistical Computing, Vienna, Austria - <http://www.R-project.org>).

Results

Velocity measurements

Microvessels mimicking catheters with a size of 200 and 700 micrometer with BMF velocities as low as 1 cm/s were adequately visualized using a linear probe (figure 2). With a convex probe, however, velocities below 2 cm/s in the 700 micron vessel and below 3 cm/s in the 200 micron vessel could not be depicted.

Measurements of velocity and diameter proved to be highly reproducible, with an overall ICC coefficient of 0.997 (95% CI 0.996–0.998) and 0.914 (0.864–0.946) respectively.

As shown in table 2, in all different settings ICC coefficient of three consecutive velocity measurements stayed above 0.9 with a variation coefficient below 1.0, except for velocities measured in the 200 micron vessel with the convex probe.

Differences between true (pump) velocity and the peak measured Doppler velocity are shown in figure 3. Overall, pulsed wave Doppler overestimated velocity with a 1.1 to 3.5-fold overestimation. This is independent of the flow visualization method in the triplex mode, as expected (figure 3B). If velocity increased, spreading of the velocities measured in the different settings seemed to be more pronounced. However, this appeared to depend almost uniquely on the highly significant differences that were seen in velocity measurements with versus without steer angle correction ($p < 0.001$). When leaving out the steer angle velocity estimates, correlation between true velocities and measured velocity ameliorated.

Overall ICC coefficient between average velocity measured by Doppler and the true velocity was 0.352 (0.269–0.442). As shown in a Bland-Altman plot (figure 4), overall agreement between true velocity (velocity pump) and velocity estimated by Doppler was poor. However, results suggest consistent overestimation.

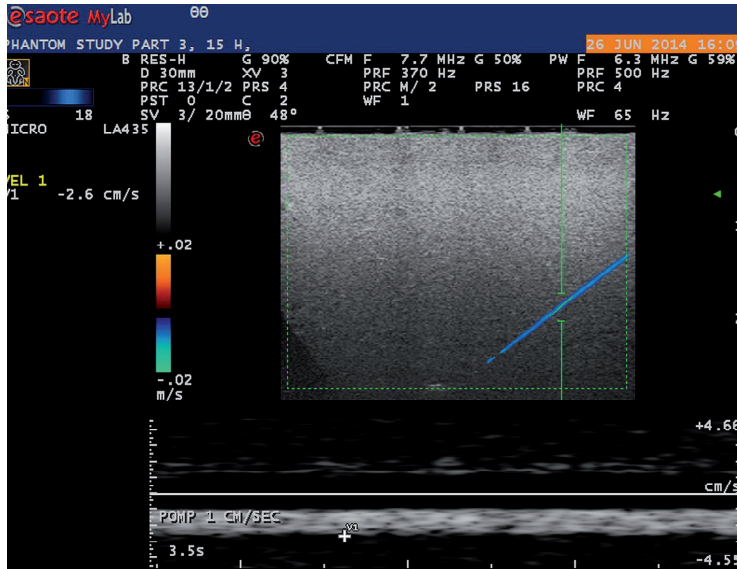


Figure 2. Ultrasound image of phantom microvessel.

Ultrasound image showing a 200 micron flow phantom catheter as depicted by a linear probe in color Doppler mode.

Table 2. Reproducibility of velocity measurements

Vessel diameter (μm)	Doppler mode	Probe	Steer angle correction	ICC (95% CI)	
200	Color	Linear	-	0.998 (0.991-1.000)	
			+	0.999 (0.996-0.999)	
		Convex	-	0.985 (0.643-0.989)	*
			+	0.991 (0.673-0.995)	*
	Power	Linear	-	0.997 (0.991-0.998)	
			+	0.997 (0.988-0.999)	
		Convex	-	0.915 (0.357-0.945)	*
			+	0.992 (0.702-0.998)	*
700	Color	Linear	-	0.999 (0.996-1.000)	
			+	0.999 (0.976-1.000)	
		Convex	-	0.986 (0.964-0.998)	**
			+	0.999 (0.992-1.000)	**
	Power	Linear	-	0.995 (0.933-0.997)	
			+	0.999 (0.996-0.999)	
		Convex	-	0.997 (0.991-0.999)	**
			+	0.999 (0.993-0.999)	**

Reproducibility of consecutive velocity measurements as showed by ICC (intra-class correlation) coefficients. Color – color Doppler, Power – power Doppler, v: velocity. * No visualization if $v \leq 2$ cm/sec. ** No visualization if $v = 1$ cm/sec

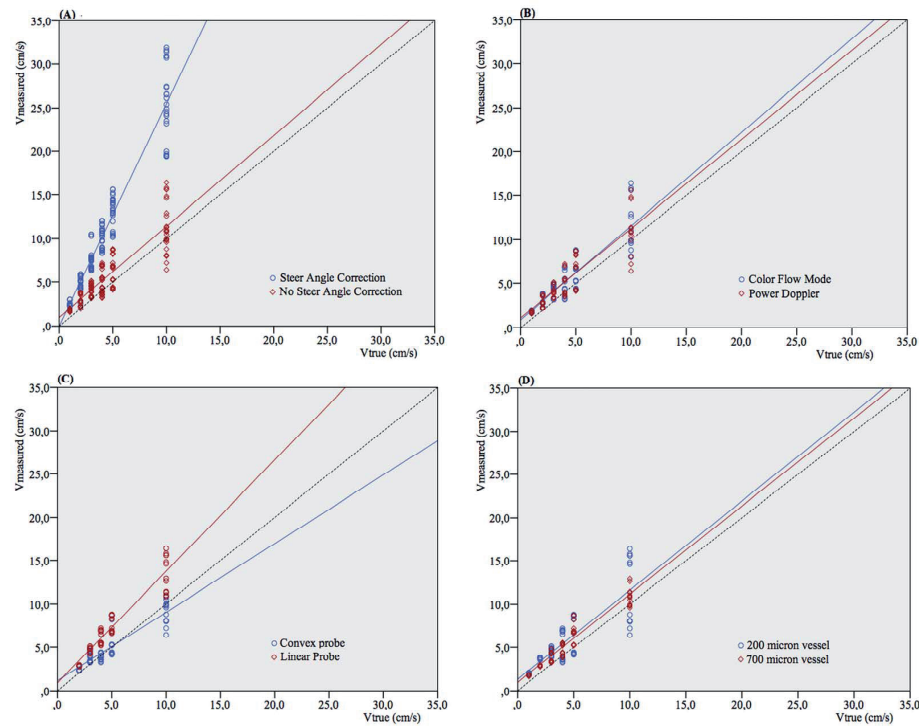


Figure 3. Pump velocity versus measured Doppler velocity. Relation between true velocity (cm/s) and velocity measured (cm/s) in different settings: (A) With or without steer angle correction, (B) Color Doppler versus Power Doppler, (C) Convex versus Linear probe, (D) vessel size. Since applying steer angle correction leads to significant ($p < 0.001$) overestimation of velocity, velocities in figure B, C and D are without applying steer angle correction. The dotted line represents the line of equality.

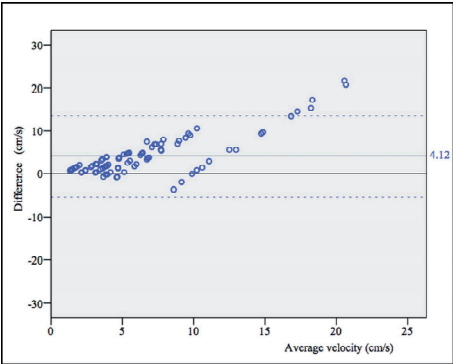


Figure 4. Agreement between true velocity and Doppler velocity. Bland-Altman plot of agreement between true velocity (V_{true}) and velocity estimated by Doppler measurements ($V_{measured}$). The mean difference is 4.12 cm/s (95%CI 3.10 - 5.15 cm/s), dotted lines represent ± 2 standard deviation borders.

Diameter measurements

Student-T test for vessel size showed significant differences in diameter estimation (p-values < 0.001 and 0.005 respectively). As shown in figure 5, vessel size was mostly overestimated by ultrasound.

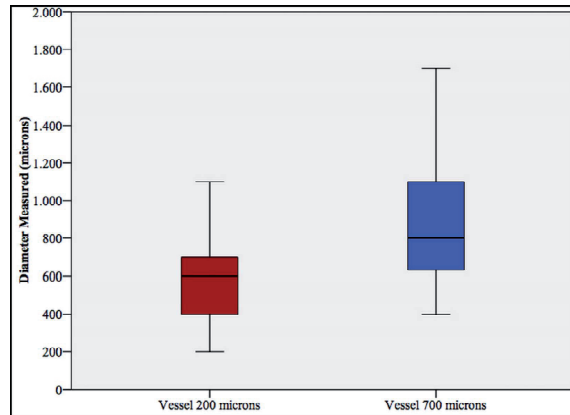


Figure 5. Vessel diameter.

Vessel diameter measured (\pm standard deviation) for the 200 micron vessel and the 700 micron vessel. Note the significant overestimation.

Discussion

In this flow phantom study we found that Doppler ultrasound imaging is able to visualize microvessel-size catheters with low flow, mimicking cerebral microcirculation. Within the different settings, reproducible velocity and diameter results can be obtained. Our overall results showed that vessel diameter and velocity are overestimated when measured by Doppler ultrasound. This corresponds with results of previous phantom studies.^{25–28} However, these studies were designed mainly to determine optimal machine settings and minimal detectable flow. To our best knowledge, this is the first in vitro experiment to calibrate for neonatal brain microcirculation.

Overestimation of flow velocity was observed in our study with convex as well as linear ultrasound probes. Previous publications^{20, 25, 29} described a similar phenomenon. Several aspects of Doppler technique and processing of the signals may contribute to this overshooting, as detailed below.

Firstly, it might be explained by sampling inaccuracy. The flow can be assumed parabolic in the low-Reynolds number regime asserted in our measurements. In such a flow, the peak velocity is two times higher than the average flow as predicted by Eq.

1. Moreover, we manually picked the maximum Doppler velocity in the PW panel, as in current clinical practice, not the average velocity. The effect of the flow profile on such Doppler-based velocity estimation is complex, but tends to overestimate the mean velocity.³⁰

A second explanation might be the way raw ultrasound data are filtered and processed within the ultrasound machine to produce an image. Most ultrasound machines consider the mean propagation speed c in tissue to be 1540 cm/s and use this value to calculate many values, of which velocity is one.^{31, 32} If the true propagation speed is higher than 1540 cm/s, this may lead to overestimation of predicted velocity. Exact propagation speed of preterm brain tissue is unknown and additionally depends on several other factors, like temperature and hydration status.³³ Also, in the process of filtering background scatter, some information might be lost or adapted, all according to the software used. At present we are not familiar with the manufacturer's confidential post processing algorithms to create an image from raw data. Especially when desiring to depict smaller vessels and lower flow velocities, insight in these methods and cooperation with the manufacturer in the development of new software might be of importance.

Thirdly, overshooting might be explained by insonation angle. Since both velocity and direction of blood flow determine Doppler shift, which is the main principle of Doppler ultrasound, insonation angle is an important determinant in calculating velocity. To make velocity quantification error as small as possible, the Doppler angle must be kept as small as possible.³² Current study was performed in a flow phantom with an insonation angle of about 60 degrees, which is considered the maximal insonation angle in clinical practice but still gives an important velocity estimation error. Additionally, increasing insonation angle worsens several Doppler artifacts, such as an intrinsic spectral broadening, which leads to a systematic overestimation in velocity measurements.³¹

Pulsed wave and color flow mode Doppler ultrasound depend on the time shift of pulsed wave echoes to calculate velocity and direction. In power Doppler, on the other hand, the color displayed is determined by the Doppler signal power rather than the effective time shift. In theory, this makes power Doppler more sensitive for visualization of low flow velocity.^{34, 35} Yet, our study shows that both directional PD and CD are able to detect flow velocities down to 1 cm/s with the linear array, which would indicate applicability of both methods in the current framework of preterm intracerebral circulation imaging. The measured velocities with PD were independent of the CD or PD visualization method, which is expected because of the independent nature of data acquisition and processing between PW Doppler and the visualization method.

As expected, applying the steer angle artificially corrects for the angle between flow direction and ultrasound beam. Since the measured Doppler value is divided by the cosine of the angle that the sonographer sets, it should always result in larger apparent velocities in the image.³⁶ This is consistent with our findings.

Considering the specific characteristics of the linear and convex ultrasound probes and their use in clinical practice, we expected the linear probe to be more suitable for microcirculation imaging. Indeed, lower flow velocities were visualized using the linear probe in the 200 micron vessel compared to the convex probe. As seen in figure 3 velocities were mainly overestimated by the linear probe, whilst the convex probe underestimated them. Apart from that, results show no obvious superiority for this probe and its specific settings, with reference to the diameter and blood flow velocity of the microvessels.

Since B-mode ultrasound is insufficiently accurate in estimating the diameter of microvessels, we tried to approach true diameter using color Doppler and power Doppler. Reproducible results were obtained, however overestimation was equally observed as in the velocity measurements. This inaccuracy in measuring diameter is a known problem of Doppler technique. Due to the relatively long transmit pulses in Doppler, axial accuracy of color Doppler systems is rather low, resulting in the encoding of the color sometimes beyond the true flow field.²⁹

Additionally, when adjusting instrument parameters, for instance increasing the gain, overestimation of vessel diameter is more likely.^{37, 38} Mitchell³⁹ stated that a jet area depicted by color imaging is likely to be more dependent on instrument parameters than on vascular anatomy or physiologic characteristics. However, current understanding of ultrasound technique and new in vitro models like this microcirculation flow model might give the opportunity to calibrate machine settings for measurement of diameter and true blood flow in near future. In a small spinoff pilot study ultrasound settings were adjusted according to flow phantom measurements allowing accurate caliber visualization during Doppler imaging, showing the feasibility of this technique.

In conclusion, Doppler ultrasound might be an additional diagnostic tool for quantification of neonatal brain blood flow. This study shows that, before starting to use velocity estimates in patients, calibration of the ultrasound machine for that purpose is needed. The ultimate goal of this type of research is to develop a sonographic tool that can be used for objectively studying regional (3D) perfusion in routine practice.

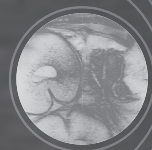
References

1. Sherlock RL, Anderson PJ, Doyle LW, Victorian Infant Collaborative Study G. Neurodevelopmental sequelae of intraventricular haemorrhage at 8 years of age in a regional cohort of elbw/very preterm infants. *Early Hum Dev.* 2005;81:909-916.
2. Volpe JJ. Brain injury in premature infants- a complex amalgam of destructive and developmental disturbances. *Lancet neurol.* 2009;110-124.
3. Petrou S, Sach T, Davidson L. The long-term costs of preterm birth and low birth weight- results of a systematic review. *Child Care Health Dev.* 2001;27:97-115.
4. Meek JH, Tyszczuk L, Elwell CE, Wyatt JS. Low cerebral blood flow is a risk factor for severe intraventricular haemorrhage. *Archives of Diseases in Childhood Fetal Neonatal Edition.* 1999;81:F15-18.
5. Kissack CM, Garr R, Wardle SP, Weindling AM. Postnatal changes in cerebral oxygen extraction in the preterm infant are associated with intraventricular hemorrhage and hemorrhagic parenchymal infarction but not periventricular leukomalacia. *Pediatr Res.* 2004;56:111-116.
6. Greisen G. Autoregulation of cerebral blood flow in newborn babies. *Early Hum Dev.* 2005;81:423-428.
7. Kuban KCK, Gilles FH. Human telencephalic angiogenesis. *Ann Neurol.* 1985;17:539-548.
8. Liem KD, Greisen G. Monitoring of cerebral haemodynamics in newborn infants. *Early Hum Dev.* 2010;86:155-158.
9. van Bel F, Lemmers PM, Naulaers G. Monitoring neonatal regional cerebral oxygen saturation in clinical practice: Value and pitfalls. *Neonatology.* 2008;94:237-244.
10. Marin T, Moore J. Understanding near-infrared spectroscopy. *Adv Neonatal Care.* 2011;11:382-388.
11. Hellström-Westas L. Continuous electroencephalography monitoring of the preterm infant. *Clinics in perinatology.* 2006;33:633-647.
12. Basu S, Dewangan S, Barman S, Shukla RC, Kumar A. Postnatal changes in cerebral blood flow velocity in term intra-uterine growth-restricted neonates. *Paediatr Int Child Health.* 2014;34:189-193.
13. Pezzati M, Dani C, Biadaioli R, Filippi L, Biagiotti R, Giani T, et al. Early postnatal doppler assessment of cerebral blood flow velocity in healthy preterm and term infants. *Dev Med Child Neurol.* 2002;44:745-752.
14. Macé E, Montaldo G, Cohen I, Baulac M, Fink M, Tanter M. Functional ultrasound imaging of the brain. *Nat Methods.* 2011;8:662-664.
15. Manual of diagnostic ultrasound. 2011:Page 17
16. Anstrom JA, Brown WR, Moody DM, Thore CR, Challa VR, Block SM. Subependymal veins in premature neonates: Implications for hemorrhage. *Pediatric Neurology.* 2004;30:46-53.
17. Vasovic LP, Jovanovic ID, Ugrenovic SZ, Andelkovic ZP. The posterior part of the human cerebral arterial circle (cac): Arterial caliber from gestational weeks 13 to 24. *J Anat.* 2007;211:612-619.
18. Kehrer M, Blumenstock G, Ehehalt S, Goelz R, Poets C, Schöning M. Development of cerebral blood flow volume in preterm neonates during the first two weeks of life. *Pediatr Res.* 2005;58:927-930.
19. Kehrer M, Krägeloh-Mann I, Goelz R, Schöning M. The development of cerebral perfusion in healthy preterm and term neonates. 2003. 2003;34:281-286.
20. Teirlinck CJPM, Bezemer RA, Kollmann C, Lubbers J, Hoskins PR, Fish P, et al. Development of an example flow test object and comparison of five of these test objects, constructed in various laboratories. *Ultrasonics.* 1998;36:653-660.
21. Ramnarine KV, Nassiri DK, Hoskins PR, Lubbers J. Validation of a new blood-mimicking fluid for use in doppler flow test objects. *Ultrasound Med Biol.* 1998;24:451-459.

22. Pfannschmidt J, Jorch G. Transfontanelle pulsed doppler measurement of blood flow velocity in the internal jugular vein, straight sinus, and internal cerebral vein in preterm and term neonates. *Ultrasound Med Biol*. 1989;15:9-12.
23. Deeg KH, Lode HM. [trans-fontanellar doppler sonography of the intracranial veins in infants—part i—normal values]. *Ultraschall Med*. 2005;26:507-517.
24. Ten Cate DF, Luime JJ, van der Ven M, Hazes JM, Kooiman K, de Jong N, et al. Very different performance of the power doppler modalities of several ultrasound machines ascertained by a microvessel flow phantom. *Arthritis Res Ther*. 2013;15:R162.
25. Schulten-Wijman MJ, Struijk PC, Brezinka C, De Jong N, Steegers EA. Evaluation of volume vascularization index and flow index: A phantom study. *Ultrasound Obstet Gynecol*. 2008;32:560-564.
26. Goertz DE, Christopher DA, Yu JL, Kerbel RS, Burns PN, Foster FS. High-frequency color flow imaging of the microcirculation. *Ultrasound Med Biol*. 2000;26:63-71.
27. Xu X, Sun L, Cannata JM, Yen JT, Shung KK. High-frequency ultrasound doppler system for biomedical applications with a 30-mhz linear array. *Ultrasound Med Biol*. 2008;34:638-646.
28. Raine-Fenning NJ, Nordin NM, Ramnarine KV, Campbell BK, Clewes JS, Perkins A, et al. Determining the relationship between three-dimensional power doppler data and true blood flow characteristics: An in-vitro flow phantom experiment. *Ultrasound Obstet Gynecol*. 2008;32:540-550.
29. Guo Z, Moreau M, Rickey DW, Picot PA, Fenster A. Quantitative investigation of in vitro flow using three-dimensional colour doppler ultrasound. *Ultrasound Med Biol*. 1995;21:807-816.
30. Ricci S, Matera R, Tortoli P. An improved doppler model for obtaining accurate maximum blood velocities. *Ultrasonics*. 2014;54:2006-2014.
31. Gill R. *The physics and technology of diagnostic ultrasound*. High Frequency Publishing; 2012.
32. Zagzebski JA. *Essentials of ultrasound physics*. Mosby; 1996.
33. Kremkau FW, Barnes RW, McGraw CP. Ultrasonic attenuation and propagation speed in normal human brain. *J Acoust Soc Am*. 1981;70:29-38.
34. Martinoli C, Derchi LE, Rizzatto G, Solbiati L. Power doppler sonography: General principles, clinical applications, and future prospects. *Eur Radiol*. 1998;8:1224-1235.
35. Murphy KJ, Rubin JM. Power doppler: It's a good thing. *Semin Ultrasound CT MR*. 1997;18:13-21.
36. Szabo TL. *Diagnostic ultrasound imaging: Inside out*. Academic Press; 2013.
37. Raine-Fenning NJ, Nordin NM, Ramnarine KV, Campbell BK, Clewes JS, Perkins A, et al. Evaluation of the effect of machine settings on quantitative three-dimensional power doppler angiography: An in-vitro flow phantom experiment. *Ultrasound Obstet Gynecol*. 2008;32:551-559.
38. Browne JE, Watson AJ, Hoskins PR, Elliott AT. Validation of a sensitivity performance index test protocol and evaluation of colour doppler sensitivity for a range of ultrasound scanners. *Ultrasound Med Biol*. 2004;30:1475-1483.
39. Mitchell DG. Color doppler imaging: Principles, limitations, and artifacts. *Radiology*. 1990;177:1-10.

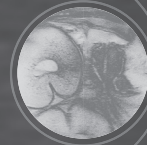
PART II

Neonatal focal brain lesions



CHAPTER 5

Risk factors, clinical presentation and neuroimaging findings of neonatal perforator stroke



G.M. Ecury-Goossen, M.M.A. Raets, M. Lequin, M. Feijen-Roon, P. Govaert, J. Dudink.

Stroke. 2013;44:2115-20.

Abstract

Background and Purpose

To date, studies on neonatal stroke have mainly focused on cortical stroke. We have focused on perforator strokes, non-cortical strokes in the arterial vascular perforator area. We sought to identify risk factors and to evaluate clinical presentation and neuroimaging findings for neonatal perforator stroke, which seems to be under-recognized.

Methods

All infants admitted to our tertiary intensive care unit in almost twelve years diagnosed with postnatal brain imaging to have a perforator stroke were enrolled in this study. Demographic, perinatal and postnatal data were evaluated.

Results

79 perforator strokes were detected in 55 patients (28 male) with a median gestational age of 37 1/7 weeks (range 24 1/7 to 42 1/7 weeks, 25 preterm). Perforator stroke was asymptomatic in most patients (58%). Initial diagnosis was predominantly made with cranial ultrasound (80%) in the first week of life (60%). Risk factors for stroke were present in all cases: maternal, fetal or perinatal. Likely pathogenic mechanisms were prolonged birth asphyxia (16%), hypoxia or hypotension (15%), embolism (15%), infection (15%), acute blood loss (9%) and birth trauma (9%).

Conclusions

Previously described risk factors for developing neonatal main artery stroke are probably also associated with neonatal perforator stroke. Perforator stroke is often asymptomatic, but cranial ultrasound is a reliable diagnostic tool in diagnosing perforator stroke.

Introduction

Advances in neuroimaging techniques have greatly improved detection and understanding of neonatal stroke.¹ Reported incidence of neonatal stroke in term newborns ranges from 1 in 2300 to 1 in 5900.¹⁻³ Benders et al. reported an incidence of 7 in 1000 preterm admissions.⁴ In most cases of neonatal stroke, the middle cerebral artery (MCA) is involved. For each of the cerebral arteries, main branch (cortical or pial) or perforator branch involvement can be distinguished.⁵ To date, studies on neonatal stroke have mainly focused on cortical stroke. Perforator stroke is apparently still under-recognized and little is known about risk factors and clinical presentation.

To gain more insight into risk factors, clinical presentation and neuroimaging findings of neonatal perforator stroke, we report the largest cohort to date of neonates diagnosed with perforator stroke.

Patients and methods

All infants admitted to our tertiary (neonatal) intensive care unit between August 1999 and April 2011 and diagnosed with perforator stroke by postnatal cranial ultrasound (CUS) and/or magnetic resonance imaging (MRI) were enrolled. The study was approved by the medical ethical committee of the Erasmus Medical Centre Rotterdam, the Netherlands.

Table 1. Perforator stroke classification

Vessel	Arterial perforator vessel	Territory
ACA	Heubner's	Rostroventral and lateral part of caudate head Lateral part of anterior limb of the internal capsule (ALIC)
MCA	Lenticulostriate	Posterior part of caudate head Lateral part of globus pallidus Putamen
PCA		Lateral, inferior and paramedian parts of thalamus
AChA		Medial part of globus pallidus Posterior limb of the internal capsule (PLIC) Amygdaloid nuclei
PCoA		Supero-anterior part of medial thalamic nuclei
Circle of Willis	Hypothalamus	
	Thalamus	Superolateral parts of thalamus

ACA= anterior cerebral artery

AChA= anterior choroidal artery

MCA= middle cerebral artery

PCA= posterior cerebral artery

PCoA= posterior communicating artery

Perforator stroke involves the perforators of the anterior choroidal artery (AChA), anterior cerebral artery (ACA), middle cerebral artery (MCA), posterior cerebral artery (PCA) and posterior communicating artery (PCoA), supplying amongst others thalamus, striatum, posterior limb of the internal capsule (PLIC) and centrum semiovale (see table 1).⁶

The anatomy of basal ganglia perforators is detailed in previous papers.^{5,6} Perforator stroke was defined as a well-delineated hyperechoic lesion in thalamus and/or striatum on CUS (see figure 1). Isolated lesions in centrum semiovale were not included, as these can not only be caused by focal arterial infarction in a terminal lateral striatal MCA branch. An alternative explanation could be by stroke of a ventriculopetal cortical arterial branch of the MCA with occlusion away from the surface as it courses in white matter. Also, isolated lesions in the centrum semiovale can be confused with punctuate white matter lesions. On MRI perforator stroke was defined as a well-lineated lesion, hypointense on T1-weighted imaging, hyperintense in T2-weighted imaging, hypointense on apparent diffusion coefficient maps and hyperintense on diffusion-weighted imaging (DWI).

All preterm infants had been screened by standard local CUS protocol, as a matter of clinical routine. This entailed at least two ultrasound studies in the first week of life, fol-

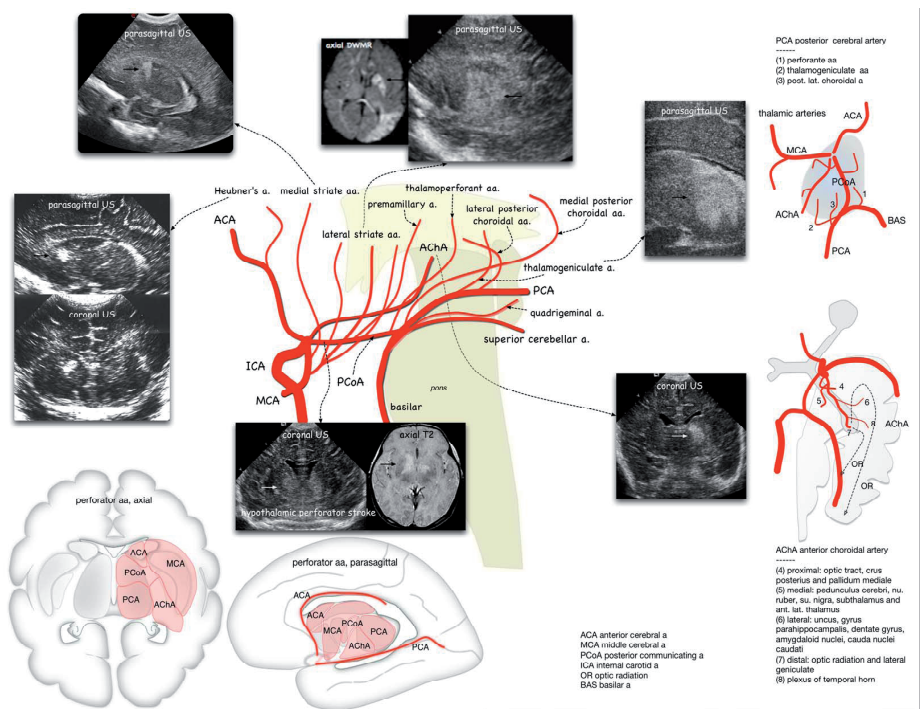


Figure 1. Axial and parasagittal perforator templates with illustrative cranial ultrasound and/or MRI images

lowed by weekly ultrasound studies until discharge. Term infants at risk for brain damage are screened with cranial ultrasound at the discretion of the attending physician. Sonograms were obtained using a Sequoia (Siemens, Mountain View, California) or an Esaote system (Mylab 70, Genova Italy). MRI scanning was performed on a 1.5-T GE EchoSpeed scanner (GE Medical Systems, Milwaukee, Wisconsin), using an MR-compatible incubator provided with a specialized high-sensitivity neonatal head coil. Perforator strokes first diagnosed with MRI (ML), were reviewed by two neonatologists (JD, PG) who also reviewed all CUS and remaining MRI studies independently and sought consensus for questionable imaging findings.

Demographic, perinatal, postnatal and short-term follow-up data were retrieved from the medical records. Perinatal data included delivery, gestational age, gender, birth weight, Apgar score, and umbilical cord pH. Postnatal data included respiratory support, CRIB (Clinical Risk Index for Babies) score⁷, the presence of central venous catheters, necrotizing enterocolitis (NEC), hypoglycemia, sepsis, and congenital heart disease. Clinical symptoms and neuroimaging findings preceding the radiological diagnosis of perforator stroke were reviewed.

Clinical phenotypes for perinatal stroke were classified by etiological mechanisms of neonatal stroke: infection, birth trauma, embolism, arteriopathy, blood loss, ECMO, asphyxia, prothrombotic condition, or unclassifiable.⁸

Results

Patient characteristics and risk factors

55 patients were included in this study, 0.7% of all 7713 patients admitted to our NICU during the study period, 0.5% of admitted preterm infants and 0.6% of admitted very low birth weight infants (birth weight < 1500 grams). Patient characteristics are shown in table 2.

Twenty-five patients were born preterm (< 37 weeks postmenstrual age), 17 of whom before 32 weeks postmenstrual age. Eight mothers had received antenatal betamethasone. Vacuum extractor was used in five cases, and was unsuccessful in one, in which emergency caesarean section was then needed. Sixteen other patients were delivered by emergency caesarean section because of suspected fetal distress. Eighteen patients were diagnosed with birth asphyxia according to Levene's criteria.⁹

Risk factors for developing stroke are summarized in table 3. Data on placental histology were recorded in only 15 cases. These data could not be retrieved for the 39 outborn children. In 8 of 15 cases the placenta was classified as abnormal (see table 3). There were no cases reported of perinatal stroke in a sibling. In two cases family history was

Table 2. Patient characteristics

	No. (%) or median (range)
Gestational age, weeks	37 1/7 (24 1/7 – 42 1/7)
Birth weight, grams	2640 (550 – 4440)
Male	28 (51%)
Singleton	48 (87%)
SGA	12 (22%)
Apgar score 1 minute (n = 53)	5 (0-10)
Apgar score 5 minutes (n = 54)	8 (2-10)
	n = 14 Apgar score ≤ 5
Umbilical cord pH (n = 31)	7,18 (6,73-7,39)
	n = 10 pH ≤ 7.05
CRIB score (n = 54)	2 (0-13)
Age at diagnosis of perforator stroke, days	6 (1-82)

SGA= small for gestational age

CRIB= Clinical Risk Index for Babies

Table 3. Risk factors for stroke

	No. (%)
Maternal	
Pre-eclampsia or HELPP syndrome	6 (11%)
Pregnancy induced- or pre-existing diabetes	3 (5%)
Placental abnormalities	8/15 (53%)
	n = 3 chorioamnionitis, n = 4 infarction, n = 1 placental abruption
Perinatal	
Complicated delivery*	21 (38%)
Perinatal asphyxia	18 (33%)
Fetomaternal transfusion	6 (11%)
Neonatal	
Sepsis or meningitis	18 (33%)
Patent ductus arteriosus	12 (22%)
Congenital heart defect	3 (5%)
ECMO	0 (0%)
Central venous catheter	45 (82%)
Hypoglycemia (< 2 mmol/l)	8 (15%)
Polycythemia (hematocrit > 65%)	8 (15%)
Prothrombotic risk factors	2/27 (7%)
NEC	6 (11%)

* forceps, vacuum extraction or emergency caesarean section.

HELPP= hemolytic anemia, elevated liver enzymes, low platelet count

ECMO= extracorporeal membrane oxygenation

NEC= necrotizing enterocolitis

positive for stroke. In both multiple family members suffered a stroke before the age of 50 years.

Thirteen children had culture proven sepsis, five had culture-proven meningitis (1 *Listeria monocytogenes*, 1 *E. Coli*, 3 *Group B Streptococcus*). Forty-five children had one or more central venous catheters before perforator stroke was diagnosed. Diagnosis of perforator stroke was followed by ultrasound evaluation of the catheter and major veins and/or heart in 24 cases. This revealed thrombosis in five (n = 2 thrombosis around the tip of the catheter, n = 3 venous thrombosis) and multiple air configurations in the liver in one patient (with an umbilical vein catheter). Prothrombotic screening was done in 27 patients, revealing heterozygosity for factor V Leiden in two cases. Etiological mechanisms leading to the perforator stroke are summarized in table 4.

Table 4. Etiological mechanisms leading to the perforator stroke

	Term (n = 30)	Preterm (n = 25)	Total
Infection			
- Sepsis	1	2	3
- Meningitis	4	1	5
Birth trauma	2	3	5
Embolism			
- Proven thrombosis of catheter	1	1	2
- Proven venous thrombosis	2	1	3
- Suspected thrombosis	2	0	2
- Suspected air embolism	0	1	1
Arteriopathy	1	1	2
Acute blood loss	3	2	5
Birth asphyxia	6	3	9
Prothrombotic condition	0	0	0
Other			
- Prolonged hypoxia/hypotension	3	5	8
Unclassifiable	5	5	10

Neuroimaging

Neuroimaging revealed 79 perforator strokes in 55 patients (see table 5); right-sided in 21, left-sided in 20, and bilateral in 14. These 14 patients had two to four perforator strokes each. Of these fourteen, none had symmetrical deep gray matter injury and only one was diagnosed with birth asphyxia according to Levene's criteria.¹⁰

In 44 patients (80%), the stroke was first identified with CUS. In 27 of them additional MRI was obtained, confirming the diagnosis of perforator stroke in all 27. In 10 patients (18%) the stroke was first diagnosed by MRI. In one patient the stroke was first diag-

Table 5. Perforator strokes in 55 neonates

	Right	Left	Total
ACA Heubner's	6	4	10
MCA	13	19	32
PCA	7	11	18
AChA	6	2	8
PCoA	5	3	8
Circle of Willis	1	2	3
	38	41	79

ACA= anterior cerebral artery

AChA= anterior choroidal artery

MCA= middle cerebral artery

PCA= posterior cerebral artery

PCoA= posterior communicating artery

nosed on a CT scan made elsewhere because of convulsions and later confirmed with MRI in our hospital.

In 33 patients (60%), the perforator stroke was diagnosed in the first week of life. Three patients with previous normal CUS findings were diagnosed with routine CUS after the age of 28 days. These were born preterm (between 28 and 31 weeks gestational age) and were diagnosed at term equivalent age.

13 patients had concomitant cortical stroke. In none of these patients perforator stroke could be explained solely by the concomitant cortical stroke. Table 6 gives an overview of all associated intracerebral lesions in this cohort.

Table 6. Associated intracerebral lesions

	No.
Cortical MCA stroke	11
Cortical PCA stroke	2
Watershed lesions	4
Grade II IVH and watershed lesions	1
Germinal matrix hemorrhage	2
Hydrocephalus	2
Cerebellar hemorrhage	1
Lissencephaly	1

MCA= middle cerebral artery

PCA= posterior cerebral artery

Presenting symptoms and clinical course

Perforator stroke was asymptomatic in 32 patients (58%), all diagnosed with routine neuroimaging. Twenty other patients (36%) had clinical seizures prior to the diagnosis of perforator stroke. Eighteen of these twenty patients were diagnosed with conditions which are known to cause seizures, such as cortical stroke, birth asphyxia and meningitis. Eight patients presented with apnea, which was probably related to prematurity, not to perforator stroke. One patient with meningitis presented with hypertonia. One patient presented with unexplained diminished arousal response and was later diagnosed with multiple perforator strokes (right MCA lateral striate stroke, left circle of Willis, left PCA thalamic stroke).

None of the patients in this cohort received thrombolytic therapy. Six patients died before the age of one month. None of these deaths was related to perforator stroke, but rather to cardiopulmonary insufficiency due to other neonatal complications.

Discussion

To our knowledge, this is the largest cohort of newborns with perforator stroke studied. Both preterm and term infants were included. We found that perforator stroke was asymptomatic in most patients (58%). Most strokes were first diagnosed using CUS (80%), predominantly in the first week of life (60%). Still, 40% were diagnosed *after* the first week of life and 5% were diagnosed with routine CUS after the age of 28 days. These numbers illustrate the importance of routine serial CUS screening in infants admitted to a neonatal intensive care unit. Right-sided lesions occurred as frequently as left-sided lesions. Various likely pathogenic mechanisms for the development of perforator stroke could be distinguished, most often birth asphyxia, prolonged hypoxia or hypotension, embolism, and infection. It seems likely that previously described risk factors for developing neonatal main artery stroke can also apply to neonatal perforator stroke. Maternal, fetal or perinatal risk factors were present in all cases.

Pregnancy is considered to be a natural prothrombotic state. Thrombosis on the fetal side of the placenta can potentially lead to embolism in the fetal brain as a result of right-to-left direction of blood flow in the fetal ductus arteriosus and patency of the foramen ovale. Placental disorders may be under-recognized in neonatal stroke, as placentas are often not adequately examined or have been discarded before stroke becomes apparent.¹¹ We had data on placental abnormalities for only 15 mothers. More than half of them had placental abnormalities that could be regarded as a risk factor for developing stroke, specifically placental infarction, chorioamnionitis and placental abruption.^{12–14}

In five patients, birth trauma was considered responsible for the occurrence of perforator stroke. Breech or forceps delivery can lead to indirect arterial injury by

traction-elongation-torsion. Subdural bleeding after a complicated delivery can lead to compression and/or spasm of the MCA or its branches, thus leading to stroke. In one case birth trauma led to tentorium tear and uncal herniation, presumably leading to compression of the PCA and thus to PCA artery stroke.¹⁵

Perinatal arterial ischemic stroke has been reported to coincide with hypoxic-ischemic encephalopathy and hypoxic-ischemic encephalopathy has been suggested to be a risk factor for perinatal stroke.¹⁶ Birth asphyxia can lead to congestion, endothelial injury and intravascular coagulation, thus leading to stroke.¹⁷ Hypoxic-ischemic encephalopathy is more often present in full-term infants than in preterm infants with stroke.¹⁸ This was also the case in the present study.

In this cohort, five perforator strokes were most likely related to meningitis. The perforator arteries course through the infected meninges to reach the brain parenchyma, and subarachnoid inflammation may encompass the major vessels of the circle of Willis. It has been suggested that local vasculopathy induced by infection and inflammation leads to thrombosis, resulting in occlusion of the arteries.¹⁹

Embolism was the most likely mechanism of stroke in 15% of patients in this cohort.

In two cases embolism was suspected, but not proven by ultrasound imaging; in one case from a femoral vein catheter used for exchange transfusion for jaundice, in another case from a suspected thrombus in a patient with an indwelling femoral vein catheter and abnormal anatomy of the inferior vena cava. In five cases proven thrombosis of a venous catheter or proven venous thrombosis most likely led to perforator stroke. In one patient abdominal ultrasound imaging revealed multiple air configurations in the liver, which probably led to air embolism, causing the stroke. These events could have been prevented by avoiding the use of central venous catheters. However, this is not always feasible, especially in a NICU setting. We recommend to critically evaluate the necessity of maintaining a central venous catheter.

In a study on risk factors for perinatal arterial stroke in preterm infants, hypoglycemia was the only independent risk factor identified in the neonatal period.¹⁸ In the present study, hypoglycemia was present in 8 patients, 7 of whom were preterm. In the subgroup of preterm infants 7 of 25 (28%) had hypoglycemia preceding the diagnosis of perforator stroke, compared to 1 of 33 term infants. It is not certain whether hypoglycemia did indeed precede perforator stroke, in view of the delay in detecting ultrasound abnormalities in infants with stroke.¹⁸

Prothrombotic screening at our institution has evolved over the years. Currently it entails antithrombin, protein S and protein C levels, factor V Leiden mutation and factor II G20210A mutation. In some cases screening is broadened to include lupus anticoagulans, MTHR C677T mutation and homocysteine levels. Twenty-eight patients (51%) in our study were not adequately screened for prothrombotic factors. Moreover, protein S, C and antithrombin levels were often not repeated after the neonatal period,

so congenital deficiencies could not be ruled out. Two patients, both with isolated perforator stroke, were diagnosed with factor V Leiden heterozygosity. It is unlikely that only the presence of factor V Leiden led to isolated perforator stroke.²⁰ These patients had multiple other risk factors, particularly acute blood loss. Earlier studies have found that prothrombotic coagulation factors are present in more than half of neonatal main artery strokes, but it has been suggested that they likely play only a minor role in the pathogenesis of stroke.^{11, 20}

In two patients stroke was most likely related to arteriopathy. One of these patients had Miller-Dieker lissencephaly, the other idiopathic infantile arterial calcification. Infantile arterial calcification has been related with cerebral infarction.²¹

Perinatal stroke is probably under-recognized because symptoms are subtle or absent and neonates may not undergo appropriate neuroimaging to identify stroke. It may be diagnosed serendipitously, as in the case of a term infant who was a control subject in a study of perinatal stroke and was diagnosed with a stroke on MRI.²² In the present study, perforator stroke was usually first identified with CUS – probably because CUS is the first choice imaging modality at our NICU. There is no evidence that CUS is superior to MRI in detecting a stroke. In 27 of 44 patients in which perforator stroke was first identified with CUS, subsequent MRI was obtained. MRI confirmed the diagnosis of perforator stroke in all of these 27 cases, illustrating that CUS is reliable in diagnosing perforator stroke. Cranial ultrasound is an essential part of the routine care in high-risk infants admitted to our NICU. Its major advantages are its safety, relatively low cost, the fact that it can be performed at bedside and can be repeated as often as necessary, making it the most suitable tool for serial imaging of the neonatal brain.²³ The value of CUS in detecting neonatal stroke has been described previously.^{5, 24}

In preterm neonates, sequential routine neuroimaging led to the diagnosis of perforator stroke. In term infants, indications for neuroimaging such as birth asphyxia and convulsions ultimately led to the diagnosis. Cortical stroke in full-term infants most often presents with seizures, apnea and non-focal neurologic signs.^{1, 25} Preterm infants are often free of symptoms, and cortical stroke is often diagnosed using routine cranial imaging. In the present study, perforator stroke was indeed asymptomatic in more than half of patients. Convulsions were a possible presenting symptom in one third of patients, mostly term neonates. In all but two patients these could be related to a more likely cause, such as concurrent cortical stroke, birth asphyxia and meningitis. The remaining two patients had multiple perforator strokes, possibly explaining the clinical presentation of seizures.

In (term) infants with perinatal stroke the left MCA is preferentially affected.⁴ In our cohort, however, there was no side preference. We have no obvious explanation for this. It is not explained by preferential direction of emboli; there was also no left-sided prefer-

ence in the subgroup of patients in whom embolism was the most likely pathogenic mechanism.

According to the definition provided by the Workshop on Ischemic Perinatal Stroke, neonatal ischemic stroke is diagnosed after birth and on or before the 28th postnatal day.²⁶ We chose to also include three neonates diagnosed after 28 days of life. These had normal CUS results prior to detection of perforator stroke. They were born preterm and were diagnosed at term corrected age with routine cranial ultrasound while still admitted. Two of them had proven thrombosis of a central venous catheter; one was diagnosed after developing NEC. This illustrates that perforator strokes in preterm infants can be diagnosed after the 28th day of life, especially when multiple risk factors are present.

Our report has limitations inherent to its retrospective design. As risk factors were studied retrospectively, risk analysis was incomplete and possibly biased. In relating the cases of perforator stroke to a clinical phenotype, ascertainment bias is inevitable.

Conclusion

In this cohort of neonatal perforator stroke various likely pathogenic mechanisms could be distinguished, notably prolonged hypoxia or hypotension, birth asphyxia, embolism, infection, acute blood loss, and birth trauma. Previously described risk factors for developing neonatal main artery stroke can probably also be applied to neonatal perforator stroke. In experienced hands, CUS is reliable in diagnosing perforator stroke. Isolated perforator strokes are most likely under-recognized, as clinical symptoms are almost always lacking. Routine serial CUS is therefore recommended, especially in preterm neonates. In combination with cortical stroke, hypoxic-ischemic encephalopathy or meningitis, convulsions can be a presenting symptom, especially in term neonates. Insight gained from ongoing follow-up of this neonatal perforator stroke cohort will help more accurately predict neurodevelopmental outcome.

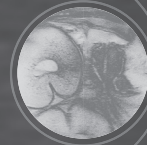
References

1. Nelson KB, Lynch JK. Stroke in newborn infants. *Lancet Neurol.* 2004;3:150-158.
2. Lee J, Croen LA, Backstrand KH, Yoshida CK, Henning LH, Lindan C, et al. Maternal and infant characteristics associated with perinatal arterial stroke in the infant. *JAMA.* 2005;293:723-729.
3. Chabrier S, Husson B, Dinomais M, Landrieu P, Nguyen The Tich S. New insights (and new interrogations) in perinatal arterial ischemic stroke. *Thromb Res.* 2011;127:13-22.
4. Benders MJ, Groenendaal F, De Vries LS. Preterm arterial ischemic stroke. *Semin Fetal Neonatal Med.* 2009;14:272-277.
5. Abels L, Lequin M, Govaert P. Sonographic templates of newborn perforator stroke. *Pediatr Radiol.* 2006;36:663-669.
6. Govaert P. Sonographic stroke templates. *Semin Fetal Neonatal Med.* 2009;14:284-298.
7. The crib (clinical risk index for babies) score: A tool for assessing initial neonatal risk and comparing performance of neonatal intensive care units. The international neonatal network. *Lancet.* 1993;342:193-198.
8. Govaert P, Ramenghi L, Taal R, Dudink J, Lequin M. Diagnosis of perinatal stroke ii: Mechanisms and clinical phenotypes. *Acta Paediatr.* 2009;98:1720-1726.
9. Levene MI LR. *Chapter: The asphyxiated newborn infant, pages 405-426.* Edinburgh: Churchill Livingstone 1995.
10. Swarte R, Lequin M, Cherian P, Zecic A, van Goudoever J, Govaert P. Imaging patterns of brain injury in term-birth asphyxia. *Acta Paediatr.* 2009;98:586-592.
11. Rutherford MA, Ramenghi LA, Cowan FM. Neonatal stroke. *Arch Dis Child Fetal Neonatal Ed.* 2012;97:F377-384.
12. Cheong JL, Cowan FM. Neonatal arterial ischaemic stroke: Obstetric issues. *Semin Fetal Neonatal Med.* 2009;14:267-271.
13. Elbers J, Viero S, MacGregor D, DeVeber G, Moore AM. Placental pathology in neonatal stroke. *Pediatrics.* 2011;127:e722-729.
14. Lynch JK. Epidemiology and classification of perinatal stroke. *Semin Fetal Neonatal Med.* 2009;14:245-249.
15. Govaert P, Vanhaesebrouck P, de Praeter C. Traumatic neonatal intracranial bleeding and stroke. *Arch Dis Child.* 1992;67:840-845.
16. Ramaswamy V, Miller SP, Barkovich AJ, Partridge JC, Ferriero DM. Perinatal stroke in term infants with neonatal encephalopathy. *Neurology.* 2004;62:2088-2091.
17. Voorhies TM, Lipper EG, Lee BC, Vannucci RC, Auld PA. Occlusive vascular disease in asphyxiated newborn infants. *J Pediatr.* 1984;105:92-96.
18. Benders MJ, Groenendaal F, Uiterwaal CS, Nikkels PG, Bruinse HW, Nievelstein RA, et al. Maternal and infant characteristics associated with perinatal arterial stroke in the preterm infant. *Stroke.* 2007;38:1759-1765.
19. Hernandez MI, Sandoval CC, Tapia JL, Mesa T, Escobar R, Huete I, et al. Stroke patterns in neonatal group b streptococcal meningitis. *Pediatr Neurol.* 2011;44:282-288.
20. Cnossen MH, van Ommen CH, Appel IM. Etiology and treatment of perinatal stroke; a role for prothrombotic coagulation factors? *Semin Fetal Neonatal Med.* 2009;14:311-317.
21. van der Sluis IM, Boot AM, Vernooij M, Meradji M, Kroon AA. Idiopathic infantile arterial calcification: Clinical presentation, therapy and long-term follow-up. *Eur J Pediatr.* 2006;165:590-593.

22. Mercuri E, Cowan F, Gupte G, Manning R, Laffan M, Rutherford M, et al. Prothrombotic disorders and abnormal neurodevelopmental outcome in infants with neonatal cerebral infarction. *Pediatrics*. 2001;107:1400-1404.
23. van Wezel-Meijler G, Steggerda SJ, Leijser LM. Cranial ultrasonography in neonates: Role and limitations. *Semin Perinatol*. 2010;34:28-38.
24. Cowan F, Mercuri E, Groenendaal F, Bassi L, Ricci D, Rutherford M, et al. Does cranial ultrasound imaging identify arterial cerebral infarction in term neonates? *Arch Dis Child Fetal Neonatal Ed*. 2005;90:F252-256.
25. Kirton A, Armstrong-Wells J, Chang T, Deveber G, Rivkin MJ, Hernandez M, et al. Symptomatic neonatal arterial ischemic stroke: The international pediatric stroke study. *Pediatrics*. 2011;128:e1402-1410.
26. Raju TN, Nelson KB, Ferriero D, Lynch JK, Participants N-NPSW. Ischemic perinatal stroke: Summary of a workshop sponsored by the national institute of child health and human development and the national institute of neurological disorders and stroke. *Pediatrics*. 2007;120:609-616.

CHAPTER 6

The clinical presentation of preterm cerebellar haemorrhage



G.M. Ecury-Goossen, J. Dudink, M. Lequin, M. Feijen-Roon, S. Horsch, P. Govaert.

Eur J Pediatr. 2010;169:1249-53.

Abstract

The objective of this study was to evaluate clinical symptoms and findings on cranial ultrasound (CUS) in preterm infants with cerebellar haemorrhage through retrospective analysis of all preterm infants with a postnatal CUS or MRI diagnosis of cerebellar haemorrhage admitted in a tertiary care centre between January 2002 and June 2009. Fifteen infants were identified; median gestational age was 25 2/7 weeks and median birth weight 730 g. We discerned six types of haemorrhage: subarachnoid ($n = 3$), folial ($n = 1$), lobar ($n = 9$, of which 4 bilateral), giant lobar ($n = 1$, including vermis) and contusional ($n = 1$). Especially in infants with lobar cerebellar haemorrhage, CUS showed preceding or concurrent lateral ventricle dilatation, mostly without intraventricular haemorrhage (IVH). Thirteen infants suffered from notable, otherwise unexplained motor agitation in the days preceding the diagnosis. In conclusion, motor agitation may be a presenting symptom of cerebellar haemorrhage in preterm infants. Unexplained ventriculomegaly can be a first sign of cerebellar haemorrhage and should instigate sonographic exploration of the cerebellum.

Introduction

Cerebellar haemorrhage in preterm infants has become a focus of attention, as it is associated with neurodevelopmental sequelae and mortality.^{1–4} Prevalences ranging from 2.3% to 19% for very low birth weight infants (VLBW) have been reported.^{3–6} With regard to neurodevelopmental sequelae, cerebellar haemorrhage may play a role in the cognitive, learning and behavioural dysfunctions known to affect survivors of preterm birth.² To our knowledge, there are no descriptions of the clinical presentation of this lesion in the early neonatal period. Early recognition of large cerebellar lesions is possible by cranial ultrasound (CUS) through the anterior fontanelle. It is thought, however, that a combination of striking clinical information and targeted scanning through mastoid or posterolateral fontanelle should facilitate recognition, even of small lesions.^{3, 5–8}

The aim of this study was to retrospectively analyse the clinical symptoms and CUS findings of preterm infants with cerebellar haemorrhage in order to increase understanding of presenting signs and symptoms.

Patients and Methods

From a detailed database we identified all preterm infants (< 37 weeks postmenstrual age) admitted to the Erasmus MC-Sophia Children's Hospital from January 2002 through June 2009 with a postnatal CUS or MRI diagnosis of cerebellar haemorrhage. Infants with chromosomal abnormalities and congenital brain anomalies were excluded. The enrolled infants had been screened by local protocol, which entailed at least two ultrasound studies in the first week of life, followed by weekly ultrasound studies until discharge. Standard imaging was performed through the anterior fontanelle. However, if a lesion in the posterior fossa was suspected, additional imaging was performed at 12–13 MHz through the mastoid fontanelle, also known as the posterolateral fontanelle.⁹ Sonograms were obtained using a Sequoia system (Siemens, Mountain View, California), and with Esaote system (Mylab 70, Genova Italy). The imaging studies were performed by neonatologists with experience in neonatal US brain imaging. Cerebellar haemorrhage was defined as a unilateral or bilateral hyperechoic change in the cerebellar hemisphere(s), vermis or subarachnoid layer. Following vaginal breech delivery, haemorrhagic changes in both inferior cerebellar areas were interpreted as contusion due to occipital osteodiastasis. Supratentorial IVH was graded using Papile's criteria.¹⁰ As CUS imaging was implicit to standard care, explicit parental consent was not requested.

Additional MRI had been performed, whenever feasible, if CUS findings suggested cerebellar haemorrhage. Scanning was performed on a 1.5-T GE EchoSpeed scanner (GE Medical Systems, Milwaukee, Wisconsin), using an MR-compatible incubator provided

with a specialised high-sensitivity neonatal head coil. All CUS and MRI studies were independently reviewed by two neonatologists (JD, PG), who reached consensus on the diagnosis.

Demographic, perinatal, postnatal and short-term follow-up data were retrieved from the medical records. Perinatal data included delivery, gestational age, gender, birth weight, Apgar score and cord pH. Postnatal data included respiratory support, use of inotrope agents, patent ductus arteriosus (PDA), sepsis and thrombocytopenia. PDA was diagnosed by echocardiography. Clinical symptoms and CUS findings preceding the radiologic diagnosis of cerebellar haemorrhage were reviewed. Ventriculomegaly was defined as a ventricular index more than two standard deviations above Levene's mean ventricular index.¹¹ The different types of cerebellar haemorrhages found were templated.

Results

We identified 15 preterm infants with a postnatal diagnosis of cerebellar haemorrhage in the period from January 2002 through June 2009, 0.5% of all 3,201 preterm infants admitted to the NICU during this period and 1% of the VLBW infants born in this period. Perinatal details are presented in Table 1.

Median gestational age was 25 2/7 weeks (range 24 6/7 to 32 1/7 weeks), and median birth weight was 730 g (range 535 to 1,905 g). Nine infants were small for gestational age, eleven were male, and seven were twins. Three mothers were diagnosed with pre-eclampsia/HELLP syndrome; three presented with preterm premature rupture of membranes, and three presented with placental abruption. Eleven mothers received antenatal betamethasone.

Five infants were born by caesarean section because they showed cardiotocographic abnormalities indicating foetal distress. Four were born following vaginal breech delivery. None were asphyxiated at birth. All required endotracheal ventilation, and ten received inotropic agents. Four were mildly thrombocytopenic on the first day of life (range 71,000–128,000/ μ L). Three infants with CUS diagnosis of cerebellar haemorrhage had become thrombocytopenic over the preceding days (range 6,000–26,000/ μ L). Eleven patients were treated for PDA. All of these were initially treated with indomethacin. Six underwent surgical ligation after treatment with indomethacin was not successful.

The initial CUS scans in 12 infants were normal prior to detection of cerebellar haemorrhage. The initial cranial sonograms of the remaining three revealed periventricular leukomalacia (infant 3), left-sided subependymal haemorrhage with lateral ventricle dilatation and left cerebellar haemorrhage (infant 11), and right-sided subependymal haemorrhage (infant 12). In 11 infants, CUS showed lateral ventricle dilatation preceding identification or coincident with cerebellar haemorrhage, which on standard CUS could

Table 1. Peri- and postnatal details of included infants

Case no, gender	GA (weeks)	Birth weight (grams)	Singleton/ twin	Delivery	Apgar score (1 and 5 min)
1, m	25 2/7	645	twin	SVD	8, 4
2, m	25 2/7	700	twin	SVD, breech	5, 8
3, f	32 1/7	1905	singleton	CS	4, 7
4, m	31 5/7	1700	singleton	SVD, breech	6, 8
5, m	25	650	singleton	SVD	8, 9
6, f	25 4/7	635	singleton	CS	1, 6
7, f	24 6/7	740	twin	SVD	2, 6
8, m	24 6/7	885	singleton	SVD, breech	2, 7
9, m	25 2/7	730	twin	CS	1, 3
10, m	24 6/7	760	singleton	SVD	4, 6
11, m	28 6/7	1110	singleton	CS	1, 7
12, m	25	730	twin	SVD	5, 8
13, m	25 1/7	720	twin	SVD	7, 8
14, f	25 5/7	535	singleton	CS, breech	1, 1
15, m	25 1/7	675	twin	SVD, breech	2, 7

CS= caesarean section

f= female

GA= gestational age

m= male

SVD= spontaneous vaginal delivery

not be explained by supratentorial IVH. Lateral ventricle dilatation was transient in all cases; none required intervention.

In 12 infants, cerebellar haemorrhage was first identified with CUS, between days 2 and 23 of life (median, 9). In six of these, subsequent MRI confirmed the diagnosis. Two patients died before MRI could be obtained (infants 13–14). In three others, cerebellar haemorrhage was first identified on MRI, which had been obtained because of the following findings on CUS: extensive periventricular leukomalacia (infant 3), grade III IVH with venous infarction (infant 4) and hyperechoic globi pallidi (infant 8).

Thirteen infants presented with striking motor agitation—as independently reported and noted in the records by at least two nurses—2 to 5 days (median, 3) preceding the diagnosis of cerebellar haemorrhage. Jerking of the extremities had been noted as a specific sign in three of those. Nine of these 13 infants received analgesics because of agitation, and one received a sedative. Generally, morphine was used for analgesia. No NSAIDs were used for analgesia. None of the infants were diagnosed with seizures, and none were treated as such.

An overview of radiological and clinical findings is provided in Table 2 and Figure 1. Figure 2 provides a CUS image of one of the included patients.

Table 2. Radiological and clinical findings

number	type of haemorrhage	ventriculo- megaly	associated lesions	motor unrest	neonatal death
3	subarachnoid unilateral (2 right, 1 left)	0	one with extensive haemorrhagic PVL	3	1
1	folial (1 left)	1	IVH grade 3	1	0
5	lobar unilateral (3 left, 2 right)	4	one with IVH grade 2	4	0
1	giant lobar unilateral (plus vermis) (left)	1	no IVH	1	0
4	lobar bilateral	4	one fetal IVH grade 3 with mantle destruction and complete cerebellar destruction	3	2
1	occipital osteodiasis (contusion of inferior surface(s))	1	no IVH	1	0

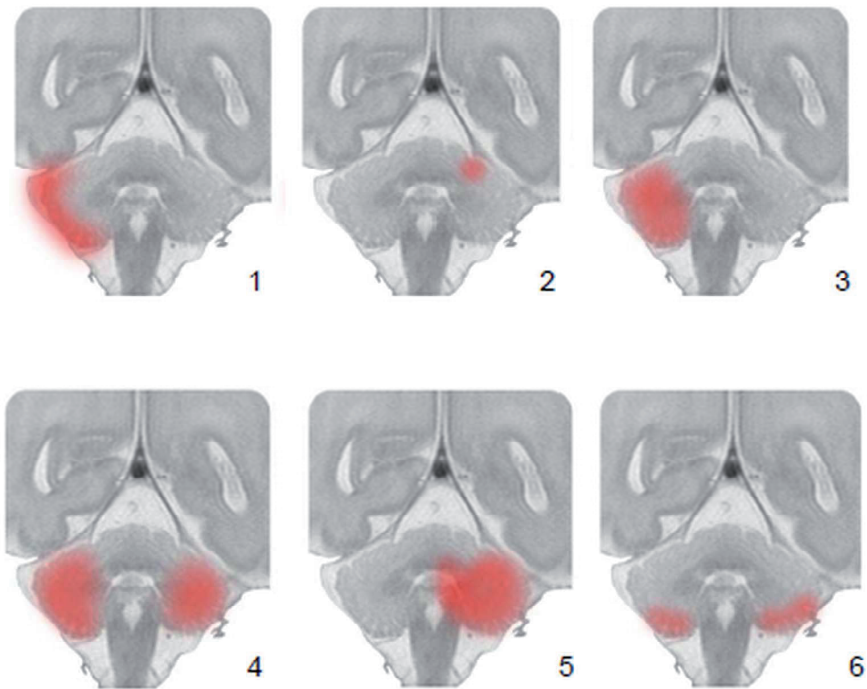


Figure 1. Cerebellar lesions templated

An overview of cerebellar haemorrhage in the included preterm infants. Six types of cerebellar haemorrhage were discerned: (1) subarachnoid, (2) folial, (3) lobar, (4) bilateral lobar, (5) giant lobar including vermis, (6) contusional.

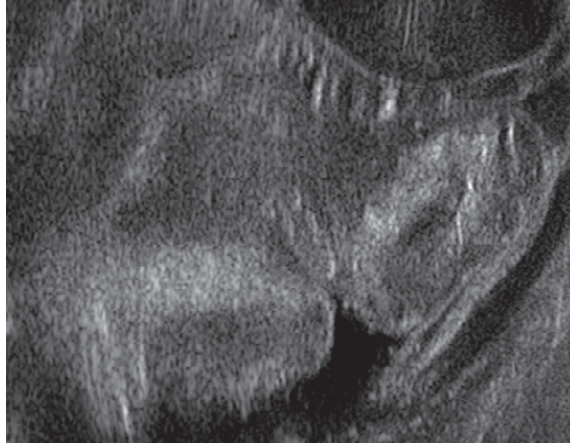


Figure 2

Bilateral cerebellar haemorrhage in one of the included patients. Coronal image reconstructed after parasagittal insonation of the cerebellum through the mastoid fontanelle.

6

Discussion

We reviewed both clinical symptoms and CUS findings in 15 preterm infants with cerebellar haemorrhage. All but two had shown otherwise unexplained motor agitation over the days preceding the diagnosis, suggesting this may be a presenting symptom of cerebellar haemorrhage. CUS preceding or coincident with identification of cerebellar haemorrhage revealed lateral ventricle dilatation in most infants with lobar haemorrhage, which could not be explained by supratentorial IVH. To our knowledge, these findings have not previously been described in preterm infants.

Cerebellar haemorrhage in preterm infants was first described as a post-mortem finding in autopsy studies and in case reports.^{12, 13} It is thought to be a multifactorial condition, with low gestational age and birth weight, vaginal delivery and instrumental or traumatic delivery as possible risk factors.^{3, 14–16} The majority of cerebellar haemorrhages in this cohort were diagnosed in extremely preterm infants; 11 of 15 patients were born after less than 26 weeks of gestation. Four patients in this cohort were born following vaginal breech delivery. Mechanisms underlying cerebellar haemorrhage are poorly understood. Some authors suggest that it follows bleeding from the germinal matrix in the subependymal layer of the fourth ventricle roof or in the subpial external granule cell layer.^{3, 17} One infant in the present study, who showed bilateral haemorrhagic changes in both lower hemispheres, probably suffered from occipital osteodystasia associated with vaginal breech delivery.¹⁸ Cerebellar haemorrhage may also develop after coagulopathy or an increase in venous pressure, for example, during extracorporeal membrane oxygenation.^{3, 16, 19} Furthermore, emergency caesarean section, PDA and early acidosis

may have an independent impact on the risk of cerebellar haemorrhage in preterm infants.⁵ One third of the infants in the present study were indeed born after emergency caesarean section, and more than two thirds were diagnosed with PDA. The latter figure is slightly lower than the 80% reported by Limperopoulos et al.⁵ Three infants in our cohort were diagnosed with lobar cerebellar haemorrhage following supratentorial IVH. Cerebellar haemorrhage has been reported to be associated with ultrasonographically detectable supratentorial lesions, mostly IVH.²⁰

Until today, it was thought that preterm cerebellar haemorrhage remains clinically silent except for apnoea.²¹ Based on our findings, we suggest, however, that otherwise unexplained motor agitation may be a symptom of cerebellar haemorrhage. The underlying mechanism could be explained as follows. The cerebellar cortex continuously inhibits signals sent to the brainstem and the thalamus by way of the efferent deep cerebellar nuclei. Destruction of cerebellar cortex, as in the case of cerebellar haemorrhage, will reduce the cortex's inhibitory capacity and thus lead to increased motor activity culminating in striking agitation.²² In addition, pain due to meningeal haemorrhage may contribute to agitation.

Eleven infants in the present study, most with lobar haemorrhage, showed noteworthy ventricular dilatation on CUS, unexplained by IVH, prior to or coincident with discovery of cerebellar haemorrhage. Merrill et al. described transient mild ventriculomegaly in one infant with cerebellar haemorrhage, but timing was not detailed.³ We conclude that the ventricular dilatation in this study is a consequence of the cerebellar haemorrhage. Large cerebellar haemorrhages can impede the liquor circulation in several ways: by compressing the fourth ventricle as a result of the swelling in the acute stage of haemorrhage, by rupture of haemorrhage into the fourth ventricle, or by subarachnoid bleeding in the cisterna magna or underneath the tentorium. Our findings suggest that ventriculomegaly in the absence of any supratentorial intracranial haemorrhage may be a sign of cerebellar haemorrhage, especially in infants with lobar cerebellar haemorrhage. Unexplained ventriculomegaly is a reason to carefully explore both cerebellar hemispheres for lobar bleeding.

The incidence of cerebellar haemorrhage in our study period (0.5%) was much lower than in previous studies.^{1, 3-5, 14} A possible explanation for this could be that we included infants less than 37 weeks gestation instead of only very low birth weight infants. Also, we may have missed cerebellar haemorrhages as ultrasound imaging through the mastoid fontanelle was not routinely used. CUS through the mastoid fontanelle can detect cerebellar injury missed by using the anterior fontanelle approach.^{3, 6, 7, 23} Posterior fossa views are generally not included, however, in standard CUS examination of preterm infants.⁶ We recommend using posterior fossa views, especially when preterm infants show either unexplained ventricular dilatation or motor agitation.

Our report has limitations inherent to its retrospective design. Reporting of motor agitation was not structured, and preterm infants may have other concurrent diagnoses that could result in motor agitation. The findings of motoric unrest and ventriculomegaly in this study can now be studied prospectively in future studies.

Conclusions

In the described cohort, we found otherwise unexplained motor agitation in preterm infants to be a presenting symptom of cerebellar haemorrhage. Furthermore, unexplained ventricular dilatation hinted towards the lesion in infants with large cerebellar lesions.

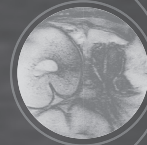
References

1. Bednarek N, Akhavi A, Pietrement C, Mesmin F, Loron G, Morville P. Outcome of cerebellar injury in very low birth-weight infants: 6 case reports. *Journal of Child Neurology*. 2008;23:906-911.
2. Limperopoulos C, Bassan H, Gauvreau K, Robertson RL, Sullivan NR, Benson CB, et al. Does cerebellar injury in premature infants contribute to the high prevalence of long-term cognitive, learning, and behavioral disability in survivors? *Pediatrics*. 2007;120:584-593.
3. Merrill J.D. PRE, Fell S.C., Barkovich A.J., Goldstein R.B. A new pattern of cerebellar hemorrhages in preterm infants. *Pediatrics* 1998;102 E62
4. Muller H, Beedgen B, Schenk JP, Troger J, Linderkamp O. Intracerebellar hemorrhage in premature infants: Sonographic detection and outcome. *J Perinat Med*. 2007;35:67-70.
5. Limperopoulos C, Benson CB, Bassan H, Disalvo DN, Kinnamon DD, Moore M, et al. Cerebellar hemorrhage in the preterm infant: Ultrasonographic findings and risk factors. *Pediatrics*. 2005;116:717-724.
6. Steggerda SJ, Leijser LM, Wiggers-de Bruine FT, van der Grond J, Walther FJ, van Wezel-Meijler G. Cerebellar injury in preterm infants: Incidence and findings on us and mr images. *Radiology*. 2009;252:190-199.
7. Enriquez G, Correa F, Aso C, Carreno JC, Gonzalez R, Padilla NF, et al. Mastoid fontanelle approach for sonographic imaging of the neonatal brain. *Pediatric Radiology*. 2006;36:532-540.
8. Miall LS, Cornette LG, Tanner SF, Arthur RJ, Levene MI. Posterior fossa abnormalities seen on magnetic resonance brain imaging in a cohort of newborn infants. *J Perinatol*. 2003;23:396-403.
9. Korsten A, Lequin M, Govaert P. Sonographic maturation of third-trimester cerebellar foliation after birth. *Pediatric Research*. 2006;59:695-699.
10. Papile LA, Burstein J, Burstein R, Koffler H. Incidence and evolution of subependymal and intraventricular hemorrhage: A study of infants with birth weights less than 1,500 gm. *Journal of Pediatrics*. 1978;92:529-534.
11. Levene MI. Measurement of the growth of the lateral ventricles in preterm infants with real-time ultrasound. *Arch Dis Child*. 1981;56:900-904.
12. Donat JF, Okazaki H, Kleinberg F. Cerebellar hemorrhages in newborn-infants. *American Journal of Diseases of Children*. 1979;133:441-441.
13. Schreiber MS. Posterior fossa (cerebellar) haematoma in the new-born. *Med J Aust*. 1963;2:713-715.
14. Dyet LE, Kennea N, Counsell SJ, Maalouf EF, Ajayi-Obe M, Duggan PJ, et al. Natural history of brain lesions in extremely preterm infants studied with serial magnetic resonance imaging from birth and neurodevelopmental assessment. *Pediatrics*. 2006;118:536-548.
15. Limperopoulos C, Robertson RL, Sullivan NR, Bassan H, du Plessis AJ. Cerebellar injury in term infants: Clinical characteristics, magnetic resonance imaging findings, and outcome. *Pediatric Neurology*. 2009;41:1-8.
16. Wigglesworth JS, Pape KE. Pathophysiology of intracranial haemorrhage in the newborn. *J Perinat Med*. 1980;8:119-133.
17. Castillo M. Selective vulnerability and the cerebellum in neonates. *American Journal of Neuroradiology*. 2007;28:20-21.
18. Hemsath FA. Birth injury of the occipital bone with a report of thirty-two cases. *Am J Obstet Gynecol* 1934;27:194-203.

19. Pape KE, Armstrong DL, Fitzhardinge PM. Central nervous system pathology associated with mask ventilation in the very low birthweight infant: A new etiology for intracerebellar hemorrhages. *Pediatrics*. 1976;58:473-483.
20. Volpe JJ. Cerebellum of the premature infant: Rapidly developing, vulnerable, clinically important. *Journal of Child Neurology*. 2009;24:1085-1104.
21. Martin R, Roessmann U, Fanaroff A. Massive intracerebellar hemorrhage in low-birth-weight infants. *Journal of Pediatrics*. 1976;89:290-293.
22. Haines DE. *Fundamental neuroscience for basic and clinical applications, 3rd edition*. . Oxford: Churchill Livingstone 2006.
23. Luna JA, Goldstein RB. Sonographic visualization of neonatal posterior fossa abnormalities through the posterolateral fontanelle. *American Journal of Roentgenology*. 2000;174:561-567.

CHAPTER 7

Serial cranial ultrasonography or early MRI for detecting preterm brain injury?



A. Plaisier, M.M.A. Raets, G.M. Ecury-Goossen, P. Govaert, M. Feijen – Roon, I.K.M. Reiss, L.S. Smit, M.H. Lequin, J. Dudink.

Arch Dis Child Fetal Neonatal Ed. 2015;100:F293-300.

Abstract

Objective

To investigate detection ability and feasibility of serial cranial ultrasonography (CUS) and early magnetic resonance imaging (MRI) in preterm brain injury.

Design

Prospective cohort study.

Setting

Level III neonatal intensive care unit.

Patients

307 infants, born below 29 weeks of gestation.

Methods

Serial CUS and MRI were performed according to standard clinical protocol. In case of instability, MRI was postponed or cancelled. Brain images were assessed by independent experts and compared between modalities.

Main outcome measures

Presence of preterm brain injury on either CUS or MRI and discrepant imaging findings on CUS and MRI

Results

Serial CUS was performed in all infants, early MRI was often postponed ($n = 59$) or canceled ($n = 126$). Injury was found in 146 infants (47.6%). Clinical characteristics differed significantly between groups that were subdivided according to timing of MRI. 61 Discrepant imaging findings were found. MRI was superior in identifying cerebellar hemorrhage; CUS in detection of acute intraventricular hemorrhage, perforator stroke and cerebral sinovenous thrombosis.

Conclusions

Advanced serial CUS seems highly effective in diagnosing preterm brain injury, but may miss cerebellar abnormalities. Although MRI does identify these lesions, feasibility is limited. Improved safety, better availability and tailored procedures are essential for MRI to increase its value in clinical care.

Introduction

Neurodevelopmental problems are common in preterm infants.^{1,2} Early objective diagnosis of brain injury is important for prognostication and decision making in neonatal intensive care. Current neuroimaging tools, such as magnetic resonance imaging (MRI), are suited for quantitative assessment of injury and can provide insight into pathogenesis of preterm brain injury.³ MRI is powerful, non-ionizing and has several advances to evaluate preterm brains: diffusion tensor imaging (DTI), functional MRI, volumetric MRI and proton MR spectroscopy allow quantification of disturbances in brain maturation and elucidate brain connectivity and functionality of infants born preterm. MRI is considered the best method to detect and quantify diffuse non-cystic white matter injury (WMI)⁴ and is increasingly performed at preterm age to provide early diagnosis of lesions.² However, MRI is expensive, time consuming and challenging for critically ill infants.

Cranial ultrasonography (CUS) is relatively cheap, directly available and allows serial bedside scanning with limited disturbance of the infant. Traditionally, CUS is used to detect germinal matrix and intraventricular hemorrhage (GMH-IVH) and periventricular leukomalacia (PVL). Its value to detect other lesions as well is increasing, owing to technical developments such as high-resolution ultrasound (< 200 micron), quantitative measurements and use of supplemental acoustic windows (mastoid and posterior fontanel).^{5–11} Limitations of CUS include observer-dependency¹², the challenge of reproducible objective measurement and problems to detect posterior fossa abnormalities and cerebral cortical changes.⁹

Based on comparative studies between MRI and CUS regarding abilities to predict outcome, MRI is proposed as imaging method of choice for high risk preterm infants^{13–15} especially when performed around term-equivalent age. However, these studies did not use additional acoustic windows, high-resolution ultrasound and Doppler imaging – as recommended by others.^{5, 16–18} And, most importantly, the limitations of MRI in clinical context are often not fully considered.

Routine MRI scans at 30 weeks gestation have the advantage of providing early detection of preterm related brain injury, which can help clinical decision making while infants are still requiring critical levels of support. Because of the critical period of brain plasticity between 30 weeks and term gestation early MRI scans seem a logical neuroimaging starting point. Currently more neonatal centers only perform routine term-equivalent-scanning, which provides important information regarding brain injury just before discharge, but lack the advantages mentioned above. Although several hospitals

perform scans at early preterm age, the clinical value of routine early MRI scans must first be established.

This study focuses therefore on feasibility of routine, clinical early MRI scanning compared to serial CUS in a vulnerable population in a prospective cohort study. Our aims were to investigate detection accuracy and clinical feasibility of serial CUS from birth until discharge compared with a routine MRI scan obtained from 30 weeks' postmenstrual age (PMA) onwards, in infants born < 29 weeks' gestational age (GA). We hypothesized that dedicated advanced serial CUS is equally effective as a single routine MRI scan at 30 weeks' PMA to diagnose common brain lesions in preterm infants and has higher clinical availability.

Methods

Patients

Between May 2010 and January 2013, infants born below 29 weeks GA were recruited prospectively. Standard clinical neuroimaging included serial CUS from birth until discharge and MRI at 30 weeks' PMA (29 4/7–30 4/7 weeks). MRI scans are timed at 30 weeks' PMA to enable early detection of brain injury and early parental counseling. Furthermore, our NICU policy includes that infants are transferred to other (non-NICU) hospitals once certain clinical criteria are met. As a result, term-equivalent scanning raises important logistic issues as most preterm infants are still admitted in other hospitals when they reach term-equivalent age. Of 336 eligible infants, 29 were excluded because of congenital malformation ($n = 18$), uncertainty regarding GA ($n = 5$) or refusal of parental informed consent ($n = 6$). The institutional review board approved this study and parental consent was obtained for all participants.

CUS

Serial CUS was performed by an experienced observer using an Esaote MyLab 70 (Genova, Italy). According to extended clinical protocol, images were obtained in standard sections; six coronal and five sagittal / parasagittal planes through the anterior fontanel, at days 0, 1, 2, 7 and subsequently, once a week until discharge. Additional images of the cerebellum and transverse sinus were acquired through the mastoid fontanel. Serial color Doppler imaging was performed to assess the intracranial (sino-) venous and arterial system (Fig. 1). Images were acquired with a convex, 8.5 MHz probe. To obtain higher resolution of superficially located areas, a high frequency linear probe (13 MHz) was used at the anterior and mastoid fontanel.

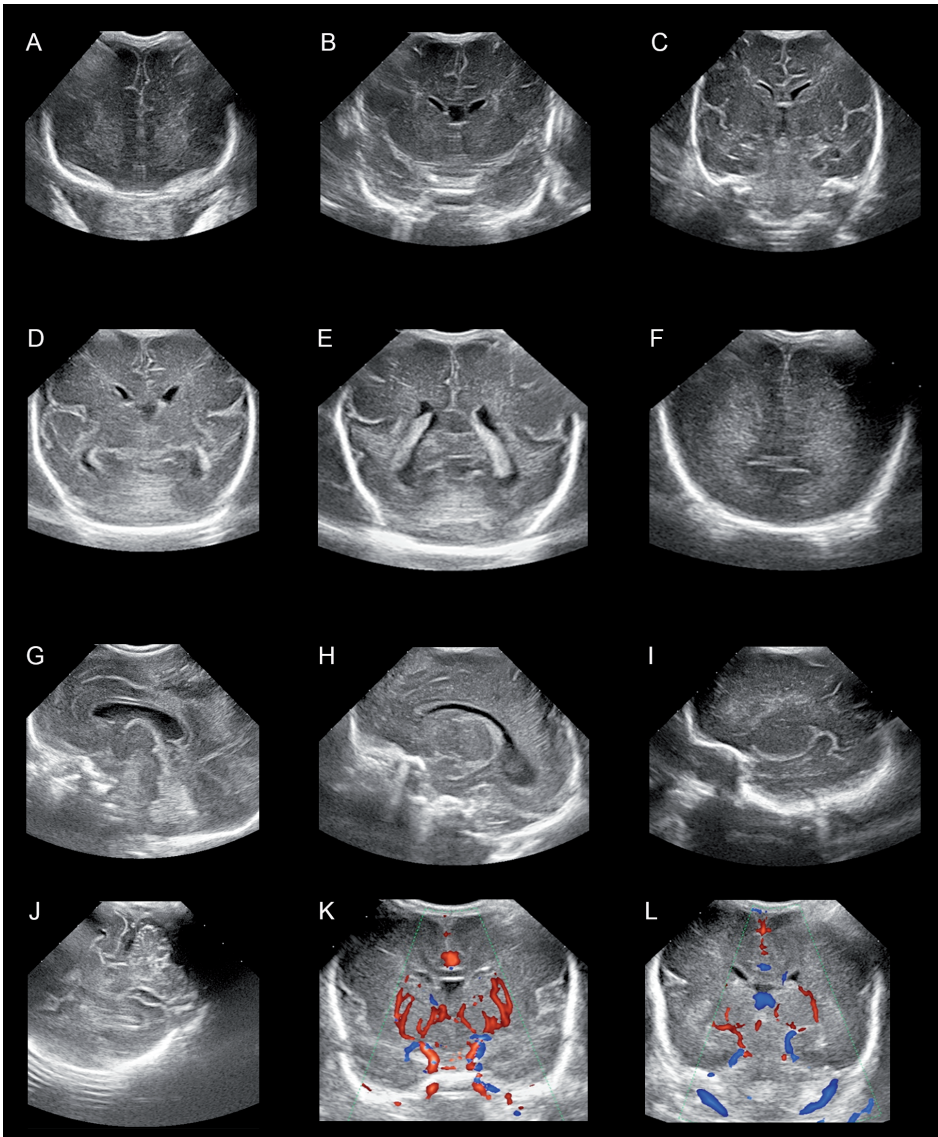


Figure 1

Ultrasound images were obtained in six coronal (A-F) and five sagittal/parasagittal planes (G-I) through the anterior fontanel. Additional images were acquired through the mastoid fontanel (J) to visualize the cerebellum and color Doppler images (K-L) were acquired to assess arterial and (sino-) venous systems.

MRI

MRI procedures were carried out according to our clinical guideline¹⁹: MRI scanning was postponed if patients were hemodynamically and respiratory unstable, which was evaluated by the attending neonatologist and nursing staff. All infants were accompanied by

trained staff and were placed in an MRI-compatible incubator, which allowed controlled temperature and humidity and MR-compatible pulse oximetry and ventilation. Moldable earplugs and neonatal earmuffs protected infants from auditory noise; sedative drugs were not administered.

Imaging data were acquired with a 1.5T GE EchoSpeed scanner (General Electric Healthcare Technologies, Waukesha, WI) (Fig. 2). Clinical imaging protocol included conventional MRI sequences and DTI. Axial T2-weighted fast-spin echo was obtained with the following parameter settings: repetition time (TR): 13100 ms; echo time (TE): 139 ms; slice thickness: 1.2 mm; field of view (FOV): 190x190 mm²; scanning time: 3:51 minutes. Axial 3D T1-SPGR was acquired using: TR: 9 ms; TE: 3 ms; slice thickness: 1.6 mm; FOV: 150x150 mm²; scanning time: 2:57 minutes. DTI was performed using a single-shot-echo-planar-imaging sequence with diffusion gradients in 25 non-collinear directions, TR: 11725 ms; TE: 85.6 ms; slice thickness: 3 mm; FOV: 220x220 mm²; *b* value: 750 s/mm²; number of non-diffusion-weighted images: 3; scanning time: 5:17 minutes.

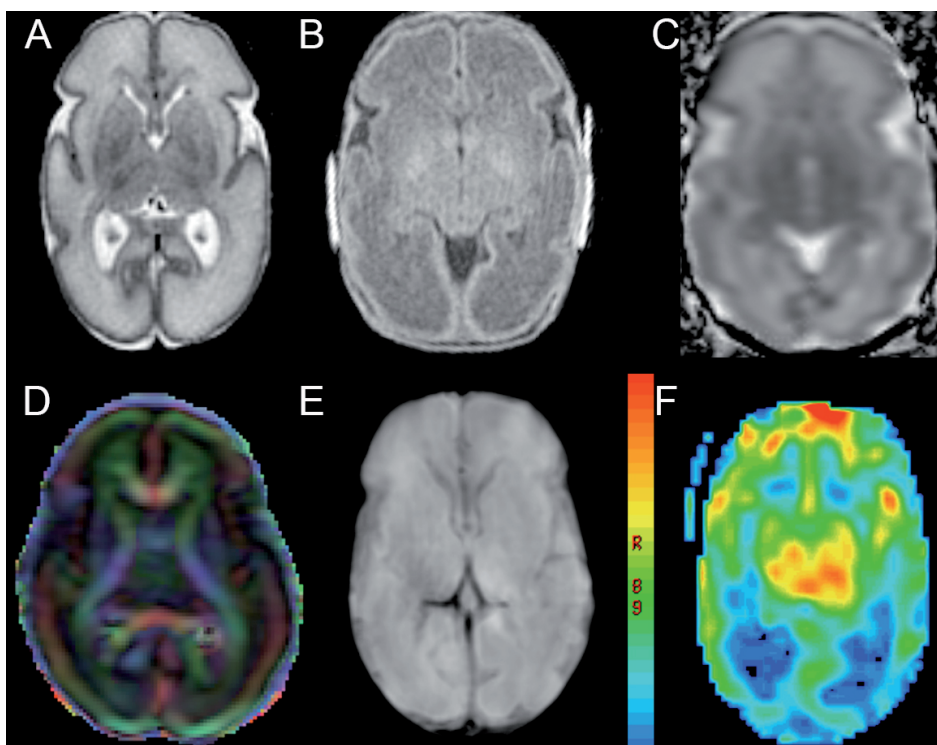


Figure 2

Applied MRI sequences: A: axial T2-weighted fast-spin echo; B: axial 3D T1-SPGR; diffusion tensor imaging, C: apparent diffusion coefficient-map and D: susceptibility weighted imaging.

For the sake of optimization during the study, advanced sequences were added to clinical scanning protocol: susceptibility weighted imaging (SWI) was performed using: TR: 75 ms; TE: 48 ms; slice thickness: 2.2 mm; FOV: 210x210 mm²; scanning time: 4:15 minutes. Arterial spin labeling was executed using: TR: 4200 ms; TE: 10 ms; post label delay: 1025 ms; slice thickness: 4 mm; FOV: 220x220 mm²; scanning time: 6:05 minutes.

Assessment of brain injury

CUS and MRI data were assessed for signs of preterm brain injury by experienced investigators independently (MR/PG for CUS and AP/ML for MRI, with > 20 years of experience in neonatal neuroimaging for PG and ML) using a detailed classification system that covers for most common types of brain injury²⁰ and has appropriately been described elsewhere.²¹ In all cases, consensus was reached between investigators. IVH was graded according to Volpe.²² WMI was classified into cystic PVL and diffuse non-cystic WMI; the latter were defined as periventricular inhomogeneous echodensities on CUS or diffuse WMI on MRI.^{4, 17} Cerebellar hemorrhage was categorized into folial or lobar cerebellar hemorrhage.²³ Presence of brain injury on CUS scans was based on cumulative findings of all serial assessments up until discharge from our NICU. Discrepancies between CUS and MRI were scored and we assessed whether CUS yielded additional diagnoses after the MRI was performed.

Statistical analysis

Statistical analysis was performed using SPSS version 20. Analysis was done in three steps: 1) description of clinical characteristics (table 1) and imaging findings (table 3) of all infants; 2) comparison of clinical characteristics between imaging groups (table 2) to highlight clinical feasibility of early MRI scanning in a vulnerable population compared to serial (bedside) CUS, and 3), comparison of imaging findings on CUS versus MRI to investigate their detection abilities (table 4). Descriptive statistics were applied to patient characteristics and neonatal morbidities. GA was calculated from the first date of the last menstrual period; severity of illness was assessed with the score for neonatal acute physiology perinatal extension²⁴; intrauterine growth restriction was defined as birth weight below two standard deviations; persistent ductus arteriosus was recorded if it required treatment and necrotizing enterocolitis was defined by pneumatosis intestinalis, hepatobiliary gas, or free intraperitoneal air on conventional X-rays. Differences between imaging groups were analyzed with one-way ANOVA for continuous variables (with post-hoc Bonferroni) and by Chi-squared tests for dichotomous/ordinal data (with post-hoc analysis using standardized residuals). Combined sum of findings by CUS and MRI served to calculate abilities of both imaging techniques to detect injury patterns. A *p*-value of < 0.05 (two-sided) was considered statistically significant.

Table 1. Subject characteristics

	Total (n = 307)
Gestational age, mean \pm SD ^a (weeks)	26.7 \pm 1.5
Birth weight, mean \pm SD (grams)	922 \pm 256
Head circumference, mean \pm SD (cm)	24.1 \pm 2.1
Sex, number of boys (%)	170 (55.4)
Apgar score at 5 minutes, mean \pm SD	7 \pm 2
Antenatal steroids	
None	28 (9.1)
1 dose, n (%)	88 (28.7)
2 doses, n (%)	187 (60.9)
Intrauterine growth restriction, n (%)	42 (13.7)
SNAPPE-score ^b , mean \pm SD	26 \pm 21
Postnatal steroids, n (%)	43 (14.0)
Necrotizing enterocolitis, n (%)	45 (14.7)
Persistent ductus arteriosus, n (%)	142 (46.3)
Death, n (%)	61 (19.9)
Postmenstrual age at MRI scan, mean \pm SD (weeks)	31.0 \pm 2.3
No signs of brain injury, n (%)	161 (52.4)

^a standard deviation; ^b score for neonatal acute physiology perinatal extension

Results

Subject characteristics

307 Infants (170 boys) were included in this study, with mean GA of 26 weeks, 5 days and birth weight of 922 grams. Additional clinical characteristics are listed in Table 1. All 307 infants were serially scanned using CUS according to imaging protocol, with a maximum delay of twelve hours. In contrast, MRI was not performed at all in 126 infants, as 57 died before 30 weeks' PMA; 55 were transferred to other hospitals before MRI scanning could be performed; and MRI was not performed in 14 due to logistic difficulties. At 30 weeks' PMA, 73 infants were considered not stable enough for MRI scanning; 59 of them were eventually scanned at a later time. Thus, three different groups with regard to MRI scanning are distinguished: group I: MRI scanning at 30 weeks' PMA ($n = 122$); group II: MRI scanning after 30 weeks' PMA ($n = 59$) and group III: no MRI scanning ($n = 126$) (Fig. 3).

Differences between imaging groups

Clinical characteristics between the three MRI imaging groups differed significantly (Table 2). Post-hoc analysis revealed that infants in imaging group I were born with higher GA and birth weight and seemed to have fewer complications: persistent ductus arteriosus, supplementation of postnatal steroids and death were significantly less com-

Table 2. Subject characteristics between imaging groups

	Group I (n = 122)	Group II (n = 59)	Group III (n = 126)	p-value
Gestational age, mean \pm SD ^a (weeks)	27.1 \pm 1.3 * ^^	26.5 \pm 1.3 *	26.5 \pm 1.6 ^^	0.001
Birth weight, mean \pm SD (grams)	994 \pm 224 ** ^^	855 \pm 191 **	884 \pm 294 ^^	< 0.001
Head circumference, mean \pm SD (cm)	24.7 \pm 1.8 * ^^	23.8 \pm 1.8 *	23.7 \pm 2.3 ^^	< 0.001
Sex, number of boys (%)	58 (47.5)	35 (59.3)	77 (61.1)	0.079
Apgar score at 5 minutes, mean \pm SD	8 \pm 1 ^	8 \pm 2	7 \pm 2 ^	0.012
Antenatal steroids				0.848
None	12 (9.8)	5 (8.5)	11 (8.7)	
1 dose, n (%)	35 (28.7)	14 (23.7)	39 (30.9)	
2 doses, n (%)	72 (59.0)	40 (67.8)	75 (59.5)	
Intrauterine growth restriction, n (%)	9 (7.4)	9 (15.3)	24 (19.0)	0.026
SNAPPE ^b -score, mean \pm SD	19 \pm 16 * ^^	27 \pm 15 *	34 \pm 25	< 0.001
Postnatal steroids, n (%)	5 (4.1)	12 (20.3)	26 (20.8)	< 0.001
Necrotizing enterocolitis, n (%)	11 (9.0)	9 (15.3)	25 (19.8)	0.138
Persistent ductus arteriosus, n (%)	44 (36.1)	42 (71.2)	56 (46.7)	< 0.001
Death, n (%)	2 (1.6)	2 (3.4)	57 (45.2)	< 0.001
Postmenstrual age at MRI scan, mean \pm SD (weeks)	30. \pm 0.3	33 \pm 3.3	-	< 0.001
No signs of brain injury, n (%)	58 (47.5)	27 (45.7)	76 (60.3)	0.05

^a standard deviation; ^b score for neonatal acute physiology perinatal extension;

Post-hoc Bonferroni analysis:

Group I versus group II: * p < 0.05; ** p < 0.01

Group I versus group III: ^ p < 0.05; ^^p < 0.01

mon and score for severity of illness was significantly lower. These characteristics differed most in comparison with imaging group III. Occurrence of necrotizing enterocolitis did not significantly differ between imaging groups (Table 2).

Patterns of preterm brain injury (Fig. 4)

Combined imaging findings

Injury patterns found either with CUS or MRI are listed in Table 3. GMH-IVH was detected in 100 infants, WML in 10, cerebellar hemorrhage in 21; cerebral sinovenous thrombosis (CSVT) in 11 and in 4 infants perforator stroke was identified.

Ultrasonographic findings

180 infants (58.6%) had normal CUS. GMH-IVH was seen in 80 infants (26.7%); in 23 this was limited to germinal matrix (7.5%), in 39 it was assigned IVH grade II (12.7%), in six IVH

Table 3. Patterns of preterm brain injury (combination of CUS and MRI findings)

	Total (n = 307)
Germinal matrix - intraventricular hemorrhage (GMH-IVH), n (%)	100 (32.6)
- GMH, n (%)	39 (12.7)
- Limited IVH grade II, n (%)	43 (14.0)
- Extensive IVH grade III, n (%)	6 (2.0)
- Periventricular hemorrhagic infarction, n (%)	12 (3.9)
White matter injury, n (%)	10 (3.3)
- Diffuse non-cystic white matter injury, n (%)	7 (2.3)
- Cystic periventricular leukomalacia, n (%)	3 (1.0)
Cerebellar hemorrhage, n (%)	21 (6.8)
- Folial hemorrhage, n (%)	9 (2.9)
- Lobar hemorrhage, n (%)	12 (3.9)
Cerebral sinovenous thrombosis, n (%)	11 (3.6)
Perforator stroke, n (%)	4 (1.3%)

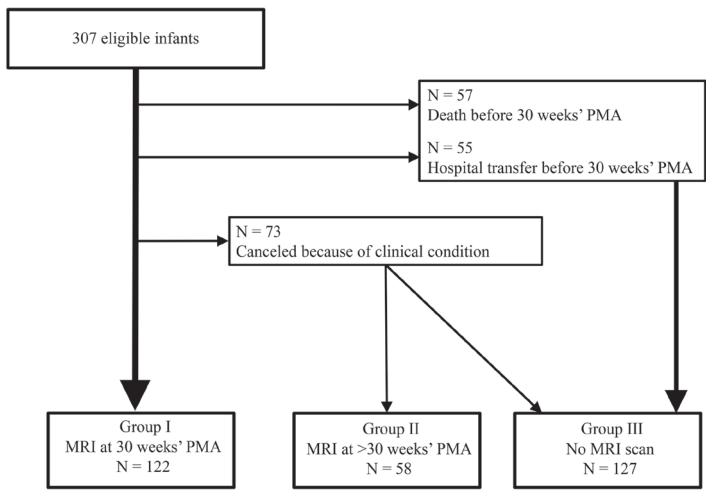


Figure 3
Flowchart of formation of neuroimaging groups.

grade III (2.0%) and in 12 (3.9%), hemorrhage was complicated by parenchymal infarction. WMI was sonographically detected in seven infants (2.2%); in four of them (1.3%) it was diffuse non-cystic WMI and in three (1.0%) cystic PVL was detected. Lobar cerebellar hemorrhage was identified in 10 infants (3.3%). Folial cerebellar hemorrhages were not

recognized with CUS. CSVT was present in 11 infants; in all, the transverse sagittal sinus was involved, in one infant there was also almost complete thrombosis of the superior sagittal sinus. Four infants presented with a perforator stroke on CUS.

MRI findings

MRI was performed in 180 infants and did not show any injury in 112 infants (62.2%). GMH-IVH was present in 43 infants (23.8%): GMH in 20 (11.1%); IVH-II in 14 (7.7%) and periventricular hemorrhagic infarction in nine infants (5.0%). WMI was detected in eight infants (4.4%); in seven (3.9%) this was diffuse non-cystic WMI and one infant had cystic PVL. Cerebellar hemorrhage was detected with MRI in 15 infants (8.3%); lobar in six and folial in nine. CSVT was identified on MRI in two infants; perforator stroke was not detected at all by MRI.

Discrepant imaging findings on CUS and MRI

Table 4 compares imaging findings of CUS with MRI findings in the 180 infants who were scanned by both techniques (group I and II). Inconsistencies were predominantly found for GMH-IVH in 38 infants, cerebellar hemorrhage in 11 and CSVT in seven infants. MRI had higher abilities to detect GMH and identified all posterior fossa abnormalities, but in 27 infants, CUS excelled in the acute detection of IVH grade II-III, perforator strokes and CSVT, as these lesions were no longer clearly visible on MRI at the time of scanning.

Table 4. Discrepant imaging findings on CUS and MRI in group I and II

	Imaging modality		
	Total	CUS	MRI
Germinal matrix - intraventricular hemorrhage (GMH-IVH), <i>n</i>	61	41 (67.2%)	43 (70.5%)
- GMH, <i>n</i>	25	9 (36.0%)	20 (80.0%)
- Limited IVH grade II, <i>n</i>	27	23 (85.2%)	14 (51.9%)
- Extensive IVH grade III, <i>n</i>	0	0	0
- Periventricular hemorrhagic infarction, <i>n</i>	9	9 (100%)	9 (100%)
White matter injury, <i>n</i>	8	5 (62.5%)	8 (100%)
- Diffuse non-cystic white matter injury, <i>n</i>	7	4 (57.1%)	7 (100%)
- Cystic periventricular leukomalacia, <i>n</i>	1	1 (100%)	1 (100%)
Cerebellar hemorrhage, <i>n</i>	15	4 (26.7%)	15 (100%)
- Folial hemorrhage, <i>n</i>	9	0	9 (100%)
- Lobar hemorrhage, <i>n</i>	6	4 (66.7%)	6 (100%)
Cerebral sinovenous thrombosis, <i>n</i>	9	9 (100%)	2 (22.2%)
Perforator stroke, <i>n</i>	2	2 (100%)	0

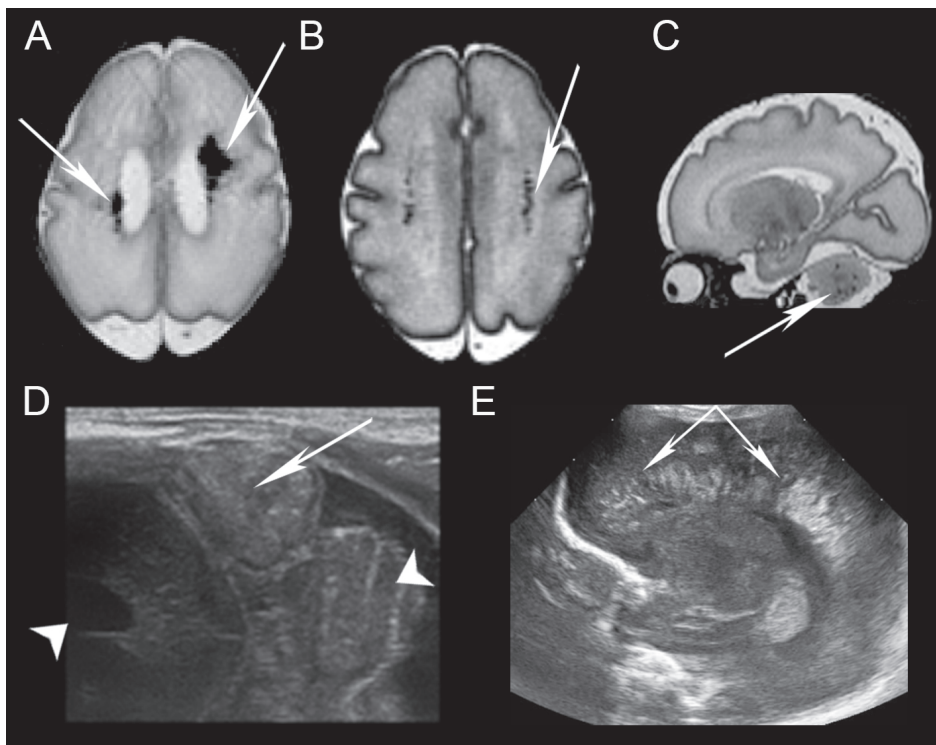


Figure 4

Examples of brain injury patterns on MRI (A-C) and CUS (D-E): A: bilateral periventricular hemorrhagic infarction on axial T2-weighted scan, note the ventricular dilatation caused by intraventricular hemorrhage; B: punctate white matter lesions on axial T2-weighted scan; C: multiple folial cerebellar hemorrhages on sagittal T2-weighted scan; D: cerebral sinovenous thrombosis in transverse sinus on cranial ultrasound, assessed through mastoid fontanel, note the large mass (arrow) between the lateral ventricle (left arrowhead) and cerebellum (right arrowhead) and E: periventricular leukomalacia on parasagittal cranial ultrasound, assessed through the anterior fontanel.

Findings for WMI were discrepant in three infants. None of the discrepancies between CUS and MRI were detected after the MRI was performed.

Discussion

This study demonstrates the high number of preterm infants with detectable brain injury (47.6%) and shows how serial advanced CUS effectively detects most common lesions. CUS has higher clinical feasibility than MRI, which cannot always be performed in severely ill infants. However, despite mastoid fontanel scanning, CUS remains inferior to identify small posterior fossa abnormalities. MRI provided important additional diag-

nostic information. Although other studies have predominantly investigated the value of MRI and CUS to detect WMI, main strength of this study is that it investigated their value for several brain injuries. In addition, this study demonstrates the complementary roles of both imaging modalities to detect common patterns of preterm brain injury: MRI was better to detect GMH and posterior fossa abnormalities, whereas CUS was better at grade II-III IVH, perforator stroke and CVST.

Although MRI performed at term-equivalent age is highly predictive of neurodevelopmental outcomes, prognostication can currently only be accurately made until that moment. Performing early MRI scans may result in earlier prognostication and may be of special interest in settings where infants are often transferred to level II hospitals once certain clinical criteria are reached. Moreover, early by proxy MRI biomarkers of future neurodevelopmental outcome can also guide randomization of future neuro-protective and -rehabilitation trials. However, before early MRI scans can be implemented as standard of care for preterm infants, clinical applicability and sensitivity must first be established. This study addressed these matters of early MRI scans in a vulnerable population.

Comprehensive application of CUS, usage of supplemental acoustic windows, color Doppler imaging, higher transducer frequencies and careful interpretation of images by an experienced observer results in high accuracy to identify certain lesions. Serial CUS outperformed MRI scan in diagnosing focal lesions in 27 infants, mostly because of higher sensitivity to detect perforator stroke and CSVST.

Clinical relevance of diagnosing perforator stroke and CSVST seems important as detection of these lesions may have therapeutic and diagnostic consequences. Infants with CSVST may need thrombolytic treatment and as with perforator strokes may prompt assessment of thrombophilic factors. Perforator strokes are small and more challenging to detect on MRI with lower resolution in this brain area than CUS. Therefore we believe that timing is not the only reason for the mismatch in diagnostic tools. Thinner slices and advanced sequences (such as SWI) may improve identification of perforator strokes using MRI.

The higher ability of CUS to detect IVH grade II seems mainly attributable to consecutive application of CUS and timing of onset of IVH. Conventional MRI did not always detect low grade IVH, possibly due to the resolving nature of IVH. Parodi et al.²⁵ recently reported a lower sensitivity (60%) of CUS to detect grade I-II GMH-IVH compared with SWI. The authors point out the unique possibilities of SWI to detect subependymal and/or intraventricular hemosiderin depositions and accentuate that dedicated timing and application of advanced MRI sequences is valuable in assessing preterm brains.

In the present study, CUS was insufficient to detect diffuse non-cystic WMI in only three infants. All other diffuse WMI on MRI were already detected on CUS by inhomogeneous echodensities on CUS. This confirms the assumption that inhomogeneous hyperechogenicities are the CUS correlates of punctate WMI and stresses the important value of advanced dedicated serial CUS to detect diffuse non-cystic WMI.^{7, 9, 16–18} However, MRI is needed to assess extent and localization of WMI for prediction of its full impact on outcome.²⁶ In this study, a low number of diffuse non-cystic white matter abnormalities were found. This could be explained by missing data, as MRI could not be performed in clinical unstable preterm infants, which are typically the ones at increased risk to develop WMI. In addition, the low number of diffuse WMI, could also be by abnormalities that are commonly seen at term-equivalent age, such as diffuse excessive high signal intensities. As we scanned at mean PMA of 31 weeks, these abnormalities may have been missed.

In correspondence with current literature^{27, 28}, MRI in the present study excelled in the detection of posterior fossa abnormalities: it confirmed all cerebellar hemorrhages detected with CUS and identified all folial and two lobar cerebellar hemorrhages that had been missed with CUS.

In addition to the detection of limited cerebellar hemorrhages, neonatal care may clearly benefit from quantitative MRI sequences that could provide early objective biomarkers of outcome.³ However, MRI is a complex technique with limitations in the very young. Our study design dictated MRI scanning at 30 weeks' PMA, but depending on clinical condition, scanning was postponed or cancelled in 185 infants (60%). Inherently, infants scanned at 30 weeks' PMA may likely have been less troubled by complications. Postponement or cancellation seems worrying because especially preterm infants with severe illness are at risk of brain injury and may benefit most from early MRI scanning.²⁹
³⁰ It would be essential, therefore, to improve applicability of MRI. This includes: 1) safety improvement: transfers and monitoring of critically ill infants to the MR suite should be optimized and MRI sequences can be shortened to reduce procedure times.^{31, 32} 2) Tailored MRI scanning: indications, usage of sequences and timing to scan should be established more individually. 3) Improved availability: a dedicated neonatal MRI scanner in the vicinity of the NICU would overcome logistic problems.

Important limitations of this study should be addressed: 1) imaging group III was heterogeneous because it included both deceased patients and infants transferred to other hospitals before the MRI could take place. Inclusion of deceased patients may have influenced clinical characteristics. However, as severe brain injury was frequently encountered in the infants that died, MRI was preferred to enable optimal clinical decision-making, but could not take place due to clinical instability. This emphasizes the

value of bedside sequential CUS and difficulties to enable safe MRI scanning in a vulnerable population; 2) due to absence of correlation between injury patterns and long term outcome in our study population, we were not able to demonstrate clinical relevance of all findings; 3) we were unable to calculate sensitivity of CUS and MRI because golden standard of preterm brain injury (for example by histopathologic findings) was not available; 4) because strategies were being optimized over the course of this study, SWI was not performed in all MRI procedures, which may have led to lower sensitivity to detect low-grade GMH-IVH compared with other studies²⁵; 5) in this study, we observed imaging findings of routine, clinical MRI scans, as such, we were not able to perform post processing of advanced MRI sequences to obtain quantitative measurements of injury. We are aware that sophisticated use of MRI sequences, such as DTI, volumetric MRI and proton MR spectroscopy, which are usually performed in the context of research, would undoubtedly result in greater value of MRI. And 6) we performed MRI scanning at 30 weeks' PMA, instead of at term-equivalent age. This could have led to loss of patients to compare. However, given the increasing demand for early quantitative biomarkers of outcome, the importance of early MRI scans will increase as well. This study therefore provides valuable information regarding practicability and clinical limitations of such early MRI scans.

Conclusion

Brain injury is frequently encountered in preterm infants (47.6%). Advanced CUS is adequate to detect and monitor preterm brain injury and therefore deserves more appreciation in neonatal neurology. MRI is invaluable as it allows objective quantitative assessment of microstructural brain properties and is superior to detect posterior fossa abnormalities. However, clinical use in preterm infants is currently limited because of safety and logistic issues. These issues need to be addressed in view of increasing demand for quantitative biomarkers of outcome using early MRI scans. Furthermore, dual use of sequential CUS and MRI provides high sensitivity to detect common patterns of preterm brain injury. Future research should therefore focus on improvement of their complementary applications.

Acknowledgement

The authors would like to thank Rogier de Jonge, clinical epidemiologist, for performing statistical analyses and interpreting the results of this study.

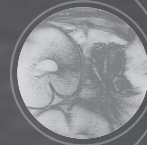
References

1. Gulland A. Fifteen million and rising—the number of premature births every year. *BMJ*. 2012;344:e3084.
2. Plaisier A, Govaert P, Lequin MH, Dudink J. Optimal timing of cerebral mri in preterm infants to predict long-term neurodevelopmental outcome: A systematic review. *AJNR Am J Neuroradiol*. 2014;35:841-7.
3. Ment LR, Hirtz D, Huppi PS. Imaging biomarkers of outcome in the developing preterm brain. *Lancet Neurol*. 2009;8:1042-1055.
4. Rutherford MA, Supramaniam V, Ederies A, Chew A, Bassi L, Groppo M, et al. Magnetic resonance imaging of white matter diseases of prematurity. *Neuroradiology*. 2010;52:505-521.
5. Leijser LM, de Vries LS, Cowan FM. Using cerebral ultrasound effectively in the newborn infant. *Early Hum Dev*. 2006;82:827-835.
6. Govaert P, De Vries LS. *An atlas of neonatal brain sonography*. London: Mac Keith Press; 2010.
7. Ciambra G, Arachi S, Protano C, Cellitti R, Caoci S, Di Biasi C, et al. Accuracy of transcranial ultrasound in the detection of mild white matter lesions in newborns. *Neuroradiol J*. 2013;26:284-289.
8. Graca AM, Cardoso KR, da Costa JM, Cowan FM. Cerebral volume at term age: Comparison between preterm and term-born infants using cranial ultrasound. *Early Hum Dev*. 2013;89:643-8.
9. van Wezel-Meijler G, Steggerda SJ, Leijser LM. Cranial ultrasonography in neonates: Role and limitations. *Semin Perinatol*. 2010;34:28-38.
10. Steggerda SJ, Leijser LM, Wiggers-de Bruine FT, van der Grond J, Walther FJ, van Wezel-Meijler G. Cerebellar injury in preterm infants: Incidence and findings on us and mr images. *Radiology*. 2009;252:190-199.
11. Leijser LM, Srinivasan L, Rutherford MA, Counsell SJ, Allsop JM, Cowan FM. Structural linear measurements in the newborn brain: Accuracy of cranial ultrasound compared to mri. *Pediatr Radiol*. 2007;37:640-648.
12. Reynolds PR, Dale RC, Cowan FM. Neonatal cranial ultrasound interpretation: A clinical audit. *Arch Dis Child Fetal Neonatal Ed*. 2001;84:F92-95.
13. Maalouf EF, Duggan PJ, Counsell SJ, Rutherford MA, Cowan F, Azzopardi D, et al. Comparison of findings on cranial ultrasound and magnetic resonance imaging in preterm infants. *Pediatrics*. 2001;107:719-727.
14. Miller SP, Cozzio CC, Goldstein RB, Ferriero DM, Partridge JC, Vigneron DB, et al. Comparing the diagnosis of white matter injury in premature newborns with serial mr imaging and transfontanel ultrasonography findings. *AJNR Am J Neuroradiol*. 2003;24:1661-1669.
15. Mirmiran M, Barnes PD, Keller K, Constantinou JC, Fleisher BE, Hintz SR, et al. Neonatal brain magnetic resonance imaging before discharge is better than serial cranial ultrasound in predicting cerebral palsy in very low birth weight preterm infants. *Pediatrics*. 2004;114:992-998.
16. Horsch S, Skiold B, Hallberg B, Nordell B, Nordell A, Mosskin M, et al. Cranial ultrasound and mri at term age in extremely preterm infants. *Arch Dis Child Fetal Neonatal Ed*. 2010;95:F310-314.
17. Leijser LM, Liauw L, Veen S, de Boer IP, Walther FJ, van Wezel-Meijler G. Comparing brain white matter on sequential cranial ultrasound and mri in very preterm infants. *Neuroradiology*. 2008;50:799-811.
18. de Vries LS, Benders MJ, Groenendaal F. Imaging the premature brain: Ultrasound or mri? *Neuroradiology*. 2013;55:13-22.
19. Plaisier A, Raets MM, van der Starre C, Feijen-Roon M, Govaert P, Lequin MH, et al. Safety of routine early mri in preterm infants. *Pediatr Radiol*. 2012;42:1205-1211.

20. Govaert P, Ramenghi L, Taal R, de Vries L, Deveber G. Diagnosis of perinatal stroke i: Definitions, differential diagnosis and registration. *Acta Paediatr.* 2009;98:1556-1567.
21. Raets MMA, Dudink J, IJsselstijn H, van Heijst AFJ, Lequin MH, Houmes RJ, et al. Brain injury associated with neonatal extracorporeal membrane oxygenation in the netherlands: A nationwide evaluation spanning two decades. *Pediatric Critical Care Medicine.* 2013;14:884-892.
22. Volpe JJ. Intracranial hemorrhage: Germinal matrix-intraventricular hemorrhage of the premature infant. *Neurology of the newborn.* Philadelphia: Saunders; 2008.
23. Ecury-Goossen GM, Dudink J, Lequin M, Feijen-Roon M, Horsch S, Govaert P. The clinical presentation of preterm cerebellar haemorrhage. *Eur J Pediatr.* 2010;169:1249-1253.
24. Richardson DK, Corcoran JD, Escobar GJ, Lee SK. Snap-ii and snappe-ii: Simplified newborn illness severity and mortality risk scores. *J Pediatr.* 2001;138:92-100.
25. Parodi A, Morana G, Severino MS, Malova M, Natalizia AR, Sannia A, et al. Low-grade intraventricular hemorrhage: Is ultrasound good enough? *J Matern Fetal Neonatal Med.* 2015;28:2261-4.
26. Woodward LJ, Anderson PJ, Austin NC, Howard K, Inder TE. Neonatal mri to predict neurodevelopmental outcomes in preterm infants. *N Engl J Med.* 2006;355:685-694.
27. Fumagalli M, Bassi L, Sirgiovanni I, Mosca F, Sannia A, Ramenghi LA. From germinal matrix to cerebellar haemorrhage. *J Matern Fetal Neonatal Med.* 2015;28:2280-5.
28. Tam EWY, Rosenbluth G, Rogers EE, Ferriero DM, Glidden D, Goldstein RB, et al. Cerebellar hemorrhage on magnetic resonance imaging in preterm newborns associated with abnormal neurologic outcome. *J Pediatr.* 2011;158:245-250.
29. Zwicker JG, Grunau RE, Adams E, Chau V, Brant R, Poskitt KJ, et al. Score for neonatal acute physiology-ii and neonatal pain predict corticospinal tract development in premature newborns. *Pediatr Neurol.* 2013;48:123-129 e121.
30. Card D, Nossin-Manor R, Moore AM, Raybaud C, Sled JG, Taylor MJ. Brain metabolite concentrations are associated with illness severity scores and white matter abnormalities in very preterm infants. *Pediatr Res.* 2013;74:75-81.
31. Rutherford M, Biarge MM, Allsop J, Counsell S, Cowan F. Mri of perinatal brain injury. *Pediatr Radiol.* 2010;40:819-833.
32. Stokowski LA. Ensuring safety for infants undergoing magnetic resonance imaging. *Adv Neonatal Care.* 2005;5:14-27; quiz 52-14.

CHAPTER 8

Neurodevelopmental outcome after neonatal perforator stroke



G.M. Ecury-Goossen, M. van der Haer, L. Smit, M. Feijen-Roon, M. Lequin, R.C.J. de Jonge, P. Govaert, J. Dudink.

Dev Med Child Neurol 2016;58:49-56.

Abstract

Aim

To assess outcome after neonatal perforator stroke in the largest cohort to date.

Method

Survivors from a cohort of children diagnosed with neonatal perforator stroke using cranial ultrasound or magnetic resonance imaging were eligible for inclusion. Recovery and Recurrence Questionnaire score, presence of cerebral palsy (CP), and crude outcome were assessed, specifically (1) the ability to walk independently, (2) participation in regular education, and (3) the presence of epilepsy.

Results

Thirty-seven patients (20 males, 17 females) aged 3 to 14 years (mean age 8y) were included in the study: 14 with isolated single perforator stroke, four with multiple isolated perforator strokes, and 19 with additional brain injury. Out of 18 children with isolated perforator stroke(s), four had CP, one could not walk independently, and one developed epilepsy. The posterior limb of the internal capsule was involved in 4 out of 18 patients; three of these patients had CP. Of 19 children with additional brain injury, 11 had CP and three were not able to walk independently. Three out of nine children with concomitant cortical middle cerebral artery stroke developed epilepsy.

Interpretation

Perforator stroke patterns can be of use in predicting long-term outcome and for guiding counselling and surveillance. Motor outcome was favourable in children with isolated perforator stroke(s), except when the posterior limb of the internal capsule was involved.

Introduction

Detection of neonatal stroke has improved in line with advances in neuroimaging techniques.¹ The reported incidence of neonatal stroke in term neonates ranges from 1 in 2300 to 1 in 5900.¹⁻³ An even higher incidence of 7 in 1000 admissions has been reported in a preterm cohort.⁴

In the classification of perinatal stroke, arterial and venous mechanisms of occlusion can be defined.⁵⁻⁷ In the case of arterial ischaemic stroke, one or more of the main cerebral arteries and/or its perforator branches can be involved.⁸ Perforator stroke involves the perforators of the anterior choroidal artery, anterior cerebral artery, middle cerebral artery (MCA), posterior cerebral artery, and posterior communicating artery, supplying among others the thalamus, striatum, and posterior limb of the internal capsule (PLIC).⁹ Strokes in the brainstem involving perforating branches of the basilar arteries are also possible. Perforator strokes are probably under recognized, as clinical symptoms are often lacking and neuroimaging diagnosis is typically an incidental finding during routine cranial ultrasound (CUS) imaging.¹⁰

In our experience, parents of neonates with brain injury first and foremost want to be informed about prognosis when their child is admitted to the neonatal intensive care unit. However, to date follow-up studies on neonatal arterial ischaemic stroke have mainly focused on cortical stroke. Large long-term follow-up studies of children with neonatal perforator stroke are lacking. Most outcome studies on paediatric perforator strokes include children who developed perforator stroke after the neonatal period.¹¹⁻¹⁵ Only a few reports focus on neonates, but these describe small groups of children during a short or unknown period of follow-up.^{8, 16-19} Therefore, the aim of our study was to evaluate the neurodevelopmental outcome in a previously described cohort of 55 infants with neonatal perforator stroke.¹⁰ Risk factors, clinical presentation, and neuroimaging findings of this cohort have been described in our previous study. The current paper focuses on simple, clinically relevant outcomes and attempts to answer common questions clinicians are faced with when counselling parents of affected children, specifically: (1) the ability to walk independently, (2) the ability to participate in regular education, and (3) the presence of epilepsy. We hypothesized that children with single isolated neonatal perforator stroke will usually have a favourable outcome, but that involvement of the PLIC could lead to motor impairment, even in case of a single isolated neonatal perforator stroke.

Method

The original cohort¹⁰ consisted of 55 infants diagnosed with perforator stroke at our tertiary (neonatal) intensive care unit between August 1999 and April 2011, using CUS or magnetic resonance imaging (MRI). Details on the definition of perforator stroke, methods of neuroimaging, and the aetiological mechanisms of stroke have been previously described.¹⁰ Children who were alive in March 2014 were eligible for inclusion in the current study. Children whose parents were not fluent in Dutch were excluded.

The local ethics committee approved this study and waived the requirement to obtain written parental informed consent.

Based on neuroimaging results at diagnosis, the children were categorized into three groups:

(1) single (unilateral) isolated perforator stroke without additional intracerebral lesions on CUS and/or MRI; (2) multiple isolated perforator strokes without other intracerebral lesions on CUS and/or MRI; and (3) concomitant intracerebral lesions on CUS and/or MRI (i.e. cortical stroke, watershed lesions, germinal matrix haemorrhage or intraventricular haemorrhage, cerebellar haemorrhage, and hydrocephalus). Involvement of the corticospinal tract in the PLIC was ascertained by visualization of a lesion in the PLIC on either CUS or – if available – MRI,⁹ or changes in the corticospinal tract on diffusion weighted imaging at the level of the mesencephalon in the acute stage (see Fig. 1).^{20, 21} The PLIC is perfused from the posterior communicating artery or anterior choroidal artery (see Fig. 1) and some lateral perforator branches from the MCA may irrigate the genu of the internal capsule and nearby corticobulbar fibers.⁹

Parents of included children were interviewed by telephone in March and April 2014 using the Recovery and Recurrence Questionnaire (RRQ). The RRQ is a modification of the Pediatric Stroke Outcome Measure that has been designed to assess a child's post-stroke function by telephone interview.^{22, 23} The RRQ contains five subscales: right sensorimotor function; left sensorimotor function; language production; language comprehension; and cognitive or behavioural deficits. Subscale scoring is 0 (no deficit), 0.5 (mild deficit, normal function), 1 (moderate deficit, decreased function), or 2 (severe deficit, missing function). Total RRQ score ranges from 0 (no deficit) to 10 (maximum deficit). A validation study of RRQ score compared to the Pediatric Stroke Outcome Measure score has been recently published.²³ In order to minimize bias all telephonic interviews were executed by the same investigator, who was blinded to the medical history of the child.

The parents were also asked specifically about their child's ability to walk independently, the presence of epilepsy, and the type and level of education their child is participating in.

If available, follow-up data were retrieved from the medical records: Bayley Scales of Infant and Toddler Development scores; the presence of CP and classification; Gross Mo-

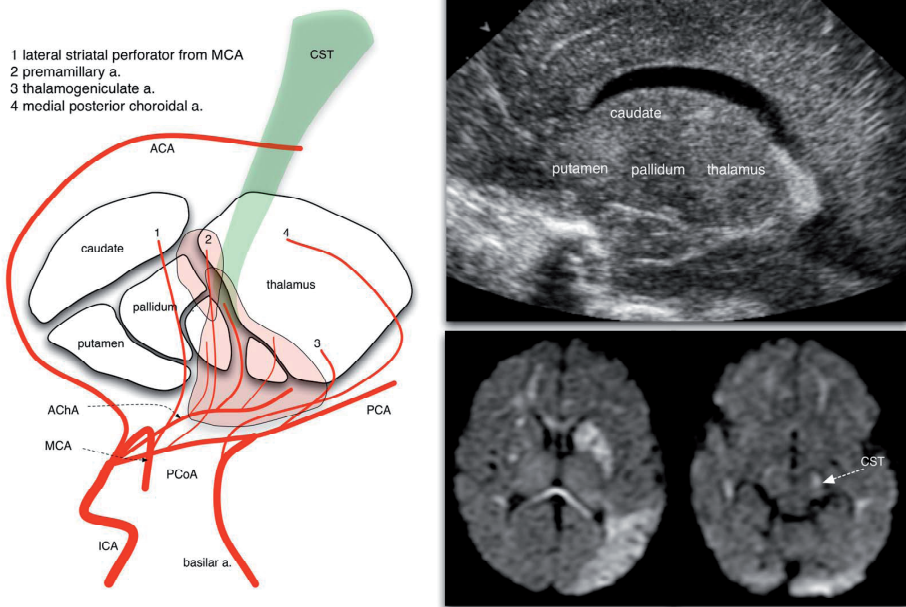


Figure 1.

Arterial irrigation of the posterior limb of the internal capsule, parasagittal ultrasound image, and axial diffusion weighted MRI image. ACA, anterior cerebral artery; AChA, anterior choroidal artery; CST, corticospinal tract; ICA, internal carotid artery; MCA, middle cerebral artery; PCA, posterior cerebral artery; PCoA, posterior communicating artery.

tor Function Classification System; and the presence of epilepsy. Neurodevelopmental follow-up was assessed at 2 and/or 3 years corrected age, using the second or third edition of the Bayley Scales of Infant and Toddler Development, depending on the year in which the child was assessed.^{24, 25} No correction was made to compensate for discrepancies between the second and third edition.²⁶ Developmental scores above minus one standard deviation (≥ 85) were regarded as average development, between one and two standard deviations below the mean (70–84) as mild developmental delay, and below minus two standard deviations below the mean (≤ 69) as significant developmental delay. A paediatric neurologist or experienced neonatologist performed neuromotor examination. Cerebral palsy (CP) was classified according to the Surveillance of Cerebral Palsy in Europe classification.²⁷ For children with CP, the level of disability was evaluated using the Gross Motor Function Classification System.²⁸ If data from the telephonic interview conflicted with data from the medical records, the most recently acquired data were used for analysis.

Results

Fifty-five patients were described in the original cohort study.¹⁰ Thirty-seven (20 males, 17 females) of these patients were included in this follow-up study. As previously described, six patients died before the age of 1 month.¹⁰ The cause of death in these infants was not related to perforator stroke, but to cardiopulmonary insufficiency caused by other neonatal complications. In addition, five patients died after the age of 1 month: three at the age of 2 months, one at 3 years and another at 7 years of age. Death of these five patients was caused by cardiopulmonary insufficiency, mostly due to infection. Of the 11 patients that died, five had isolated single perforator stroke, four had multiple perforator strokes, and two had concomitant intracerebral lesions. Six children were lost to follow-up, one child was excluded because the parents were not fluent in Dutch.

Characteristics of the 37 included patients are presented in Table 1. The age at assessment ranged from 3 to 14 years (median 8 years). Twenty-one children were born preterm (< 37wks' gestation), of whom thirteen were very preterm (< 32wks' gestation). Fourteen

Table 1. Patient characteristics

	Isolated unilateral stroke (n = 14)	Multiple perforator strokes (n = 4)	Additional lesions (n = 19)	Total
Gestational age, weeks	32 [24 6/7 – 42]	34 [28 1/7 – 37 4/7]	37 5/7 [27 2/7 – 41 5/7]	35 5/7 [24 6/7 – 42]
Birth weight, grams	1668 [720 – 3666]	1735 [680 – 2560]	3240 [620 – 4440]	2320 [620 – 4440]
Male	9 (64%)	1 (25%)	10 (53%)	20 (54%)
Singleton	11 (79%)	3 (75%)	17 (89%)	31 (84%)
SGA	3 (21%)	2 (50%)	3 (16%)	8 (22%)
Apgar score 1 minute (n = 34)	5 [0 – 10], 2 missing	7 [3 – 10]	7.5 [1 – 9], 1 missing	6.5 [0 – 10]
Apgar score 5 minutes (n = 35)	7 [5 – 10], 1 missing	10 [8 – 10]	9 [3 – 10], 1 missing	8 [3 – 10]
Umbilical cord pH (n = 21)	7.17 [6.73 – 7.39], 4 missing	7.11 [6.96 – 7.25], 2 missing	7.15 [6.86 – 7.32], 10 missing	7.16 [6.73 – 7.39]
CRIB score (n = 34)	5 [0 – 11], 2 missing	6 [0 – 9], 1 missing	0 [0 – 13]	1 [0 – 13]
Age* at assessment RRQ, years	7.7 [3.1 – 14.6]	8.6 [4.8 – 12]	8.9 [3.3 – 13.5]	8.3 [3.1 – 14.6]

Data are presented as median [range] or number (percentage)

Abbreviations:

SGA= small for gestational age

CRIB= Clinical Risk Index for Babies

RRQ= Recovery and Recurrence Questionnaire

*Age not corrected for prematurity

patients had single isolated unilateral perforator stroke, four had multiple isolated perforator strokes, and 19 had additional brain injury. None received antithrombotic or thrombolytic therapy and none were diagnosed with recurrent stroke later on in childhood. One patient received postnatal corticosteroids because of bronchopulmonary dysplasia. Follow-up data from medical records was available for 31 out of 37 patients.

Group 1: single isolated unilateral perforator stroke

Imaging findings and neurodevelopmental outcome for the 14 patients with isolated single unilateral perforator stroke are presented in Table 2. Two children had CP, one was unable to walk independently, 6 out of 13 children reaching school age did not participate in regular education, and one developed epilepsy. The median RRQ score was 0.5 (range 0–7.5).

Group 2: multiple isolated perforator strokes

Results for the four patients with isolated multiple perforator strokes are presented in Table 3. Two developed CP, all were able to walk independently, two did not participate in regular education, and none developed epilepsy. The median RRQ score was 1.5 (range 0–3).

Thus, 4 out of the 18 patients with isolated (single or multiple) perforator stroke(s) developed CP. Three of these patients had involvement of PLIC. On the other hand, the PLIC was involved in 4 out of 18 patients with isolated perforator stroke(s). Three of these children developed CP.

Group 3: additional intracerebral lesions

Results for the 19 patients with additional intracerebral lesions are shown in Table 4. Eleven patients had CP, three were not able to walk independently, 9 out of 17 children reaching school age did not participate in regular education, and four developed epilepsy. The median RRQ score was 0.5 (range 0–10). The PLIC was involved in nine children; seven of these children developed CP. In 7 out of the 11 children with CP, PLIC was involved. When focusing on the nine children with concomitant MCA cortical stroke, seven had developed CP (five of whom had involvement of PLIC), one was not able to walk independently, five did not participate in regular education, and three developed epilepsy. The median RRQ score for these children was 1 (range 0–8).

Discussion

In this study we report on the follow-up findings of a cohort of children previously diagnosed with neonatal perforator stroke. As expected, motor outcome was generally more

Table 2. Outcome isolated unilateral perforator strokes

PT ID	Perforator stroke type	PLIC involvement	GA (weeks)	M/F	Aetiological mechanism stroke ²⁹	Age at assessment (y)	RRQ score	CP type	GMFCS	Walking independently	Regular education	Epilepsy	BSID
1	ACA Heubner right	No	30.7	F	Birth asphyxia	11	0	-	n/a	Yes	Yes	No	2y: MDI 108, PDI 112 3y: MDI 105, PDI 121
2	ACA Heubner right	No	24.9	M	Unclassifiable	3	0	-	n/a	Yes	n/a	No	2y: MDI 95, PDI 94 (BSID-III)
3	ACHA left	Yes	38.4	M	Sepsis	8	7.5	Spastic bilateral, right > left	IV	No	No	Yes	n.a.
4	MCA lateral striate right	Yes	31.1	M	Embolism	13	4	Spastic unilateral, left	I	Yes	No	No	3y: MDI 82, PDI 58
5	MCA medial striate left	No	30.9	F	Prolonged hypoxia/hypotension	14	0	-	n/a	Yes	Yes	No	2y: MDI 110, PDI 95
6	MCA thalamic left	No	42	M	Prolonged hypoxia/hypotension	7	3	-	n/a	Yes	No	No	n.a.
7	MCA lateral striate left	No	32.1	F	Unclassifiable	5	0	-	n/a	Yes	Yes	No	2y: MDI 115, PDI 107 (BSID-III)
8	MCA lateral striate right	No	27.9	M	Acute blood loss	5	2	-	n/a	Yes	No	No	3y: MDI 60, PDI not assessed
9	PCA thalamic left	No	33.6	M	Birth asphyxia	12	0	-	n/a	Yes	Yes	No	n.a.
10	PCA thalamic left	No	34.9	M	Acute blood loss	11	1	-	n/a	Yes	No	No	n.a.
11	PCA thalamic left	No	33.6	M	Sepsis	6	0	-	n/a	Yes	Yes	No	n.a.
12	PCA thalamic left	No	29.4	F	Unclassifiable	7	3	-	n/a	Yes	Yes	No	n.a.
13	PCoA thalamic left	No	33.9	M	Birth trauma	14	6	-	n/a	Yes	No	No	2y: MDI 63, PDI 95
14	PCoA thalamic right	No	31.7	F	Prolonged hypoxia/hypotension	5	0	-	n/a	Yes	Yes	No	2y: MDI 85, PDI 91 (BSID-III) 3y: MDI 90, PDI 91 (BSID-III)
Total/ range		2/14	24.9– 42			3–14	0–7.5	2/14		13/14	7/13	1/14	

PT ID, patient identification; PLIC, posterior limb of internal capsule; GA, gestational age; M, male; F, female; RRQ, Recovery and Recurrence Questionnaire; CP, cerebral palsy; GMFCS, Gross Motor Function Classification System; BSID, Bayley Scales of Infant and Toddler Development; ACA, anterior cerebral artery; MDI, mental development index; PDI, psychomotor developmental index; BSID-III, Bayley Scales of Infant and Toddler Development, third edition; AChA, anterior choroidal artery; n/a, not applicable; MCA, middle cerebral artery; n.a., not available; PCA, posterior cerebral artery; PCoA, posterior communicating artery; y, years.

Table 3. Outcome multiple perforator strokes

PT ID	Perforator stroke type	PLIC involvement	GA (weeks)	M/F	Aetiological mechanism stroke ²⁹	Age at assessment (y)	RRQ score	CP type	GMFCS	Walking independently	Regular education	Epilepsy	BSID
15	MCA thalamic + lateral striate, PCA thalamic left	No	28.1	F	Embolism	12	0	-	n/a	Yes	Yes	No	1 y 9 mo: MDI 121, PDI 99
16	MCA lateral striate left and right	Yes	31	F	Birth asphyxia	11	2.5	-	n/a	Yes	No	No	2y: MDI 63, PDI not assessed
17	Right AChA, left MCA lateral striate + MCA other	Yes	37.6	M	Unclassifiable	4	3	Spastic bilateral, right > left	II	Yes	No	No	2y: MDI 90, PDI not assessed (BSID-III)
18	Right MCA lateral striate, left circle of Willis + PCA thalamic	No	37.1	F	Embolism	5	0.5	Spastic unilateral, left	I	Yes	Yes	No	n.a.
Total/ range		2/4	28.1– 37.6			4–12	0–3	2/4		4/4	2/4	0/4	

PT ID, patient identification; PLIC, posterior limb of internal capsule; GA, gestational age; M, male; F, female; RRQ, Recovery and Recurrence Questionnaire; CP, cerebral palsy; GMFCS, Gross Motor Function Classification System; BSID, Bayley Scales of Infant and Toddler Development; MCA, middle cerebral artery; PCA, posterior cerebral artery; n/a, not applicable; MDI, mental developmental index; PDI, psychomotor developmental index; AChA, anterior choroidal artery; BSID-III, Bayley Scales of Infant and Toddler Development, third edition; n.a., not available; y, years.

Table 4. Outcome additional intracerebral lesions

PTID	Additional lesion	Perforator stroke type	PLIC involvement	GA	M/F	Aetiological mechanism stroke ²⁹	Age at assessment (y)	RRQ score	CP type	GMFCS	Walking independently	Regular education	Epilepsy	BSID
19	Cortical MCA stroke left	MCA lateral striate left and right	Yes	41.7	M	Embolism	10	8	Spastic bilateral	V	No	No	Yes ^a	n.a.
20	Cortical MCA stroke left	MCA lateral striate	Yes	38.7	F	Unclassifiable	9	2	Spastic unilateral, right	I	Yes	Yes	No	3y: MDI 115, PDI not assessed
21	Cortical MCA stroke right	PCA thalamic left	No	37	F	Birth asphyxia	8	0.5	Spastic unilateral, left	I	Yes	No	No	3y: MDI <55, PDI not assessed
22	Cortical MCA stroke left	MCA lateral striate right	Yes	37.3	M	Meningitis	7	4	Spastic unilateral, right	I	Yes	No	Yes	2y: MDI <55, PDI <55
23	Cortical MCA stroke right	ACHA right, ACA Heubner left, MCA left	No	41	F	Unclassifiable	6	1	Spastic unilateral, left	I	Yes	No	No	2y: MDI 85, PDI not assessed
24	Cortical MCA stroke right	ACA Heubner left	Yes	41	F	Acute blood loss	3	0.5	Spastic unilateral, left	I	Yes	n/a	No	n.a.
25	Cortical MCA stroke left	PCoA bilateral	No	30.9	M	Sepsis	3	0	-	n/a	Yes	n/a	No	2y: MDI 85, PDI 91 (BSID-III)
26	Cortical MCA stroke right	PCoA right	yes	37.7	M	Unclassifiable	7	0.5	Spastic unilateral, left	I	Yes	Yes	No	n.a.
27	Cortical MCA stroke left	MCA	Yes	41.7	M	Embolism	8	1.5	-	n/a	yes	no	yes	2y: MDI 92, PDI 112 At 3y: MDI 109, PDI 113
28	Cortical PCA stroke left	PCA thalamic left	No	36.9	M	Birth trauma	10	0.5	-	n/a	Yes	Yes	No	2y: MDI 88, PDI 89
29	Cortical PCA stroke right	PCA thalamic bilateral	No	39.3	F	Embolism	9	0.5	-	n/a	Yes	Yes	No	n.a.
30	Watershed lesions	MCA right, MCA and PCA left	No	38	M	Meningitis	13	0	Spastic bilateral, left>right	I	Yes	No	No	n.a.

Table 4. Outcome additional intracerebral lesions (continued)

PT ID	Additional lesion	Perforator stroke type	PLIC involvement	GA	M/F	Aetiological mechanism stroke ^a	Age at assessment (y)	RRQ score	CP type	GMFCS	Walking independently	Regular education	Epilepsy	BSID
31	Watershed lesions	PCA thalamic right	No	35.7	F	Prolonged hypoxia/hypotension	12	2	Spastic unilateral, left	I	Yes	No	No	n.a.
32	Watershed lesions	PCA thalamic right	No	41	M	Birth asphyxia	9	0.5	-	n/a	Yes	Yes	No	n.a.
33	Grade II IVH left + watershed	MCA lateral striate left	Yes	36.2	M	Arteriopathy	10	10	Spastic unilateral, right	V	no	No	Yes	n.a.
34	GMH bilateral	PCA thalamic right	No	29	F	Prolonged hypoxia/hypotension	11	0.5	-	n/a	Yes	Yes	No	n.a.
35	GMH left	ACHA right + MCA lateral striate left	Yes	27.3	M	Embolism	6	0.5	-	n/a	Yes	Yes	No	2y: MDI 95, PDI 83
36	Hydrocephalus	MCA medial striate bilateral	No	39	F	Prolonged hypoxia/hypotension	4	1.5	-	n/a	Yes	Yes	No	2y: MDI 105, PDI 91 (BSID-III)
37	Cerebellar haemorrhage bilateral	ACHA right	Yes	27.9	F	Birth trauma	4	4	Spastic bilateral	IV	No	No	No	n.a.
Total/ range			9/19	27.3–41.7			3–13	0–10	11/19		16/19	8/17	4/19	

^aWest syndrome.

PT ID, patient identification; PLIC, posterior limb of internal capsule; GA, gestational age; M, male; F, female; RRQ, Recovery and Recurrence Questionnaire; CP, cerebral palsy; GMFCS, Gross Motor Function Classification System; BSID, Bayley Scales of Infant and Toddler Development; MCA, middle cerebral artery; n.a., not available; MDI, mental developmental index; PDI, psychomotor developmental index; PCA, posterior cerebral artery; ACHA, anterior choroidal artery; ACA, anterior cerebral artery; n/a, not applicable; PCoA, posterior communicating artery; BSID-III, Bayley Scales of Infant and Toddler Development, third edition; y, years.

favourable in children with isolated perforator strokes than in those with concomitant cortical stroke or other additional brain injury. However, this was not the case when the PLIC was involved in children with isolated perforator stroke. Epilepsy was rare in children with isolated perforator stroke compared to those with concomitant cortical stroke.

It has been suggested that perinatal stroke may have a relatively favourable outcome because of the plasticity of the developing brain.¹ However, perinatal arterial stroke can lead to motor deficits, epilepsy, and cognitive impairment.³⁰ These severe sequelae are often caused by MCA stroke.⁵ The reported outcome after neonatal stroke varies among studies, which is likely caused by differences in stroke type, the population studied, and length of follow-up.¹ In a review of studies of perinatal stroke over a period of 30 years, 40% of infants with perinatal stroke were neurologically normal, 57% were neurologically or cognitively abnormal, and 3% had died.³¹

To our knowledge, the present study is the first to focus on the long-term neurodevelopmental outcome in children diagnosed with neonatal perforator stroke. Age at assessment in our cohort ranged from 3 to 14 years. Previous outcome studies have included small numbers of patients and reported the outcome after a short or unspecified follow-up period. In a study involving 24 infants with neonatal cerebral infarction, 2 children with lenticulostriate branch infarction were included.¹⁹ At school age one showed asymmetry on neurologic examination, the other scored poorly (third centile) on the Movement Assessment Battery for Children.¹⁸ In another report, 23 infants with infarction in the MCA territory were described, including 13 infants (10 preterm) with lenticulostriate branch involvement.¹⁷ Two of the preterm infants had concomitant intraventricular haemorrhage and two had concomitant cystic periventricular leukomalacia. Outcome was assessed between 9 and 36 months corrected age. However, 2 of the 13 children with lenticulostriate branch infarction were less than 6 months old. Of the remaining 11 infants two developed CP, three showed global delay, two mild tone asymmetry, and four had no sequelae.¹⁷

Brower et al.³² described 36 children, including three newborn infants, with ischaemic infarction of the basal ganglia, internal capsule, or thalamus. Residual impairment was described as severe in five patients, moderate in one, and mild in 16. In a study by Inagaki et al.,¹⁴ 4 out of 14 children with basal ganglia ischaemic stroke developed hemiparesis and one child developed a gait disturbance. Those who developed hemiparesis all had lesions of the internal capsule. Other motor sequelae after childhood perforator stroke include gait disturbance and dystonia.^{11,13-15} Complete recovery was seen in some cohorts: 36% (5/14) of the children in a study by Inagaki et al.¹⁴; 39% (14/36) children in the cohort reported by Brower et al.³²; and 80% (4/5) children in a study by Garg et al.¹²

It has been suggested that the neurological morbidity rate in perinatal stroke survivors is higher than that in children with similar lesions acquired later in infancy or

childhood.^{33,34} However, in a study comparing neonatal to childhood MCA stroke, dystonia was present in 39% in the childhood-onset group, but was not seen in the neonatal-onset group after a median follow-up period of 5.5 years.¹⁶ This finding could be explained by different underlying aetiologies in neonatal and childhood ischaemic stroke, and differences in tissue maturation, corticomotor–neuronal connectivity, and plasticity within basal ganglia.¹⁶ Thus, results from outcome studies in older children with perforator strokes cannot be extrapolated to survivors of neonatal stroke.

As we hypothesized, in our cohort the children with isolated (single or multiple) perforator strokes had a more favourable outcome than those with additional intracerebral lesions. To illustrate this, seven out of the nine children with concomitant MCA cortical stroke had developed CP and one was not able to walk independently. In contrast, 4 out of 18 children with isolated perforator stroke developed CP and one was not able to walk independently. In the latter group, the development of CP is most likely explained by involvement of the PLIC, which was seen in three out of the four children. One child with isolated single perforator stroke (patient 3 in Table I) was severely affected and unable to walk independently. The stroke had been diagnosed after *Escherichia coli* sepsis. We hypothesize that hypoxia and hypotension during the sepsis had caused diffuse brain damage, which was not visible on neuroimaging during admission to hospital. Another child (patient 18 in Table II) had multiple perforator strokes without involvement of the PLIC and developed CP. We hypothesize that CP in this patient is explained by the MCA lateral striate perforator stroke that affected the internal capsule, and that this involvement was not clear on neuroimaging. We found that childhood epilepsy was rare in children with isolated neonatal perforator strokes and more frequent in children with concomitant cortical stroke. This could be explained by sparing of the cortex as described by Kirton et al.⁶ However, infants with early thalamic injury have an increased risk of developing postneonatal epilepsy and electrical status epilepticus in slow wave sleep,³⁵ possibly as a result of alterations in thalamocortical networks.³⁶ The incidence of electrical status epilepticus of sleep spectrum disorder in our cohort is unknown, as electroencephalography was only obtained because of a history of suspected seizures.

With regard to language, cognitive or behavioural deficits, and special education needs, there is no evident difference in our cohort between children with isolated perforator stroke and those with concomitant brain injury. In contrast, in a cohort of 59 children with (delayed presentation of) presumed perinatal ischaemic stroke, adverse cognitive/behavioural outcomes were strongly associated with cortical involvement.⁶ However, the group of patients with subcortical strokes in that study consisted primarily of children with periventricular venous infarction ($n = 12$); only four children with lenticulostriate stroke were included in this group. Furthermore, only children born at term were included, whereas most of the patients in our cohort were born prematurely. Taking the heterogeneity of our cohort into account, it is plausible that extreme pre-

maturity, underlying aetiological mechanisms of stroke (such as asphyxia, birth trauma, and sepsis/meningitis), and development of West syndrome have had a more profound effect on cognitive and behavioural outcomes. Moreover, deficits in language, cognition, behaviour, and other higher brain functions have been reported in up to 60% of children with arterial perinatal stroke.³⁷

Our report has several limitations inherent to its design. The cohort described is a very heterogeneous group, with children born at term and preterm, different perforator strokes, different aetiological mechanisms (e.g. asphyxia, sepsis/meningitis, birth trauma), congenital anomalies (e.g. heart defects), and 19 out of 37 children were diagnosed with additional brain injury. All of these factors can be expected to influence neurodevelopmental outcome. However, the 18 children with isolated single or multiple perforator stroke still constitute the largest follow-up cohort of children with neonatal perforator stroke. Because of the large variety of perforator strokes, it was not possible to determine which type of perforator strokes (besides PLIC involvement) are most harmful. Moreover, it is difficult to define the typical outcome associated with a particular type of brain injury because recovery occurs as part of a much broader and very complex developmental course.³⁸

This study focused on simple, clinically relevant outcomes, based on commonly asked questions by parents of affected children. Extensive neurological and neuropsychological assessment is needed to establish more subtle morbidities. We are aware that parental impressions of a child's recovery after stroke can be an underestimation as well as an overestimation of neurological deficits compared to assessment by a trained paediatric neurologist.³⁹ A recent validation study showed good reliability between RRQ score and Pediatric Stroke Outcome Measure score, the subcomponents right sensorimotor function, left sensorimotor function, and language production scores. Reliability for language comprehension and cognition/behaviour was moderate. Interobserver reliability and test-retest validity were not assessed.²³

Because the full spectrum of neuropsychological sequelae in children with perinatal brain injury becomes clearer in the course of time, a longer follow-up period with neuropsychological testing is required to appreciate the full spectrum of perinatal stroke.⁶ Follow-up in the present study ranged from 3 to 14 years, longer than that in previous studies that included newborn infants or children with perforator stroke. Long-term outcome studies with a prospective design are needed to determine whether apparently healthy children grow into deficits with maturation and whether deficits resolve, remain stable, or become more pronounced over time. Because MRI was not performed in all included patients, we were not able to assess findings that may further aid in prognostication, such as diffusion weighted changes in the cerebral peduncle.

For a comprehensive evaluation of outcome of neonatal perforator stroke, a well-designed, prospective multicentre follow-up study is needed. It should be realized,

however, that perforator stroke is probably under recognized and can be missed with MRI (because of lower resolution than with recent CUS techniques) and with CUS in inexperienced hands. We emphasize that routine serial CUS is needed to diagnose perforator stroke in neonates admitted to the neonatal intensive care unit.

Conclusion

This study describes the neurodevelopmental outcome of neonatal perforator stroke. Perforator stroke patterns can aid in early prediction of outcome, thus enabling clinicians to provide prognostic information and early intervention or rehabilitation where needed. Motor outcome was favourable in children with isolated neonatal perforator stroke, except when the PLIC was involved.

Acknowledgement

We thank J Hagoort, MA, linguist, Department of Pediatric Surgery, Erasmus MC-Sophia Children's Hospital, Rotterdam, The Netherlands, for revision of the manuscript.

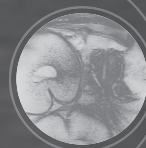
References

1. Nelson KB, Lynch JK. Stroke in newborn infants. *Lancet Neurol* 2004;3:150-8.
2. Lee J, Croen LA, Backstrand KH, et al. Maternal and infant characteristics associated with perinatal arterial stroke in the infant. *JAMA* 2005;293:723-9.
3. Chabrier S, Husson B, Dinomais M, Landrieu P, Nguyen The Tich S. New insights (and new interrogations) in perinatal arterial ischemic stroke. *Thromb Res* 2011;127:13-22.
4. Benders MJ, Groenendaal F, De Vries LS. Preterm arterial ischemic stroke. *Semin Fetal Neonatal Med* 2009;14:272-7.
5. Kirton A, deVeber G. Advances in perinatal ischemic stroke. *Pediatr Neurol* 2009;40:205-14.
6. Kirton A, Deveber G, Pontigon AM, Macgregor D, Shroff M. Presumed perinatal ischemic stroke: Vascular classification predicts outcomes. *Ann Neurol* 2008;63:436-43.
7. Raju TN, Nelson KB, Ferriero D, Lynch JK, NICHD-NINDS Perinatal Stroke Workshop Participants. Ischemic perinatal stroke: Summary of a workshop sponsored by the national institute of child health and human development and the national institute of neurological disorders and stroke. *Pediatrics* 2007;120:609-16.
8. Abels L, Lequin M, Govaert P. Sonographic templates of newborn perforator stroke. *Pediatr Radiol* 2006;36:663-9.
9. Govaert P. Sonographic stroke templates. *Semin Fetal Neonatal Med* 2009;14: 284-98.
10. Ecury-Goossen GM, Raets MM, Lequin M, Feijen-Roon M, Govaert P, Dudink J. Risk factors, clinical presentation, and neuroimaging findings of neonatal perforator stroke. *Stroke* 2013;44:2115-20.
11. Demierre B, Rondot P. Dystonia caused by putamino-capsulo-caudate vascular lesions. *J Neurol Neurosurg Psychiatry* 1983;46:404-9.
12. Garg BP, DeMyer WE. Ischemic thalamic infarction in children: Clinical presentation, etiology, and outcome. *Pediatr Neurol* 1995;13:46-9.
13. Giroud M, Lemesle M, Madinier G, Manceau E, Osseby GV, Dumas R. Stroke in children under 16 years of age. Clinical and etiological difference with adults. *Acta Neurol Scand* 1997;96:401-6.
14. Inagaki M, Koeda T, Takeshita K. Prognosis and MRI after ischemic stroke of the basal ganglia. *Pediatr Neurol* 1992;8:104-8.
15. Kappelle LJ, Willemse J, Ramos LM, van Gijn J. Ischaemic stroke in the basal ganglia and internal capsule in childhood. *Brain Dev* 1989;11:283-92.
16. Boardman JP, Ganesan V, Rutherford MA, Saunders DE, Mercuri E, Cowan F. Magnetic resonance image correlates of hemiparesis after neonatal and childhood middle cerebral artery stroke. *Pediatrics* 2005;115:321-6.
17. de Vries LS, Groenendaal F, Eken P, van Haastert IC, Rademaker KJ, Meiners LC. Infarcts in the vascular distribution of the middle cerebral artery in preterm and fullterm infants. *Neuropediatrics* 1997;28:88-96.
18. Mercuri E, Barnett A, Rutherford M, et al. Neonatal cerebral infarction and neuromotor outcome at school age. *Pediatrics* 2004;113:95-100.
19. Mercuri E, Rutherford M, Cowan F, et al. Early prognostic indicators of outcome in infants with neonatal cerebral infarction: A clinical, electroencephalogram, and magnetic resonance imaging study. *Pediatrics* 1999;103:39-46.
20. De Vries LS, Van der Grond J, Van Haastert IC, Groenendaal F. Prediction of outcome in new-born infants with arterial ischaemic stroke using diffusion-weighted magnetic resonance imaging. *Neuropediatrics* 2005;36:12-20.

21. Kirton A, Shroff M, Visvanathan T, deVeber G. Quantified corticospinal tract diffusion restriction predicts neonatal stroke outcome. *Stroke* 2007;38:974-80.
22. Lo W, Zamel K, Ponnappa K, et al. The cost of pediatric stroke care and rehabilitation. *Stroke* 2008;39:161-5.
23. Lo WD, Ichord RN, Dowling MM, et al. The pediatric stroke recurrence and recovery questionnaire: Validation in a prospective cohort. *Neurology* 2012;79: 864-70.
24. Bayley N. Bayley Scales of Infant Development (2nd edition). San Antonio, TX: Pearson, 1993.
25. Bayley N. Bayley Scales of Infant and Toddler Development (3rd edition). San Antonio, TX: Pearson, 2006.
26. Moore T, Johnson S, Haider S, Hennessy E, Marlow N. Relationship between test scores using the second and third editions of the bayley scales in extremely preterm children. *J Pediatr* 2012;160:553-8.
27. Group SC. Surveillance of cerebral palsy in Europe: A collaboration of cerebral palsy surveys and registers. Surveillance of cerebral palsy in Europe (SCPE). *Dev Med Child Neurol* 2000;42:816-24.
28. Palisano RJ, Rosenbaum P, Bartlett D, Livingston MH. Content validity of the expanded and revised gross motor function classification system. *Dev Med Child Neurol* 2008;50:744-50.
29. Govaert P, Ramenghi L, Taal R, Dudink J, Lequin M. Diagnosis of perinatal stroke ii: Mechanisms and clinical phenotypes. *Acta Paediatr* 2009;98:1720-6.
30. Golomb MR. Outcomes of perinatal arterial ischemic stroke and cerebral sinovenous thrombosis. *Semin Fetal Neonatal Med* 2009;14:318-22.
31. Lynch JK, Nelson KB. Epidemiology of perinatal stroke. *Curr Opin Pediatr* 2001;13:499-505.
32. Brower MC, Rollins N, Roach ES. Basal ganglia and thalamic infarction in children. Cause and clinical features. *Arch Neurol* 1996;53:1252-6.
33. Ganesan V, Hogan A, Shack N, Gordon A, Isaacs E, Kirkham FJ. Outcome after ischaemic stroke in childhood. *Dev Med Child Neurol* 2000;42 455-61.
34. Lansing AE, Max JE, Delis DC, et al. Verbal learning and memory after childhood stroke. *J Int Neuropsychol Soc* 2004;10:742-52.
35. Kersbergen KJ, de Vries LS, Leijten FS, et al. Neonatal thalamic hemorrhage is strongly associated with electrical status epilepticus in slow wave sleep. *Epilepsia* 2013;54:733-40.
36. Blumenfeld H. From molecules to networks: Cortical/subcortical interactions in the pathophysiology of idiopathic generalized epilepsy. *Epilepsia* 2003;44(Suppl 2):7-15.
37. Kirton A, DeVeber G. Life after perinatal stroke. *Stroke* 2013;44:3265-71.
38. Stiles J, Moses P, Roe K, et al. Alternative brain organization after prenatal cerebral injury: Convergent fMRI and cognitive data. *J Int Neuropsychol Soc* 2003;9:604-22.
39. deVeber GA, MacGregor D, Curtis R, Mayank S. Neurologic outcome in survivors of childhood arterial ischemic stroke and sinovenous thrombosis. *J Child Neurol* 2000;15:316-24.

CHAPTER 9

General discussion and future perspectives



General discussion

Rates of preterm birth are increasing^{1,2} and advances in fetal and neonatal care have increased rates of survival of children born preterm.³ Despite these advances, many of these children develop long term neuromotor and neurocognitive deficits.³⁻⁶ Previous studies have shown that cerebrovascular instability is a key factor in the sensitivity of the preterm brain to extra-uterine life.⁷ This can lead to common types of brain injury such as germinal matrix or intraventricular hemorrhage with or without venous infarction and white matter injury.^{7,8} Injury to the preterm brain may result in long term morbidity, involving cognitive, motoric and behavioral problems.³ In order to identify brain injury in critically ill infants, neuroimaging plays an important role in daily clinical practice in the NICU. Unfortunately, once preterm brain injury is diagnosed, therapeutic options are still lacking. In clinical practice, the focus is therefore on prevention of brain injury, *e.g.* through hemodynamic monitoring. At the same time, early recognition of brain injury and monitoring of brain development are important for designing and evaluating therapeutic and/or neuroprotective treatment strategies. CUS can play an important role in this process, as it allows safe, serial, bedside neuroimaging of the preterm brain – even when a patient is clinically unstable.

Traditionally, neuroimaging with CUS in NICU's mainly focused on detection of two commonly recognized types of preterm brain injury mentioned earlier; (1) germinal matrix or intraventricular hemorrhage with or without venous infarction, and (2) white matter injury. However, with improved techniques, use of alternative acoustic windows and Doppler techniques other patterns of brain injury are increasingly recognized; *e.g.* cerebellar lesions, perforator stroke, and cerebral sinovenous thrombosis. The general aim of this thesis was to provide more insight into neonatal cerebellar hemorrhage, perforator stroke and cerebral blood flow, with dedicated use of Doppler CUS in the NICU.

We describe our approach of advanced Doppler CUS in **chapter 2**. This approach is suited for both routine clinical care and research purposes. We describe optimal settings, use of different probes, multiple acoustic windows, and Doppler techniques. This approach allows for better imaging quality and improves detection of brain injury. For example, with Doppler CUS cerebral sinovenous thrombosis can be detected at an early stage, creating a window of opportunity for therapeutic intervention prior to thrombosis-induced tissue damage.

One should be aware of the potential risks and burden of CUS in critically ill neonates. Most of these can be prevented or reduced with fairly simple precautions. For example, the infant can be supported by a health care worker or parent according to the principles of Newborn Individualized Developmental Care and Assessment Program.⁹ In our experience, infants often show signs of discomfort during CUS imaging through the

mastoid fontanel. We hypothesize that this could be explained by the mechanism of auditory response to pulses of radiofrequency energy.¹⁰

At tissue level, ultrasound energy is converted into heat which may increase local temperature. Doppler imaging has higher output potential compared to standard B-mode imaging.¹¹ We therefore recommend to keep the duration of exposure to a minimum, especially with Doppler imaging. In various published guidelines thermal and mechanical indices below one are considered safe.¹¹ Standard settings should be kept within these guidelines, as well as when adjusting settings during CUS examination. All in all, until now there is no evidence of adverse effects of ultrasound examination in neonates.¹¹

Using Doppler imaging, a large number of intracranial vessels can be visualized in preterm neonates. Flow in these vessels can be evaluated and peak systolic velocity (PSV), end-diastolic velocity (EDV) and RI can thus be obtained. RI is defined as $(PSV - EDV) / PSV$.¹² In current neonatal clinical practice, RI is typically assessed in the anterior cerebral artery. In term birth asphyxia, low RI is considered a possible sign of luxury perfusion. A patent ductus arteriosus (PDA) is considered to be the usual cause for elevated RI in preterm infants.¹² In previous work RI in cerebral arteries has been described in healthy term infants, small groups of clinically stable preterm neonates or small numbers of sick infants. In these studies, only small numbers of very preterm infants were included and RI was only described during a short timeframe. However in recent years, more infants born at extremely low gestational age are treated. Reference values for RI of cerebral arteries in these infants are currently lacking. In **chapter 3** we present prospectively gathered values for RI in seven intracranial arteries in a cohort of 235 very preterm infants born at < 29 weeks of gestation, throughout their stay in our NICU. We compared RI in these arteries and assessed the relationship between RI in intracranial arteries and the presence of a hemodynamically significant PDA. We found a considerable intersubject difference in RI between the larger internal carotid artery, anterior cerebral artery and basilar artery on one hand and the smaller pial and striatal arteries on the other hand.¹³ Ergo, RI differs depending on the size of the insonated intracranial artery; the larger the artery, the higher RI. This can be explained by differences in PSV and EDV between the greater and smaller cerebral arteries; in lenticulostriate arteries velocities are lower than in the great cerebral arteries, but the diastolic component is proportionally higher.¹⁴ Thus, for accurate follow-up and comparison of RI, it is essential to serially assess the same artery at the same level of its course.

We found no definitive cut-off value for RI in intracranial arteries indicative of the presence of echocardiographic hemodynamically significant PDA. RI values in infants without PDA were lower than in those with echocardiographic hemodynamically significant PDA, but this difference was very small and was statistically significant in some, but not all of the evaluated arteries. Moreover, RI values in these two groups of patients

were overlapping for all arteries. It may be that the presence of a echocardiographic hemodynamically significant PDA does not always significantly affect cerebral perfusion, especially in the smaller cerebral arteries such as striatal and pial arteries.

Assessment of RI is non-continuous and represents a snapshot in time. Also, as RI is an index, it will not be change when both PSV and EDV are similarly affected. Consequently RI may be unaffected in a critical situation, such as low blood flow. Although the value of cerebral artery RI has been established for term and moderate to late preterm infants, our study suggests that cerebral artery RI may have limited value as a clinical tool in the very preterm infant born at < 29 weeks of gestation. For a better understanding of the relationship between systemic arterial blood pressure and intracerebral blood flow, cerebral oxygenation and functional state, simultaneous multimodal monitoring could be useful; *e.g.* simultaneous monitoring of RI, invasive arterial blood pressure, regional cerebral saturation and fractional tissue oxygen extraction using near infrared spectroscopy, evaluation of microcirculation¹⁵ and EEG. Eventually such research may gain insight into the relationship between cerebral blood flow and the evolution of brain injury in very preterm infants. Ultimately this could lead to development of neuroprotective or therapeutic treatment strategies in order to prevent brain injury in these infants.

In addition to the larger intracranial vessels, current techniques and customized ultrasound settings allow visualization of intracranial vessels with a diameter of about 200 micron and flow velocities around 2 cm/sec.¹⁵ Consequently, visualizing and evaluating the so-called preterm “cerebral microcirculation” might be possible with CUS Doppler. This could aid in evaluating cerebral blood flow during adaptation, during the evolution of brain injury or to monitor the effect of neuroprotective or therapeutic interventions in the NICU. In order to assess whether visualization and velocity measurements of preterm cerebral perfusion using Doppler ultrasound techniques are accurate, we conducted an in vitro experiment using a microvessel flow phantom as described in **chapter 4**. Visualization of the microvessels and flow through the microvessels was indeed feasible and reproducible results were obtained for measuring velocity and diameter. However, velocity and vessel diameter were almost constantly overestimated with the settings used in clinical practice. This implies that before velocity measurements of preterm microcirculation can be used in the NICU, calibration of the ultrasound machine used for that purpose is needed. The ultimate goal of such research is to develop a sonographic tool that can be used to objectively study 3D regional cerebral perfusion in routine clinical practice. Again, this could lead to the development of therapeutic or neuroprotective strategies in order to prevent brain injury in critically ill infants.

In the second part of this thesis focus is on cerebellar hemorrhage and perforator stroke, which are probably still under-recognized in preterm as well as critically ill

term neonates. In **chapter 5** we describe the largest cohort to date of 55 infants with neonatal perforator stroke, specifically the clinical presentation, risk factors and imaging findings of perforator stroke. We found that perforator stroke was asymptomatic in most cases (58%), being diagnosed with routine neuroimaging. In the majority of cases (80%), perforator stroke was first diagnosed with CUS. The timing of diagnosis was predominantly in the first week of life (60% of cases). However, 40% were diagnosed after the first week of life and 5% were diagnosed with routine CUS *after* the age of 28 days. These numbers illustrate the importance of ongoing routine serial CUS imaging in infants admitted to a NICU, even in the absence of clinical symptoms of brain injury. We also found that previously described risk factors for developing neonatal main artery stroke were present in our cohort of neonatal perforator stroke as well. This study raised questions about the implications of neonatal perforator stroke on neurodevelopmental outcome. In our experience, parents of neonates with brain injury first and foremost want to be informed about prognosis while their child is still admitted to the NICU. To date, follow-up studies on neonatal arterial ischemic stroke have mainly focused on cortical stroke. Reports on outcome of perforator stroke mostly include children who develop stroke after the neonatal period^{16–20} or describe small numbers of children with neonatal stroke for a short or unknown follow-up period.^{21–25} We therefore evaluated neurodevelopmental outcome of our cohort of children with neonatal perforator stroke in **chapter 8**. The focus in this study was on simple, clinically relevant outcomes, based on common questions clinicians are faced with when counselling parents of affected children, *e.g.* ability to walk independently and presence of epilepsy in childhood. To the best of our knowledge, this study contains the largest follow-up cohort of children with previous neonatal perforator stroke. The children were 3 to 14 years old (median 8 years) at assessment. We found that motor outcome (presence of CP and/or ability to walk independently) was generally more favorable in children with isolated perforator stroke than in those with concomitant cortical stroke or other additional brain injury. However this was not the case when the corticospinal tract in the posterior limb of internal capsule or at the level of the mesencephalon was involved. Childhood epilepsy was rare in children with isolated perforator stroke compared to those with concomitant cortical stroke. There were no evident differences between children with isolated perforator stroke and those with concomitant brain injury with regard to cognitive or behavioral deficits. The cohort described is a very heterogeneous group, with children born term and preterm, different perforator strokes, different etiological mechanisms of stroke (*e.g.* asphyxia, sepsis/meningitis, birth trauma), and some with congenital anomalies (*e.g.* heart defects). Taking the heterogeneity of our cohort into account, it is possible that factors such as extreme prematurity, underlying etiological mechanisms, and development of West syndrome have had more effect on cognitive and behavioral outcome. Furthermore, deficits in cognition, language, behavior and other higher brain functions

have been reported in up to 60% of children with arterial perinatal stroke.²⁶ In the end, it is difficult to define the typical outcome associated with a particular type of brain injury because recovery occurs as part of a much broader and very complex developmental course.²⁷ Even longer prospective follow-up is needed to determine whether apparently normal children grow into deficits with maturation and whether deficits resolve, remain stable or become more pronounced over time. Suggestions for a multi-center setup of such a trial are most welcome, as well as potential participating centers.

In **chapter 6** clinical symptoms and CUS findings are evaluated in a cohort of preterm infants with cerebellar hemorrhage. We discerned six types of hemorrhage: subarachnoid, folial, lobar unilateral, lobar bilateral, giant lobar (including vermis), and contusional. Especially in infants with lobar cerebellar hemorrhage, CUS preceding or coincident with identification of cerebellar hemorrhage showed lateral ventricle dilatation, which could not be explained by intraventricular hemorrhage. Unexplained ventriculomegaly can be a first sign of cerebellar hemorrhage and should instigate sonographic evaluation of the cerebellum through the mastoid fontanel. Another finding was that most neonates showed otherwise unexplained motor agitation in the days preceding the diagnosis, suggesting that this may be a presenting symptom of cerebellar hemorrhage in preterm infants. Previously, it was thought that preterm cerebellar hemorrhage is clinically silent except for apnea.²⁸ The findings of motoric unrest and ventriculomegaly in this study can now be verified prospectively in future studies.

Neonatal neuroimaging has seen some major advances over the past decades. Currently, CUS and MRI are used for brain imaging of critically ill neonates and both techniques have their advantages and limitations. Based on previous work comparing the ability of MRI and CUS to predict outcome, MRI has been proposed as the imaging method of choice for high risk preterm infants, especially when performed around term-equivalent age.^{29–31} However, these studies did not use high-resolution ultrasound, additional acoustic windows, and Doppler imaging – as recommended by others.^{32–35} Furthermore, the limitations of MRI in clinical context are often not fully considered. In **chapter 7**, we therefore prospectively compared a single clinical early MRI scan to serial advanced dedicated CUS regarding clinical feasibility and detection accuracy for common types of preterm brain injury. 307 infants born < 29 weeks of gestation were included in this study. CUS excelled in clinical feasibility, as a high percentage of MRI scans had to be postponed or cancelled due to suboptimal conditions of many infants or for logistic reasons. As previously described, CUS can be an adequate diagnostic tool in most common types of preterm focal brain injury.^{32, 33} As expected, MRI was superior in detecting fossa posterior abnormalities, despite CUS scanning through the mastoid fontanel. CUS was better in detecting acute intraventricular hemorrhage, perforator stroke and cerebral

sinovenous thrombosis. This study illustrates that combined use of advanced serial CUS and MRI improves detection of common patterns of brain injury. Future research should therefore focus on improvement of complimentary applications of these two imaging techniques.

All in all, with further research and advancing technologies, we believe CUS can provide even more insight into brain injury and cerebral perfusion in critically ill neonates. This will hopefully lead to development of effective treatment and neuroprotective strategies in the future.

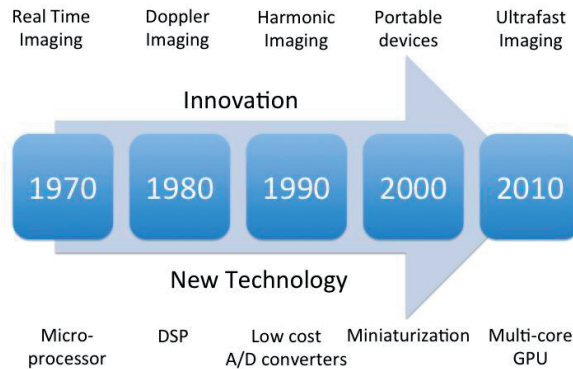
Future perspectives

Because ultrasound holds several major clinical advantages as diagnostic modality (i.e. real-time and bedside imaging, non-ionizing property, low cost), ultrasound has had a significantly impact in several clinical fields. Innovations in ultrasound therefore always show to have enormous potential. Especially in the field of neonatal neuroimaging ultrasound plays an important role because critically ill newborns admitted to the neonatal intensive care, are at high risk for brain injury and prognosis depends mainly on proper diagnosis of brain damage. MRI brain scans and ultrasound scans are regarded complementary in neonatal neuroimaging, mainly because MRI holds some key features which ultrasound lacks: such as clear fossa posterior views, quantification of tissue microstructure (e.g. diffusion tensor imaging, magnetic resonance spectroscopy), volumetric anatomical imaging, and diffusion imaging. However new technological breakthroughs will allow ultrasound to compete with some of these MRI modalities.³⁶

In the history of ultrasound new technological innovations have always been the major catalysts behind the clinical use. Since its establishment as medical imaging device in the 1960s, roughly one or two major breakthroughs are seen every decade (see figure).^{37, 38}

This last decade the incredible demands in processing and display performances needed for the gaming industry have boosted medical imaging technology. Multicore central processing units (CPU's), and new graphical processing units (GPU's) allow parallel processing on thousands of channels simultaneously. This technology has become available for the ultrasound industry, leading to several new exciting future applications in neonatal cerebral ultrasound imaging.³⁶

Conventional ultrasound imaging is performed by sequential insonification, using focused beams. Each focused beam allows reconstruction of one image line and ultrasound systems are designed to process one image line at a time. Limitations of this conventional ultrasound approach become clear as soon as higher frame rates



Figure

Abbreviations: DSP= digital signal processor, GPU= graphical processing unit, A/D= analog-to-digital

are required. Parallelization has been considered to overcome these limitations. Most current systems have “multiline capabilities”: for each transmit beam, several lines are computed. Multiline processing can be used to (1) increase the frame rate (for echocardiography for example) or (2) to increase the number of lines computed per image (for 3D imaging). However, advanced commercial data-acquisition modules have enabled full data capture of the ultrasound probe, which means that all data can be processed in multi-core CPU’s instead of the conventional mode with dedicated hardware. This enables **ultrafast imaging**, in which the frame rate shifts from a few tens of frames per second to at least a few hundred of frames per second. Such a system is able to compute in parallel as many lines as requested and is therefore capable of computing a full image from one single transmit. In such a system the image frame rate is no longer limited by the number of lines reconstructed, but by the time of flight of a single pulse ‘from’ and ‘back’ to the transducer.³⁹

In most current systems the maximum number of angles that can be used to compute an image is limited by the acquisition “Pulse Repetition Frequency” needed to measure the desired Doppler velocity scale. New ultrafast imaging systems allow an increase in temporal resolution and sensitivity. **Ultrafast Doppler** also allows clinicians to merge Color flow imaging and Pulsed wave Doppler modes in a single acquisition and with this, increase the accuracy of the examination. It will provide more insight into effects of treatment strategies and clinical conditions on local brain perfusion.

Ultrasound imaging provides both morphological (gray scale images) and functional imaging (Doppler flow imaging) of soft tissue. Using ultrafast imaging, a third dimension can be added to ultrasound: physio-pathological information. This can be done through the assessment of tissue viscoelasticity. Ultrafast imaging can be used to capture phe-

nomena that have never been imaged on commercial ultrasound devices: transient shear waves propagating in soft tissue. **Shear wave imaging** leads to quantification of tissue elasticity.⁴⁰

There are three different sources of transient shear waves in the human body:

(1) natural body vibrations: heart beating, arterial pulses, muscle fasciculations. This is a free source of information, but the assessment of reliable information is challenging outside of the vicinity of the vibrating organ.

(2) External vibrators that create controlled transient pulses.⁴¹

(3) Acoustic radiation force induced by ultrasound beams.⁴² Radiation force from an ultrasound focused beam generates a transverse bipolar shear wave.

Another promising development in ultrasound is image registration. Using probe tracking devices it is now possible to register ultrasound scans on previously uploaded MR or CT scans. Allowing optimal use of both techniques: such as the high resolution of high frequency ultrasound probes (< 150 micron) or Doppler qualities of current ultrasound.

Volumetric measurements can now be performed using extended field imaging techniques, allowing 3D reconstruction of brain tissue (including 3D segmentation of cerebral arteries; *Toshiba 500 series*).

Finally, small wireless ultrasound probes are now being developed opening a whole new range of ultrasound monitoring possibilities. Thanks to technological development of dedicated integrated circuits (IC), the functionality of a full ultrasound scanner is being miniaturized in few dedicated ICs the size of post stamp. This not only allows small hand-held wireless probes which facilitate the work flow on the neonatal care units, it also opens up the possibilities of continuous ultrasound monitoring. In such an application, the probe components are mounted inside the cap that the preterm infant is wearing, recording a detailed gray-scale or Color flow mode image every ten minutes, and transferring this wirelessly or minimally-wired to the central host computer for inspection. Automated image analysis may find early proof of e.g. hemorrhage or differences in microstructural appearance between the left and right hemisphere. Because of minimal interference with the general or even Kangaroo care, this monitoring device may be used over prolonged periods (days) during the critical days of the infant. Such a device could help gain more insight into the pathophysiology of neonatal brain injury, the effect of critical illness on the neonatal brain and assess the effect of neuroprotective strategies and possible therapeutic options. Moreover, by interleaved use over periods of weeks, this method could image the brain and microcirculation development over a longer period of time, thus truly becoming a bedside monitoring tool.

References

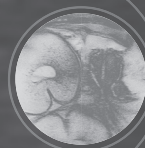
1. Blencowe H, Cousens S, Oestergaard MZ, Chou D, Moller AB, Narwal R, et al. National, regional, and worldwide estimates of preterm birth rates in the year 2010 with time trends since 1990 for selected countries: A systematic analysis and implications. *Lancet*. 2012;379:2162-2172.
2. Blencowe H CS, Chou D, Oestergaard M, Say L, Moller AB, Kinney M, Lawn J; Born Too Soon Pre-term Birth Action Group. Born too soon: The global epidemiology of 15 million preterm births. *Reprod Health* 2013 10:52.
3. Saigal S, Doyle LW. An overview of mortality and sequelae of preterm birth from infancy to adulthood. *Lancet*. 2008;371:261-269.
4. Larroque B, Ancel PY, Marret S, Marchand L, Andre M, Arnaud C, et al. Neurodevelopmental disabilities and special care of 5-year-old children born before 33 weeks of gestation (the epipage study): A longitudinal cohort study. *Lancet*. 2008;371:813-820.
5. Moore T, Hennessy EM, Myles J, Johnson SJ, Draper ES, Costeloe KL, et al. Neurological and developmental outcome in extremely preterm children born in england in 1995 and 2006: The epicure studies. *BMJ*. 2012;345:e7961.
6. Marlow N, Wolke D, Bracewell MA, Samara M, Group EPS. Neurologic and developmental disability at six years of age after extremely preterm birth. *N Engl J Med*. 2005;352:9-19.
7. Liem KD, Greisen G. Monitoring of cerebral haemodynamics in newborn infants. *Early Hum Dev*. 2010;86:155-158.
8. Greisen G, Borch K. White matter injury in the preterm neonate: The role of perfusion. *Dev Neurosci*. 2001;23:209-212.
9. Als H, Lawhon G, Brown E, Gibes R, Duffy FH, McAnulty G, et al. Individualized behavioral and environmental care for the very low birth weight preterm infant at high risk for bronchopulmonary dysplasia: Neonatal intensive care unit and developmental outcome. *Pediatrics*. 1986;78:1123-1132.
10. Elder JA, Chou CK. Auditory response to pulsed radiofrequency energy. *Bioelectromagnetics*. 2003;Suppl 6:S162-173.
11. Houston LE, Odibo AO, Macones GA. The safety of obstetrical ultrasound: A review. *Prenat Diagn*. 2009;29:1204-1212.
12. Lowe LH, Bailey Z. State-of-the-art cranial sonography: Part 1, modern techniques and image interpretation. *AJR Am J Roentgenol*. 2011;196:1028-1033.
13. van den Bergh R, van der Eecken H. Anatomy and embryology of cerebral circulation *Progress in brain research, 30th edition* Amsterdam Elsevier 1968:1-25
14. Couture A, Veyrac C. *Transfontaneller doppler imaging in neonates*. . Berlin Heidelberg: Springer-Verlag; 2001.
15. Raets MMA GP, Goos TG, Reiss IKM, de Jonge RCJ, Dudink J. Preterm cerebral microcirculation assessed with colour doppler: A pilot study. *J Pediatr Neuroradiol*. 2014;3:155-160.
16. Demierre B, Rondot P. Dystonia caused by putamino-capsulo-caudate vascular lesions. *J Neurol Neurosurg Psychiatry*. 1983;46:404-409.
17. Garg BP, DeMyer WE. Ischemic thalamic infarction in children: Clinical presentation, etiology, and outcome. *Pediatr Neurol*. 1995;13:46-49.
18. Giroud M, Lemesle M, Madinier G, Manceau E, Osseby GV, Dumas R. Stroke in children under 16 years of age. Clinical and etiological difference with adults. *Acta Neurol Scand*. 1997;96:401-406.
19. Inagaki M, Koeda T, Takeshita K. Prognosis and mri after ischemic stroke of the basal ganglia. *Pediatr Neurol*. 1992;8:104-108.

20. Kappelle LJ, Willemse J, Ramos LM, van Gijn J. Ischaemic stroke in the basal ganglia and internal capsule in childhood. *Brain Dev.* 1989;11:283-292.
21. Abels L, Lequin M, Govaert P. Sonographic templates of newborn perforator stroke. *Pediatr Radiol.* 2006;36:663-669.
22. Boardman JP, Ganesan V, Rutherford MA, Saunders DE, Mercuri E, Cowan F. Magnetic resonance image correlates of hemiparesis after neonatal and childhood middle cerebral artery stroke. *Pediatrics.* 2005;115:321-326.
23. de Vries LS, Groenendaal F, Eken P, van Haastert IC, Rademaker KJ, Meiners LC. Infarcts in the vascular distribution of the middle cerebral artery in preterm and fullterm infants. *Neuropediatrics.* 1997;28:88-96.
24. Mercuri E, Barnett A, Rutherford M, Guzzetta A, Haataja L, Cioni G, et al. Neonatal cerebral infarction and neuromotor outcome at school age. *Pediatrics.* 2004;113:95-100.
25. Mercuri E, Rutherford M, Cowan F, Pennock J, Counsell S, Papadimitriou M, et al. Early prognostic indicators of outcome in infants with neonatal cerebral infarction: A clinical, electroencephalogram, and magnetic resonance imaging study. *Pediatrics.* 1999;103:39-46.
26. Kirton A, Deveber G. Life after perinatal stroke. *Stroke.* 2013;44:3265-3271.
27. Stiles J, Moses P, Roe K, Akshoomoff NA, Trauner D, Hesselink J, et al. Alternative brain organization after prenatal cerebral injury: Convergent fmri and cognitive data. *J Int Neuropsychol Soc.* 2003;9:604-622.
28. Martin R, Roessmann U, Fanaroff A. Massive intracerebellar hemorrhage in low-birth-weight infants. *Journal of Pediatrics.* 1976;89:290-293.
29. Maalouf EF, Duggan PJ, Counsell SJ, Rutherford MA, Cowan F, Azzopardi D, et al. Comparison of findings on cranial ultrasound and magnetic resonance imaging in preterm infants. *Pediatrics.* 2001;107:719-727.
30. Miller SP, Cozzio CC, Goldstein RB, Ferriero DM, Partridge JC, Vigneron DB, et al. Comparing the diagnosis of white matter injury in premature newborns with serial mr imaging and transfontanel ultrasonography findings. *AJNR Am J Neuroradiol.* 2003;24:1661-1669.
31. Mirmiran M, Barnes PD, Keller K, Constantinou JC, Fleisher BE, Hintz SR, et al. Neonatal brain magnetic resonance imaging before discharge is better than serial cranial ultrasound in predicting cerebral palsy in very low birth weight preterm infants. *Pediatrics.* 2004;114:992-998.
32. Leijser LM, de Vries LS, Cowan FM. Using cerebral ultrasound effectively in the newborn infant. *Early Hum Dev.* 2006;82:827-835.
33. Horsch S, Skiold B, Hallberg B, Nordell B, Nordell A, Mosskin M, et al. Cranial ultrasound and mri at term age in extremely preterm infants. *Arch Dis Child Fetal Neonatal Ed.* 2010;95:F310-314.
34. Leijser LM, Liauw L, Veen S, de Boer IP, Walther FJ, van Wezel-Meijler G. Comparing brain white matter on sequential cranial ultrasound and mri in very preterm infants. *Neuroradiology.* 2008;50:799-811.
35. de Vries LS, Benders MJ, Groenendaal F. Imaging the premature brain: Ultrasound or mri? *Neuroradiology.* 2013;55 Suppl 2:13-22.
36. Szabo TL, Diagnostic Ultrasound Imaging: Inside Out, second edition. Elsevier Science 2014.
37. Szabo TL, Diagnostic Ultrasound Imaging: Inside Out. Elsevier Academic Press 2004.
38. Von Ramm OT, Smith SW, Pavy HG, Jr. High-speed ultrasound volumetric imaging system. II. Parallel processing and image display. *Ultrasonics, Ferroelectrics and Frequency Control, IEEE Transactions.* 1991;38:109-115.
39. Minin IV, Minin OV. Ultrasound Imaging - Medical Applications. InTech 2011. Chapter 1 'Ultrafast Ultrasound Imaging' by Jeremy Bercoff.

40. Sandrin L, Catheline S, Tanter M, Vinçonneau C, Fink M. 2D transient elastography. *Acoust. Imaging* 2000;25:485-492.
41. Catheline S, Wu F, Fink M. A solution to diffraction biases in sonoelasticity: the acoustic impulse technique. *J Acoust Soc Am* 1999;105:2941-50.
42. Sarvazyan AP, Rudenko OV, Swanson SD, Fowlkes JB, Emelianov SY. Shear wave elasticity imaging: a new ultrasonic technology of medical diagnostics. *Ultrasound Med Biol.* 1998;24:1419-35.

CHAPTER 10

Summary



Summary

The brain of critically ill term and preterm neonates admitted to the Neonatal Intensive Care Unit (NICU) is at risk for damage. Preterm infants are born in a critical period of brain development and maturation, in which the brain is extremely vulnerable. Common types of acquired brain injury diagnosed in the NICU are described in **Chapter 1**, the general introduction. Cranial ultrasound (CUS) and magnetic resonance imaging (MRI) are the neuroimaging modalities currently used for imaging of the brain in critically ill neonates. Advances in neuroimaging techniques have led to a better understanding of neonatal brain injury and to improved recognition of various lesion patterns, such as cerebellar lesion, perforator strokes, and sinovenous thrombosis.

The general aim of this thesis was to provide more insight into neonatal cerebellar hemorrhage, perforator stroke and cerebral blood flow, with dedicated use of Doppler CUS in the NICU. The first part of the thesis focused on cerebral blood flow and the use of advanced Doppler CUS. In the second part cerebellar hemorrhage and perforator stroke in critically ill term and preterm neonates were described – brain lesions which are probably still under-recognized.

Advanced Doppler cranial ultrasound

CUS is a valuable tool for brain imaging in critically ill neonates. Its main advantages are its safety, relatively low cost and the ease with which it can be performed at bedside, even in clinically unstable patients. CUS imaging possibilities have expanded with advancing techniques, but in many NICU's these possibilities are not used to their full potential. We described our approach of advanced Doppler CUS in neonates in **chapter 2**, with focus on the use of different probes, optimal settings, Doppler techniques, and multiple acoustic windows. This results in better imaging quality and improved diagnostic value of CUS in experienced hands. For example, Doppler CUS allows detection of cerebral sinovenous thrombosis at an early stage, allowing therapeutic intervention prior to the development of hemorrhage or stroke. Traditionally, images are obtained through the anterior fontanel. Use of additional acoustic windows (mastoid fontanel, posterior fontanel and temporal window) improves detection of brain injury. Examples of imaging using these alternative windows were described. Issues regarding equipment, data storage and safety were also addressed.

A frequently used application of Doppler CUS in the NICU is assessment of resistive index (RI) in cerebral arteries, a non-invasive way to evaluate cerebral blood flow. In current neonatal clinical practice, RI is typically assessed in the anterior cerebral artery. In pre-term infants, a patent ductus arteriosus is considered to be the usual cause for elevated RI. In recent years more infants born at extremely low gestational age are treated. Little

is known about cerebral artery RI in these infants. RI values in various cerebral arteries in a cohort of preterm infants born at < 29 weeks gestation are presented in **chapter 3**. RI was assessed in the internal carotid arteries, basilar artery, anterior cerebral artery, pial and striatal arteries in the first three days of life and weekly after that until discharge or death.

771 examinations were performed in 235 infants. RI differed between the various arteries: vessels with larger diameters (i.e. internal carotid arteries, basilar arteries and anterior cerebral artery) showed significantly higher RIs compared to the smaller vessels (pial and striatal arteries). Thus, when serially assessing RI, measurements must be made in the same artery to ensure valid comparison.

RI in infants without patent ductus arteriosus was lower than that in infants with hemodynamically significant patent ductus arteriosus (median in anterior cerebral artery 0.75 vs 0.82, $p < 0.001$), but this difference did not reach statistical significance in all arteries. There was no difference in pre- and postligation RI in infants who underwent patent ductus arteriosus ligation. We found no significant relation between RI and gestational age, SNAPPE-II score, or sex.

With current Doppler techniques and customized ultrasound settings it is possible to visualize small intracranial vessels of 200 micron in diameter and with very low flow (about 2 cm/sec). This implies that visualization of microvessels in the preterm brain – the so-called preterm “cerebral microcirculation” – is possible. To assess whether visualization and flow velocity estimates of preterm cerebral perfusion are accurate with the use of Doppler techniques, an in vitro experiment using a flow phantom was conducted as described in **chapter 4**. The flow phantom contained two microvessels (inner diameter 200 and 700 microns) with an attached syringe pump filled with blood-mimicking fluid, which was used to generate non-pulsatile flow. Measurements were performed at various flow velocities and depths, using a variety of ultrasound settings. Measurements of velocity and diameter were highly reproducible (intra class correlation 0.997 (95% CI 0.996–0.998) and 0.914 (0.864–0.946). Microvessels with velocities as low as 1 cm/sec were adequately visualized using a linear ultrasound probe. With a convex probe velocities < 2 cm/sec could not be visualized. The size of vessels was exaggerated with the used ultrasound colour Doppler techniques. Set flow and measured flow did not correspond: mean velocity was overestimated up to 3-fold, especially in high velocity ranges.

This study showed that visualization of microvessel size catheters mimicking small brain vessels is possible. Although reproducible velocity and diameter results were obtained, important overestimation of the values was observed. Before velocity estimates of microcirculation can be used in clinical practice, calibration of the ultrasound machine used for that purpose is essential.

Focal lesions

Previous studies on neonatal stroke have mainly focused on cortical stroke. **Chapter 5** described, to our knowledge, the largest cohort of neonatal perforator strokes, non-cortical strokes in the arterial vascular perforator area. Risk factors, clinical presentation and neuroimaging findings of this seemingly under-recognized brain injury were evaluated. All infants with a postnatal neuroimaging diagnosis of perforator stroke in a twelve-year period were enrolled. A total of 79 perforator strokes were detected in 55 patients. 28 patients were male, median gestational age was 37 1/7 weeks (range 24 1/7 to 42 1/7 weeks), and 25 were born preterm. In 58% perforator stroke was asymptomatic. 60% were diagnosed in the first week of life and 80% were initially diagnosed with CUS. Previously described maternal, fetal or perinatal risk factors for developing neonatal main artery stroke were present in all cases. Clinical phenotypes for perinatal stroke were classified by etiological mechanisms of neonatal stroke: birth asphyxia (16%), infection (15%), embolism (15%), hypoxia or hypotension (15%), birth trauma (9%), and acute blood loss (9%), arteriopathy (4%), unclassifiable (18%). We concluded that isolated perforator stroke is probably under-recognized, as clinical symptoms are almost always lacking. CUS is a reliable diagnostic tool in diagnosing perforator stroke.

In **chapter 6** clinical symptoms and CUS findings were evaluated in a cohort of 15 preterm infants with a postnatal CUS or MRI diagnosis of cerebellar hemorrhage. Median gestational age was 25 2/7 weeks (range 24 6/7 weeks to 32 1/7 weeks), median birth weight was 730 grams (range 535 to 1905 grams). Six types of cerebellar hemorrhages were discerned: subarachnoid ($n = 3$), folial ($n = 1$), lobar ($n = 9$, of which 4 bilateral), giant lobar ($n = 1$, including vermis) and contusional ($n = 1$). CUS showed preceding or concurrent lateral ventricle dilatation, mostly without intraventricular haemorrhage (IVH), especially in infants with lobar cerebellar hemorrhage. Thirteen infants suffered from notable, otherwise unexplained motor agitation in the days preceding the diagnosis of cerebellar hemorrhage. Motor agitation may be a presenting symptom of cerebellar haemorrhage in preterm infants. Unexplained ventriculomegaly may be a first sign of cerebellar haemorrhage and should prompt sonographic exploration of the cerebellum.

As previously mentioned, CUS and MRI are currently used for brain imaging of critically ill neonates. Both techniques have their advantages and limitations. Advancing technology, use of alternative acoustic windows and Doppler techniques have improved the possibility of CUS for detecting preterm brain injury. Also, CUS allows for repeated bedside scanning, even in critically ill infants. MRI currently entails several advanced techniques to evaluate the preterm brain. In previous work comparing MRI and CUS on their ability to predict outcome, Doppler imaging, additional acoustic windows and high-resolution ultrasound were not used. Also, the limitations of MRI in the clinical

context of critically ill neonates were often not fully considered. Therefore, a prospective study comparing a single clinical early MRI scan at 30 weeks postmenstrual age to serial advanced dedicated CUS regarding clinical feasibility and detection accuracy for common types of preterm brain injury was described in **chapter 7**. 307 infants born at < 29 weeks of gestation were included in this study. Serial CUS was performed in all patients, while MRI was often postponed ($n = 59$) or cancelled ($n = 126$). Preterm brain injury was found in 146 infants (47.6%). Discrepancies between the two imaging techniques were found in 61 of 180 infants in whom neuroimaging was performed with both imaging modalities. MRI was superior in detecting germinal matrix hemorrhage and posterior fossa abnormalities; CUS in identifying acute intraventricular hemorrhage, cerebral sinovenous thrombosis and perforator stroke. We concluded that advanced serial CUS seems highly effective in diagnosing most preterm brain injury, but may miss cerebellar lesions. These lesions are detected with MRI, but the feasibility of this technique for preterm neonates is limited. Therefore, improved safety and availability and tailored procedures are needed to increase the value of early MRI in clinical care of preterm infants in the NICU.

Neurodevelopmental outcome in survivors of neonatal perforator stroke was described in **chapter 8**. Thirty-seven patients of the original neonatal cohort of 55 patients were included: 14 with isolated single perforator stroke, 4 with multiple isolated perforator stroke, and 19 with additional brain injury. Age at assessment was 3 to 14 years (mean age 8 years). In the group of 18 children with isolated perforator stroke(s), four had CP, one could not walk independently, and one developed epilepsy. The posterior limb of the internal capsule was involved in 4 out of 18 patients; three of these patients had CP. In the group of 19 children with additional brain injury, 11 had CP and three were not able to walk independently. Three out of nine children with concomitant cortical middle cerebral artery stroke developed epilepsy. We concluded that perforator stroke patterns can aid in early prediction of outcome, enabling clinicians to provide prognostic information and early intervention of rehabilitation where needed. Motor outcome was favourable in children with isolated perforator stroke, except when the posterior limb of the internal capsule was involved.

In **chapter 9** the main findings of this thesis were described in the light of current literature and recommendations for future research were discussed.

Samenvatting

Kritisch zieke term geboren en prematuur geboren neonaten die opgenomen zijn op een Neonatale Intensive Care Unit (NICU) hebben een verhoogd risico op hersenschade. Premature neonaten worden geboren in een kritieke periode van hersenontwikkeling en –rijping, waarin het brein zeer kwetsbaar is. Veel voorkomende soorten hersenschade die worden gediagnosticeerd bij patiënten op de NICU werden besproken in **hoofdstuk 1**, de algemene introductie. Schedelechografie en magnetic resonance imaging (MRI) zijn de beeldvormingstechnieken die momenteel meestal gebruikt worden voor het afbeelden van de hersenen van kritisch zieke neonaten. Ontwikkelingen in beeldvormingstechnieken hebben geleid tot toenemend inzicht in neonatale hersenschade en betere herkenning van diverse schadepatronen, zoals cerebellaire letsels, perforator infarct en cerebrale sinoveneuze trombose.

Het doel van dit proefschrift was om middels schedelechografie meer inzicht te verkrijgen in neonatale cerebellaire bloedingen, perforator infarct en de cerebrale doorbloeding. In het eerste deel van het proefschrift stond de doorbloeding van hersenen en geavanceerde schedelechografie centraal. In het tweede deel werden diverse aspecten van cerebellaire bloedingen en perforator infarct beschreven, letsels die waarschijnlijk vaak niet herkend worden.

Schedelechografie en Doppler

Schedelechografie is een waardevolle beeldvormingstechniek bij kritisch zieke pasgeborenen. De belangrijkste voordelen zijn dat het veilig en relatief goedkoop is en dat het aan het bed van de patiënt kan worden uitgevoerd, zelfs bij de ziekste neonaten. De mogelijkheden van schedelechografie zijn toegenomen door verbeterde technieken, maar in veel NICU's worden deze mogelijkheden niet optimaal benut. In **hoofdstuk 2** beschreven we onze methode van geavanceerde Doppler schedelechografie bij neonaten, met de nadruk op het gebruik van diverse probes, optimale instellingen, Doppler technieken en beeldvorming via verschillende fontanellen. Deze methode leidt tot verbetering van de kwaliteit van beeldvorming en van de diagnostische waarde van schedelechografie. Zo kan bijvoorbeeld cerebrale sinoveneuze trombose in een vroeg stadium worden vastgesteld, waardoor de mogelijkheid bestaat tot therapeutisch ingrijpen om bloeding of infarctering te voorkomen.

Over het algemeen worden met schedelechografie beelden via de voorste fontanel gemaakt. Door het gebruik van andere fontanellen voor beeldvorming kunnen meer hersenletsels worden opgespoord. Voorbeelden hiervan werden besproken, evenals aspecten ten aanzien van de apparatuur, data opslag en veiligheid.

Een veel gebruikte toepassing van Doppler schedelechografie in de NICU is het bepalen van de resistive index (RI) in de cerebrale bloedvaten. Dit is een niet-invasieve methode om de doorbloeding van de hersenen in kaart te brengen. Bij premature neonaten wordt een open ductus arteriosus beschouwd als de meest voorkomende oorzaak van een hoge RI. Er worden steeds meer extreem vroeg geboren kinderen behandeld en er is nog weinig bekend over de RI in de cerebrale arteriën van deze kinderen. RI waarden in verschillende cerebrale arteriën werden beschreven in **hoofdstuk 3**. RI werd bepaald in de arteria carotis interna, arteria basilaris, arteria cerebri anterior, piale – en striatale arteriën, gedurende de eerste drie levensdagen en wekelijks nadien tot aan ontslag of overlijden.

Er werden in totaal 771 meetmomenten uitgevoerd bij 235 kinderen. RI was significant hoger in de grotere bloedvaten (de arteria carotis interna, arteria basilaris en arteria cerebri anterior) dan in de kleinere bloedvaten (piale en striatale vaten). Om seriële RI metingen echt met elkaar te kunnen vergelijken, is het dus van belang om deze steeds in dezelfde arterie te meten.

RI was lager bij zuigelingen zonder open ductus arteriosus dan bij zuigelingen met een hemodynamisch significante open ductus arteriosus (mediane RI in de arteria cerebri anterior 0.75 vs 0.82, $p < 0.001$), maar dit verschil was niet statistisch significant in alle arteriën. Bij de zuigelingen waarbij een ductusligatie was uitgevoerd, werd geen verschil gevonden in de RI voor en na ductusligatie. Er werd geen significante relatie gevonden tussen RI en zwangerschapsduur, geslacht of SNAPPE-II score (Score for Neonatal Acute Physiology, Perinatal Extension, Version II).

Met de huidige Dopplertechnieken en aangepaste echografie instellingen is het mogelijk om zeer kleine bloedvaten met een diameter van 200 micron en lage bloedstroomsnelheden (ongeveer 2 cm/seconde) te visualiseren. Dit impliceert dat het mogelijk moet zijn om microbloedvaten in de hersenen van neonaten – de zogenaamde “premature cerebrale microcirculatie” – te visualiseren. Om na te gaan of de visualisatie en geschatte snelheden van de cerebrale doorbloeding bij prematuren middels Doppler correct zijn, werd een in vitro experiment met een fantoom uitgevoerd. Zoals beschreven in **hoofdstuk 4** bevatte het fantoom twee microvaten met een binnenste diameter van 200 en 700 micron. Via een spuitpomp werd vocht (speciaal gemaakt om bloed te simuleren) door de microvaten gespoten. Er werden metingen met diverse snelheden en op meerdere diepten uitgevoerd, met verschillende instellingen van het echo apparaat. De metingen van de snelheid en diameter waren goed te reproduceren (intra class correlation 0.997 (95% CI 0.996–0.998) en 0.914 (0.864–0.946). Snelheden tot 1 cm/seconde konden adequaat worden afgebeeld met een lineaire echoprobe. Met een convexe echoprobe konden snelheden onder de 2 cm/seconde niet worden afgebeeld. De diameter van de bloedvaten werd groter weergegeven dan de werkelijke diameter.

De ingestelde snelheid en de gemeten snelheid kwamen niet overeen: de gemiddelde snelheid werd tot 3 keer te hoog weergegeven, vooral bij hoog ingestelde snelheden.

Deze studie laat zien dat het mogelijk is om microvaten af te beelden, maar dat de snelheid en diameter worden overschat. Voordat deze techniek in de klinische praktijk wordt toegepast, dient de gebruikte echoapparatuur geijkt te worden.

Focale letsels

Eerder uitgevoerde onderzoeken naar neonatale infarcten waren vooral gericht op corticale infarcten. In **hoofdstuk 5** werd, naar ons weten, het grootste cohort beschreven van neonatale perforator infarcten. Van 55 zuigelingen met in totaal 79 perforator infarcten werden de risicofactoren, klinische presentatie en bevindingen bij beeldvorming beschreven. De mediane zwangerschapsduur bij geboorte was 37 1/7 week (range 24 1/7 tot 42 1/7 week) en 25 zuigelingen waren prematuur geboren. Het merendeel (58%) was asymptomatisch. Bij 60% werd het perforator infarct in de eerste levensweek gediagnosticeerd en bij 80% werd de diagnose als eerste met schedelechografie vastgesteld. Maternale, foetale en perinatale risicofactoren voor het ontwikkelen van corticale infarcten die eerder in de medische literatuur werden beschreven waren in alle gevallen aanwezig. De etiologie mechanismen waren in dit cohort als volgt ingedeeld; perinatale asfyxie (16%), infectie (15%), embolie (15%), hypoxie of hypotensie (15%), geboortetrauma (9%), acuut bloedverlies (9%), arteriopathie (4%) en onduidelijk of onbekend (18%). We concludeerden dat perforator infarct waarschijnlijk vaak niet wordt herkend, aangezien klinische symptomen meestal ontbreken. Schedelechografie is een betrouwbare beeldvormingstechniek om een perforator infarct te diagnosticeren.

In **hoofdstuk 6** werden de klinische symptomen en bevindingen bij schedelechografie bij 15 premature neonaten met een cerebellaire bloeding geëvalueerd. De mediane zwangerschapsduur was 25 2/7 weken (range 24 6/7 weken tot 32 1/7 weken), het mediane geboortegewicht bedroeg 730 gram (range 535–1905 gram). Zes typen cerebellaire bloedingen werden onderscheiden: subarachnoïdale (n = 3), foliale (n = 1), lobaire (n = 9, waarvan 4 bilateraal), grote lobaire (n = 1, inclusief vermis) en contusionele (n = 1) bloedingen. Schedelechografie toonde voorafgaand aan of ten tijde van de diagnose laterale ventrikeldilatatie, meestal zonder intraventriculaire bloeding, in het bijzonder bij zuigelingen met lobaire cerebellaire bloeding. Onverklaarde ventriculomegalie kan dus een eerste teken zijn van een cerebellaire bloeding. Dertien zuigelingen presenteerden zich met opmerkelijke, onverklaarde motorische onrust in de dagen voorafgaand aan de diagnose cerebellaire bloeding. Motorische agitatie kan een symptoom zijn van cerebellaire bloeding bij premature neonaten.

Zoals eerder vermeld, worden schedelechografie en MRI gebruikt voor beeldvorming van de hersenen van ernstig zieke pasgeborenen. Beide technieken hebben hun voordelen en beperkingen. In eerdere onderzoeken waarbij schedelechografie en MRI met elkaar werden vergeleken qua diagnostische – en voorspellende waarde wat betreft latere ontwikkeling, werd niet standaard gebruik gemaakt van Doppler, beeldvorming via meerdere fontanellen en hoge resolutie echografie. Ook werd niet altijd stilgestaan bij de beperkingen van MRI ten aanzien van veiligheidsaspecten en logistiek in de dagelijkse klinische praktijk bij kritisch zieke neonaten. In **hoofdstuk 7** werd een prospectieve studie beschreven waarin één MRI-scan bij een postmenstruele leeftijd van 30 weken wordt vergeleken met seriële geavanceerde schedelechografie wat betreft de klinische uitvoerbaarheid en het diagnosticeren van hersenschade. 307 neonaten, geboren na een zwangerschapsduur van < 29 weken, werden geïnccludeerd in dit onderzoek. Seriële schedelechografie werd uitgevoerd bij alle patiënten, terwijl MRI vaak werd uitgesteld (n = 59) of geannuleerd (n = 126). Bij 146 (47.6%) kinderen werd hersenletsel vastgesteld. Bij 61 van de 180 kinderen waarbij beide beeldvormingstechnieken waren toegepast, werden tegenstrijdige bevindingen vastgesteld tussen MRI en schedelechografie. MRI was beter in het opsporen van germinale matrix bloedingen en afwijkingen in de achterste schedelgroeve, schedelechografie bij het diagnosticeren van acute intraventriculaire bloeding, cerebrale sinoveneuze trombose en perforator infarct. Concluderend lijkt schedelechografie dus zeer effectief in het diagnosticeren van de meeste hersenletsels bij prematuren, maar moet men erop bedacht zijn dat vooral cerebellaire letsels kunnen worden gemist. Deze letsels worden wel gediagnosticeerd met een MRI, maar de klinische toepasbaarheid van deze techniek bij kritisch zieke prematuren is nu matig. Om de bruikbaarheid van vroege MRI scans voor premature pasgeborenen op de NICU te verhogen, is het van belang dat de veiligheid wordt verbeterd en dat logistieke procedures worden aangepast.

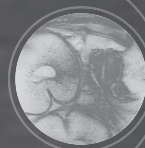
De neurologische uitkomsten van de overlevende kinderen die een neonataal perforator infarct hadden doorgemaakt, werden beschreven in **hoofdstuk 8**. We beschreven 37 patiënten van het oorspronkelijke cohort van 55 patiënten: 14 met een enkel geïsoleerde perforator infarct, 4 met meerdere geïsoleerde perforator infarcten, en 19 met nog ander hersenletsel naast het perforator infarct. De leeftijd bij de beoordeling van de neurologische uitkomst was 3 tot 14 jaar, met een gemiddelde leeftijd van 8 jaar. In de groep van 18 kinderen met geïsoleerde perforator infarct(en), hadden 4 een cerebrale parese, 1 kon niet zelfstandig lopen, en 1 ontwikkelde epilepsie. De achterste poot van de capsula interna was betrokken bij 4 van de 18 patiënten; drie van deze patiënten hadden een cerebrale parese. In de groep van 19 kinderen met extra hersenletsel, hadden 11 een cerebrale parese en konden 3 kinderen niet zelfstandig lopen. 3 van de 9 kinderen met een corticaal arteria cerebri media infarct ontwikkelden epilepsie.

We concludeerden dat perforator infarct patronen kunnen helpen bij een vroege voorspelling van de prognose, waardoor artsen ouders in een vroeg stadium beter kunnen voorlichten en waar nodig vroegtijdige begeleiding of revalidatie kunnen inschakelen.

In **hoofdstuk 9** werden de belangrijkste bevindingen van dit proefschrift beschreven in het licht van de huidige literatuur en werden aanbevelingen voor toekomstig onderzoek gedaan.

PART III

Appendices



About the author

Ginette Ecury-Goossen was born in Delft on 2 September 1982. Less than a year later, she moved with her parents to their home country Suriname. In 1988 the family moved to Curaçao, where she went to primary and secondary school. Like many of her friends and her high school sweetheart Björn she moved to the Netherlands after graduating in 2000. She studied Medicine at the Radboud University in Nijmegen and received her medical degree in November 2006. The next year she started working at Sint Franciscus Gasthuis in Rotterdam as a pediatric resident-not-in-training. In 2008 she began working in the Erasmus MC-Sophia in Rotterdam and six months later she started her official pediatric training in the NICU in that hospital. During her time in the NICU her interest in neonatal brain injury and neuroimaging developed and she participated in a research project. Over time more projects followed and in 2013 she returned to the NICU for her Neonatology (clinical) fellowship. She was encouraged by the head of the NICU department (prof. dr.I.K.M. Reiss) and her mentors (dr. J. Dudink and dr. P. Govaert) to continue the research projects during her fellowship, which eventually led to this PhD thesis. In July 2015 she finished her clinical fellowship and a month after that she and her husband Björn welcomed their first child, Myles. Shortly thereafter they moved back home to Curaçao, where Ginette now works as a pediatrician-neonatologist and the three of them live happily together.

List of publications

Goossen GM, Woensel JBM van, Noesel MM van, Zaaijer HL, Wetering MD van de. Influenza bij kinderen die chemotherapie ondergaan. *Ned Tijdschr Geneeskd* 2007;151;2154–7

Ecury-Goossen GM, Huysman WA, Man P de, Verhallen-Dantuma JCTM. Sequential intravenous-oral antibiotic therapy for neonatal osteomyelitis. *Pediatr Infect Dis J* 2009;28:72–73.

Goossen GM, Kremer LCM, van de Wetering MD. Influenza vaccination in children being treated with chemotherapy for cancer. *Cochrane Database Syst Rev* 2009;(2):CD006484.

Ecury-Goossen GM, Dudink J, Lequin M, Feijen-Roon M, Horsch S, Govaert P. The clinical presentation of preterm cerebellar haemorrhage. *Eur J Pediatr* 2010;169(10):1249–53

Goossen GM, Kremer LC, van de Wetering MD. Influenza vaccination in children being treated with chemotherapy for cancer. *Cochrane Database Syst Rev* 2013;(8):CD006484.

Ecury-Goossen GM, Raets M, Lequin M, Feijen-Roon M, Govaert P, Dudink J. Risk factors, clinical presentation and neuroimaging findings of neonatal perforator stroke. *Stroke* 2013;44(8):2115–20

Ecury-Goossen GM, Hoffmann-Haringsma AKE, Kamerbeek A. Neonatale geïnfecteerde cefaal hematomen. *Tijdschr Kindergeneeskde* 2013;81(6):159–162.

Camfferman FA, **Ecury-Goossen GM**, La Roche JE, de Jong N, van 't Leven W, Vos HJ, et al. Calibrating Doppler imaging of preterm intracerebral circulation using a microvessel flow phantom. *Front Hum Neurosci* 2015;8:1068.

Plaisier A, Raets MM, **Ecury-Goossen GM**, Govaert P, Feijen-Roon M, Reiss IK, Smit LS, Lequin MH, Dudink J. Serial cranial ultrasonography or early MRI for detecting preterm brain injury? *Arch Dis Child Fetal Neonatal Ed* 2015 Jul;100(4):F293–300.

Ecury-Goossen GM, Camfferman FA, Leijser LM, Govaert P, Dudink J. State of the art cranial ultrasound imaging in neonates. *J Vis Exp* 2015;96:e52238.

Ecury-Goossen GM, van der Haer M, Smit LS, Feijen-Roon M, Lequin M, de Jonge RC, Govaert P, Dudink J. Neurodevelopmental outcome after neonatal perforator stroke. *Dev Med Child Neurol* 2016;58(1):49–56.

Ecury-Goossen GM, Raets MM, Camfferman FA, Vos RH, van Rosmalen J, Reiss IK, Go-vaert P, Dudink J. Resistive indices of cerebral arteries in very preterm infants: values throughout stay in the neonatal intensive care unit and impact of patent ductus arterio-sus. *Pediatr Radiol* 2016;46:1291–300.

PhD portfolio

Name PhD student: G.M. Ecury-Goossen
 Erasmus MC Department: IC Neonatology
 PhD period: 2010–2016
 Promotor: Prof. dr. I.K.M. Reiss
 Supervisor: Dr. J. Dudink

1. PhD training

	Year	Workload (ECTS)
<i>Courses</i>		
Teach the teacher course	2012	0.3
Good Clinical Practice, BROK (Basiscursus Regelgeving Klinisch Onderzoek), Erasmus University	2014	1
NLS course	2014	0.4
Biomedical English Writing	2014	0.5
<i>Seminars</i>		
Ipokrates seminar Neonatal Neurology, Valencia	2015	0.7
<i>Presentations</i>		
Annual Flemish-Dutch neonatal neurology symposium	2010	1
NVK symposium neonatal cerebellar pathology	2010	1
Annual Flemish-Dutch neonatal neurology symposiums	2013 – 2015	3
Annual Dutch neonatal fellow meetings	2014 – 2015	2
5 th Congress of the European Society for Pediatric Research Barcelona, Spain	2014	1
<i>(Inter)national conferences</i>		
Annual Flemish-Dutch neonatal neurology symposium	2010	0.3
NVK symposium neonatal cerebellar pathology	2010	0.1
Annual Flemish-Dutch neonatal neurology symposium	2013 – 2015	0.9
54 th annual meeting European Society for Pediatric Research Porto, Portugal	2013	1
Annual Dutch neonatal fellow meetings	2014 – 2015	1.2
5 th Congress of the European Society for Pediatric Research Barcelona, Spain	2014	1.2

2. Teaching

Nurses education (Neonatology/Obstetrics and Gynaecology)	2013 – 2015	2
Teaching medical students	2014 – 2015	1.4
Cranial ultrasound: medical students, residents, pediatricians, radiologists	2013 – 2016	3
Supervising students:		
- microcirculation and phantom study (J. la Roche)	2014	2
- outcome neonatal perforator strokes (M. van der Haer)	2014	2

Dankwoord

"Feeling gratitude and not expressing it is like wrapping a present and not giving it."

William Arthur Ward

Curaçao, september 2016

Wat is het tot stand komen van dit boekje een bijzonder avontuur geweest... Een avontuur waarbij ik door veel mensen aangemoedigd en geholpen ben en ik met veel plezier met een aantal mensen nauw heb mogen samenwerken. Ik kan dan ook met een enorm dankbaar hart terugkijken naar de mooie tijd die ik heb gehad op de ICN in Rotterdam.

Allereerst wil ik de ouders en patiënten bedanken die hebben deelgenomen aan het onderzoek. Dit proefschrift is er dankzij jullie, maar ook voor jullie.

Mijn promotor; Prof.Dr. I.K.M. Reiss. Beste Irwin, hartelijk dank voor de prachtige kans die je me hebt gegeven voor het fellowship Neonatologie in Rotterdam en dat je me daarnaast op jouw unieke manier hebt weten te motiveren om te promoveren. Het was een onvergetelijke tijd!

Mijn co-promotor; Dr. J. Dudink, de motor achter dit promotietraject. Beste Jeroen, toen ik als arts-assistent op de ICN begon was je mijn mentor en dat ben je altijd gebleven. Jaren geleden een eerste "projectje" met jou mogen doen, wie had ooit gedacht dat dit het eindresultaat zou zijn... Enorm bedankt voor je altijd positieve en enthousiaste begeleiding, je vlotte terugkoppeling, je steun en alle gezellige momenten. Dat Caribische Neonatale Neurologie Congres gaan we echt nog samen organiseren!

De leden van de kleine commissie: Prof.Dr. L.S. de Vries, Prof.Dr. A. van der Lugt en Prof. Dr. E.A.P. Steegers, hartelijk dank voor jullie bereidwilligheid zitting te nemen in de kleine commissie en voor het lezen en beoordelen van mijn proefschrift.

De overige commissieleden: Prof.Dr.Ir. N. de Jong, veel dank voor de mooie samenwerking met de ICN en voor uw onmisbare bijdrage aan de fantoomstudie.

Prof.Dr. A.F. Bos en Prof.Dr. E.H.H.M. Rings, hartelijk dank voor het plaatsnemen in de grote commissie.

Paul Govaert, deze Japanse spreuk zegt het wat mij betreft het best: "Better than a thousand days of diligent study, is one day with a great teacher." Wat was het bijzonder met

u te mogen werken. Hartelijk dank voor alle leerzame en gezellige momenten, ik mis de dolle donderdagen!

Collega's van de afdeling ICN in het Sophia Kinderziekenhuis: wat een geweldig team! Ik kan het niet vaak genoeg zeggen; ik heb het zo goed gehad bij jullie! Mede door de positieve energie die ik haalde uit het werken met jullie is het gelukt dit proefschrift af te ronden. Bedankt voor de support en voor de mooie momenten die ik met jullie heb mogen meemaken. Een aantal collega's wil ik hier speciaal noemen.

Ten eerste Karin Suvaal, mijn hulplijn voor al het regelwerk vanuit Curaçao, hartelijk dank daarvoor! Een speciaal woord van dank aan René; als opleider en als persoon heb je me enorm gesteund, gemotiveerd en geprikkeld tijdens de opleiding én het promotietraject. Beste Rogier, bedankt voor je kritische blik op de manuscripten en voor jouw gave om statistiek begrijpelijk te maken, ik heb veel van je geleerd! Beste Marijn, ik heb veel bewondering voor de manier waarop jij je vak uitoefent. Bedankt voor het persoonlijk ophalen van het manuscript voor de kleine commissie. En natuurlijk een enorm *merci* voor Marit, mijn lieve fellow-maatje en mede-allochtoontje op de fellowkamer. Je begreep me als geen ander, we hebben lief en leed met elkaar gedeeld, wat ben ik dankbaar dat we samen fellow waren en wat bijzonder dat je op deze dag aan mijn zijde staat!

De neurogroep: bedankt voor het kritisch beoordelen en meelezen van manuscripten, voor de gezellige samenwerking en voor jullie hulp. Ik wil speciaal Marlou en Annemarie noemen, eerst collega's op de NICU, jaren later wetenschappelijk samenwerken... Het was in beide gevallen in één woord super, bedankt voor jullie luisterend oor, steun en de vele gezellige momenten.

Alle mede-auteurs die ik nog niet genoemd heb, heel veel dank voor de fijne samenwerking. Ko Hagoort, hartelijk dank voor de vlotte en waardevolle correcties van de manuscripten. De studenten die ik heb mogen begeleiden: Marit en Jhuresy, bedankt voor jullie enthousiasme en inzet, ik wens jullie veel succes in jullie verdere carrière.

Dr. M.D. van de Wetering, lieve Marianne, onder jouw hoede heb ik de eerste stapjes in de wetenschap gezet. Hartelijk dank voor de kans die je me hebt geboden en voor je begeleiding.

Mijn opleiders Kindergeneeskunde: Prof.Dr. M. de Hoog, Dr. W.A. Huysman en Dr. H.T.M. Jongejan, veel dank voor jullie vertrouwen en steun, geweldig dat ik ná de opleiding tot kinderarts mag promoveren!

Mijn nieuwe collega's op Curacao: *masha danki* voor jullie support en voor het warme welkom, ik voelde me meteen thuis!

Nena Abbad en mijn tante Anita, twee personen die deze dag helaas niet mee kunnen maken. Jullie hebben elk op jullie eigen manier mij gestimuleerd en geïnspireerd om dit traject af te leggen.

Mijn lieve familie en vrienden *ront mundo* die me altijd hebben gesteund en voor heel wat mooie en gezellige momenten hebben gezorgd door de jaren heen. Ik wil hier speciaal mijn oudste vriendinnen noemen: lieve Ann, Zetsia en Zoë, so many memories together, has it really been that long? Ik mis jullie! Wat bijzonder om jou op deze dag naast me te hebben, Zets! En mijn jongste vriendin/oudste "kind" Larissa, je bent een schat! Lieve tante Juud, al sinds m'n geboorte zo betrokken bij mij, priceless!

Mijn lieve schoonfamilie: *masha danki* voor de hartelijke ontvangst in de familie en voor jullie interesse en support! Lieve Jeanne en Boy, 15 jaar later wonen we eindelijk weer wat dichterbij elkaar, maar ondanks de enorme afstand weten we dat jullie in gedachten altijd dichtbij ons zijn geweest en ons altijd gesteund hebben.

Mijn lieve sissies Gail en Michelle (Li en Donsje), wat zou ik zonder jullie moeten... Zoveel met jullie gedeeld, samen gehuild (the ugly cry), samen gelachen (humor die weinig anderen begrijpen)... Love you so much! Miss you Donsje!

Mijn lieve ouders, waar moet ik beginnen... Jullie onvoorwaardelijke liefde en steun waren elke dag tastbaar, ook al die jaren op zo'n 8000 km afstand. En nu we weer dichtbij jullie wonen des te meer, het afronden van dit traject was zonder jullie niet gelukt. Zo bijzonder dat jullie er op deze dag ook bij zijn, love you so much!

En dan mijn twee lieve mannetjes... Lieve Myles, jij hebt het laatste stukje van het promotietraject voor zoveel vreugde gezorgd, eerste trappelend in m'n buik en nu trap-pelend op schoot met een aanstekelijke big smile. Lieve Björn, *my homebase*, jij geloofde nog meer dan ik dat dit mogelijk was en hebt me zo enorm gesteund, nooit geklaagd wanneer ik weer eens aan het schrijven was... Zonder jou was dit niet gelukt! Love you guys so much! ♥

